A COMPARATIVE ANALYSIS OF STABILITY AND STRUCTURE-FUNCTIONAL RELATIONSHIPS OF DIFFERENT XYLANASES

SACHA TABOSA-VAZ

Submitted in complete fulfilment for the Degree of Master of Technology (Biotechnology) in the Department of Biotechnology and Food Technology, Faculty of Applied Sciences, Durban University of Technology, Durban, South Africa.

Final Copy Approved For Submission

_____ _____
Supervisor Date
Prof. S. Singh (Ph. D)

_____ _____
Supervisor Date
Prof. K. Permaul (Ph. D)

_____ _____
Supervisor Date
Dr. A. Kumar (Ph. D)

DECLARATION

I hereby declare that this dissertation is my own, unaided work. It is being submitted for the degree, Master of Technology, to the Durban University of Technology, Durban, South Africa. It has not been submitted before for any degree or dissertation to any other institution.

_____

S. TABOSA-VAZ

2012

CONTENTS

ACKNOWLEDGEMENTS

I would like to thank the following people:

My supervisors, Prof. Suren Singh, Prof. Kugen Permaul and Dr. Ajit Kumar for all their guidance, helping me find solutions for any problems that arose and for pushing and motivating me.

Prof. Eva Nordberg-Karlsson and Ms. Tania Posso for organising my visits to Lund and ensuring that not only was I able to extend my research and experience life in other labs but also for making me feel welcome.

The NRF for funding my studies.

The staff and students of the Biotechnology department especially the M. Tech enzyme girls for making the days, where nothing seemed to be moving forward, tolerable.

My family and friends for the unwavering support and love. The weekends helped me focus and give my all during the week.

Lastly I would like to thank God, with His love, anything thing is possible.

LIST OF ABBREVIATIONS

2D	Secondary structure
3D	Tertiary structure
4D	Quaternary structure
CD	Circular dichroism
DEP	Diethyl pyrocarbonate
DNS	3,5 dinitrosalicylic acid
DSF	Differential scanning fluorometry
EX	Endoxylanases
F	Fluorescence observed in the folded state
GdnHCl	Guanidine hydrochloride
Hv_{em}	Emission energy of a fluorophore
Hv_{ex}	Photon of given energy
K	Constant of unfolding
LCC	Lignincarbohydrate complexes
MRW	Mean residue weight of the protein
MW	Molecular weight
NMR	nuclear magnetic resonance
OPTA	*o*-phthalaldehyde
PCR	Polymerase chain reaction
Phe	Phenylalanine
R	Gas constant
RT-PCR	Real time polymerase chain reaction
TNBS	Trinitrobenzenesulphonic acid
TRP	Tryptophan
Tyr	Tyrosine
T	Absolute temperature
U	Fluorescence observed in the unfolded state
WRK	Woodwards Reagent K
α	Fraction of folded protein
ΔG	Gibbs free energy of unfolding
θ	CD signal in milli degrees

LIST OF FIGURES

LIST OF TABLES

ABSTRACT

A comparative thermostability analysis of different partially purified xylanases from *Rhodothermus marinus, Bacillus halodurans, Thermomyces lanuginosus* and Pulpzyme HC was studied using differential scanning fluorometry (DSF), fluorescence spectroscopy and circular dichroism (CD). The *R. marinus* xylanase was found to have an optimum temperature and pH of 90ºC and 6 respectively while the *B. halodurans* xylanase was optimally active at 70ºC and a broad range of alkaline pH of 8 - 10. The commercially available xylanase from *T. lanuginosus* showed optimal activity at 50ºC and pH 7 while the Novozyme xylanase Pulpzyme HC showed optimal activity at 60ºC and pH 7.

Fluorescence spectroscopy monitored the microenvironment and fluorescence emission of Trp residues. In their native folded state, Trp are generally located in the core of the protein but during unfolding they become exposed. The fluorescence changes as the enzyme undergoes denaturation due to conformational changes and exposure of Trp residues.

Differential scanning fluorometry (DSF) monitors thermal unfolding of proteins in the presence of a fluorescent dye such as Spyro Orange. A wide range of buffers were tested for their ability to increase the xylanase stability. *T. lanuginosus* had the greatest increase in melting temperature with 0.73M Bis Tris pH 6.5 and peaked highest at 78°C. The *B. halodurans* xylanase exhibited high pH stability (pH 4-10) and exhibited very little change in melting temperature, from 74°C-77°C over the twenty four different conditions. The *R. marinus* xylanase had no increase in melting temperature showing a maximum melting temperature of 90ºC.

Circular dichroism (CD) measures unequal absorption of right- and left-handed circularly polarized light by the molecule. The xylanase from *R. marinus* exhibited the lowest ΔG of 34.71kJ at 90°C as was expected. The *B. halodurans* xylanase showed a much higher

ΔG of -52.71 at its optimum temperature of 70°C when compared with the xylanases from *R. marinus* and *T. lanuginosus*. When comparing the three xylanases activities at 70°C, it can be seen that the *B. halodurans* xylanase exhibited a lower relative activity then both *R. marinus* and T. *lanuginosus* xylanases.

All three techniques offered different information on the structure and function relationship. Fluorescence spectroscopy, the change in conformation due to fluorescence emission as a result of increased temperature and salt concentrations. DSF, optimal conditions for increased stability and activity at higher temperatures and CD, conformational changes, the fraction of folded protein and change in Gibbs free energy over a range of temperature.

CHAPTER 1: INTRODUCTION AND LITERATURE REVIEW

Biotechnology has played a major role in the advancement of the paper and pulp industry and has attracted considerable interest as a way to overcome many ecological and economical problems related to conventional industrial technologies (Shatalov and Pereira, 2007). Enzymes provide a viable economic and environment friendly alternative as compared to chemical processes used in the pulp and paper industry. The application of enzymes in fibre processing has been mainly directed towards the degradation or modification of hemicelluloses and lignin, while retaining the cellulosic portion (Janardhnan and Sain, 2006). Their activity at high temperatures and ranging pH is necessary in the processes in pulp and paper industries, where most of the enzymes become susceptible to denaturation and inactivity. Fluorescence spectroscopy and conventional methods can be used to study the enzyme denaturation and correlate their optimum activity with respect to temperature and pH (Edward *et al*., 2002). Fluorescence spectroscopy has been widely used to study the xylanase conformation (Nath, 2001; George *et al.,* 2001). Attempts to decipher the residues involved in the active site of xylanase are made by subjecting them to modification with different group specific reagents such as *o*-phthalaldehyde (OPTA), Woodwards Reagent K (WRK), trinitrobenzenesulphonic acid (TNBS) and diethyl pyrocarbonate (DEP).

Proteins are composed of complex and hierarchically organised structures. In an aqueous solvent the protein polypeptide chain generally only folds into a sole three-dimensional conformation and this unique fold and structure ensures an active protein. On the other hand, this conformation exhibits a marginal stability, equivalent to the energy of very few hydrogen bonds (Privalov, 1979). This is the reason so many researches study the folding

and unfolding of proteins and how proteins react and change conformation under denaturation conditions.

The question of how a protein folds into its unique, compact highly ordered, and functionally active form is one of the most intriguing and perplexing questions of structural and cellular biology (Jagtap and Rao, 2009). Jaenicke (1987) states that a protein in its biologically active conformation is as a result of not only folding and assembly but a series of complex reactions that involve the formation of secondary and tertiary structures, domains and oligomerization of folded monomers. The stability of proteins is often studied by the additions of chemical denaturants such as guanidine hydrochloride (GdnHCl) and urea. They are involved in unfolding proteins by providing increased stability for the unfolded state when compared with the native state. Chemical denaturation is the standard method in determining the stability of proteins and in investigating the kinetics and mechanisms of protein folding reactions (Jagtap and Rao, 2009). Refolding of the denatured proteins in vitro has been an important issue at the fundamental as well as at the biotechnological level. Denaturation and renaturation are thermodynamic processes, involving a change in free energy and large changes in conformation between the denatured and the native states (Arai and Kuwajima, 2000).

Despite the complexity of these molecules, there are four generally recognized levels of protein structure. Primary structure refers to the amino acid sequence and the location of disulfide bonds, secondary structure is the defined spatial relationship of adjacent amino acids in localized stretches, tertiary structure describes the three-dimensional conformation of an entire polypeptide chain, and quaternary structure involves the spatial relationship of multiple polypeptide chains (subunits) in stable associations (Nelson and Cox, 2000 and

Rawn, 1989). Proteins all have unique three-dimensional structure that determines its function. These three-dimensional structures are stabilized through multiple weak interactions, including hydrophobic interactions, hydrogen bonds, and ionic interactions (Nelson and Cox, 2000; Rawn, 1989). Nelson and Cox (2000) describe treatments that disrupt interactions and severely impact or destroy the three-dimensional structure of proteins with a subsequent loss of protein function. This demonstrates the relationship between the native protein structure and conformation and its function and activity.

1.1. Enzymes: Biocatalysts of nature

In nature, the rate or velocity of biochemical reactions are increased by enzymes and the most important factor is these reactions is the fact that the vast majority of enzymes remain unchanged and are reusable in the catalyzing of reactions. Historically enzymes have assisted in the process of the baking of bread as well as the fermentation and brewing of beer. Such processes were dependant on the production of the enzymes by growing microorganisms or with the addition of preparations such as rumen or papaya fruit. Therefore, the enzymes were not used in any pure or characterised form (Kirk *et al.,* 2002). As research continues and knowledge expands the complex interactions of enzymes and substrates has allowed for the discovery of novel enzymes and reactions. This knowledge has allowed for the integration of cleaner, more environmentally friendly enzyme assisted processes where harsher chemicals were once used. Therefore the demand for enzymes showing increased stability and action with respect to both temperature and pH has greatly increased.

There are more than 500 commercial products which use these enzymes in their synthesis and two of the most popular are aspartane, a low calorie sweetener and amoxcillin an antibiotic (Schoemaker *et al.,* 2003). The world market for industrial enzymes was in the

range of 1.7 and 2 billion US dollars in 2000 and this value is expected to increase several fold (Bhat, 2000). The industrial enzyme market is divided into three application segments. The largest segment with 65% of sales is technical enzymes and include enzymes in the detergent, starch, textile, leather, pulp and paper, and personal care industries. Enzymes in the food industry, the second largest segment comprising 25% of the market, includes enzymes employed in the dairy, brewing, wine and juice, fats and oils, and baking industries. Finally, feed enzymes, encompassing enzymes used in animal feeds, contribute approximately 10% of the market (McCoy, 2000; Kirk *et al*., 2002; Hibbert and Dalby, 2005). The global market for industrial enzymes has continued to increase over the years and was estimated to be around $3.3 billion in 2010 and this market is expected to reach around $4.4 billion by the year 2015 (Fig. 1.1)

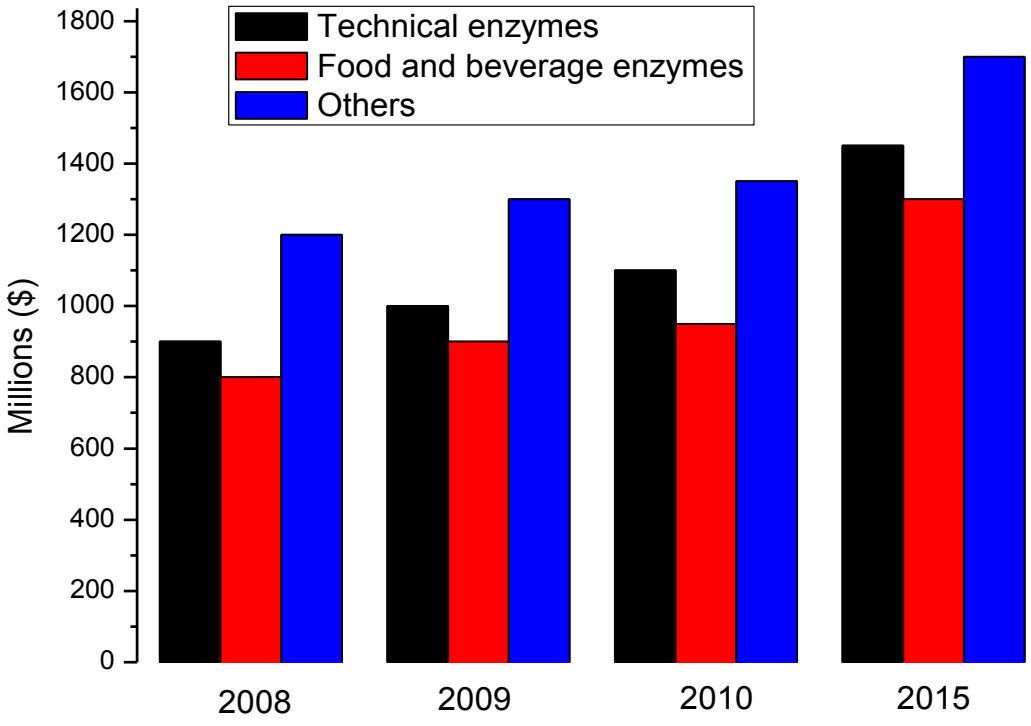

Fig. 1.1: Growth of the global enzyme market and its application sectors projected from 2008 to 2015. (www.bccresearch.com/report/enzymes-industrial-applications.html)

1.2. Extremozymes: the need for stability

There are many advantages to replacing harsher chemical treatments with more environmentally friendly enzyme substitutes. However, such enzymes use must provide a viable economic and results orientated alternative.

The microorganisms that produce xylanases and other glycosidases have been found in extremely diverse natural habitats such as *Rhodothermus marinus,* isolated from an intertidal hot spring in Isafjardardjup in northwestern Iceland (Bjornsdottir *et al.,* 2011), bacteria isolated from high altitude Andean lakes are placed in Puna desert over 4400 m above sea level (Dib *et al.,* 2009) and gram-positive bacteria designated as IMU-1 and IMU-2 that were isolated from Asian desert dust (Sasaki *et al.,* 2009). Under mesophilic growth conditions, xylanolytic activity has been reported in a wide variety of different genera and species of bacteria, fungi, and yeasts (Gilkes *et al*., 1991). There are also many different microorganisms inhabiting and thriving in extreme environmental conditions such as temperatures above 50 ºC and pH over 9, as well as high ionic strength aqueous systems containing salt approaching saturating conditions (Wong *et al*., 1988). Environmental conditions such as temperature, level of hydration, salinity and pressure have a marked influence on protein stability and therefore on enzyme reaction kinetics. Investigating the underlying mechanisms behind protein stability and the structure and function aspect can be achieved by comparing the functionality of proteins adapted to very different temperatures (Jaenicke *et al.,* 1996 and Zavodszky *et al.,* 1998). Thermozymes, proteins that have become adapted to extremely high temperatures, are produced by thermophilic or hyperthermophilic organisms that occupy areas with temperatures ranging from 70 °C to far above 100 °C. Such an organism is *R. marinus* isolated from an intertidal hot spring (Bjornsdottir *et al.,* 2011). They remain folded and functional at elevated temperatures, and are often less active at lower

temperatures. In contrast, similar mesophilic organisms, very similar in structure and with high sequence homology, keep their specific conformation and their functionality only up to approximately 60 °C. Introduction some structural properties have been related to increased thermostability, such as additional hydrogen bonds and salt bridges, shorter loop regions and increased internal hydrophobicity (Fittera *et al.*, 2001).

There are many microorganisms that are able to grow and even flourish in extreme environmental conditions. *Thermotoga maritima* (Winterhalter and Liebl, 1995), *Dictyoglomus* sp. (Mathrani and Ahring, 1991), *Caldocellum saccharolyticum* (Luthi *et al*., 1992) and *Rhodothermus marinus* (Dahlberg *et al.*, 1995). Research has been intensified on thermostable enzymes such as thermophilic xylanases from *Thermonospora sp.* and *Actinomadura sp.* because of their biotechnological applications (Perez *et al*., 2002*).* Danson *et al.* (1996) reported the hyperthermophilic and thermophilic enzymes showing optimum temperature marginally above or equal to growth conditions of the source organism. Therefore a thermoactive enzyme at 100 °C would have a much higher rate of reaction than that of a mesophile at 37 °C. The structure and conformation of such enzymes relates to properties such as thermostability and mode of action and it is these characteristics that are vital when selecting enzymes for processes in industry. Thermostable enzymes are often chosen ahead of mesophilic species as most industrial processes operate at high temperatures. Other advantages of thermostable enzymes include reducing the risk of mesophilic contamination and improving the bioavailability of organic compounds which therefore facilitates bioremediation (Becker, 1997). Higher reaction rates are also achieved due to decreased viscosity (Krahe *et al.*, 1996) and an increased diffusion coefficient of substrates and higher process yields due to improved solubility of substrates and products and favourable equilibrium displacement in endothermic reactions (Kumar and Swati, 2001).

The structure of many thermophilic extremozymes such as *R. marinus* (Abou-Hachem, 2003), *Thermotoga thermarum* (Sunna *et al.*, 1996) and *Dictyoglomus* sp. (Mathrani & Ahring, 1991), have been elucidated and compared to similar species in using structural alignment and homology modelling and some interesting data has been uncovered. The eventual goal of such research is to elucidate and understand an underlying mechanism for thermostability. Palardarni *et al.* (2002) suggested three main factors that combine and work together to promote thermostability. Firstly, an increase of surface charge, secondly, increased protein hydrophobicity and lastly, the replacement of exposed 'thermolabile' amino acids. Everly and Alberto (2000) also suggested that other adaptations are also important for thermostability such as the use of chaperonins that assist in the refolding of proteins into their native, active form.

Biotechnologically useful extremozymes have not only a commercial value but garner a high level of interest from various industrial sectors. Eichler (2001) suggested that this translates into the thermozymes needing to possess the ability to flourish and maintain high activity at both high temperatures and a range of different pH's which allows them to be used in a variety of different industrial applications. A few examples of extremozymes and their industrial applications are highlighted in Table 1.1. High throughput screening technology has allowed hundreds of different enzymes to be screened to search for variants with differing and enhanced capabilities. Enzymes have evolved and mutated, allowing them to bind and actively degrade or change a myriad of different substrates but technology has improved such that scientists and researchers are able to design enzymes that are tailored to suit the current and changing needs of industry. This has closed the gap between what nature has provided

and what is actually needed from an enzyme to retain functionality under the conditions of most industrial processes (Johannes & Zhao, 2006).

Table 1.1. Industrial extremozymes and their applications in industry (adapted from Shiraldi and De Rosa, 2002).

Microorganisms	**Enzymes**	**Applications**
Thermophiles	Amylases & glycosylases	Starch processing & saccarification
(50 °C – 110 °C)	Lipases	Detergent Formulations
	Xylanases	Paper bleaching
	Proteases	Food processing & detergents
	DNA polymerases	Genetic engineering
	Esterases	Stereo-specific reactions
Psychrophiles	Amylases, lipases & proteases	Polymer degrading agents
(0 °C – 20 °C)	Dehydrogenases	Biosensors
Alkalophiles	Cellulases & proteases	Polymer degrading agents
(pH≥9)	Amylases & lipases	Food additives

1.3. Applications

Over the years the number of possible applications of xylanases in the pulp and paper industry has increased steadily, and several are in, or are approaching, commercial use. Currently, the most effective application of xylanase is in prebleaching of kraft pulp to minimize use of harsh chemicals in the subsequent treatment stages of kraft pulp. While many applications of enzymes in paper industries are still in the research and developmental stage, several applications have found their way into the mills in an unprecedented short period of time in the last decade (Bajpai, 1999). Xylanases have various other applications other than in the pulp and paper industry. In the food industry xylanases are added in wheat flour so as to improve dough handling and increase the quality of baked products (Maat *et al.*, 1992), in the clarification of fruit juices, when used in conjunction with pectinase and cellulase (Biely, 1985), and as food additives to poultry (Bedford and Classen, 1992). Xylanases are also found in assisting the extraction of coffee, plant oils and starch (Wong and Saddler, 1992). In the agricultural and animal feed industry xylanases are used to improve the nutritional properties of agricultural silage and grain feed (Kuhad and Singh, 1993). Xylanases can also be utilized in the degumming of plant fibre sources such as flax, hemp, jute and ramie (Kapoor *et al.*, 2001; Puchart *et al.*, 1999; Sharma, 1987).

Enzymatic usage, when compared with harsher traditional chemical methods, has many benefits. Increasing specificity in reactions, providing a process that is more environmentally friendly and saving energy which all leads to a decrease in costs (Covarrubias, 2006). In the pulp and paper industry the treatment of wood pulps with enzymes is labelled fibre modification. This involves treatment of the wood pulps with hydrolysing enzymes that work on the fibre cellulose which helps reduce mechanical treatment that is usually used to achieve the desired fibre properties. The use of enzymatic

fibre modification is one such process that has helped in improve upon traditionally chemical based processes.

The pulp and paper industry generates a high volume of toxic and highly persistent chlorinated organic by products by using chlorine as a chemical bleach agent for the pre-treatment of pulp. The environmental and legislative pressures have forced the pulp and paper industry to modify its pulping, bleaching and effluent treatment technologies to reduce the environmental impact of mill effluents (Bajpai *et al.,* 1994). The more environmentally friendly processes, biobleaching and bioprocessing of pulps, is one way the pulp and paper industry is attempting to use biological means to minimise waste production (Beg *et al.,* 2001). Paice *et al.* (1992) states that xylanases are being used primarily to remove the lignincarbohydrate complexes (LCC) that are created during Kraft pulp processes. These LCC act as physical barriers that decrease the permeability of bleaching chemicals on the pulp. Xylanases acting as bleaching boosters is still a recent application of biotechnology to the pulp and paper industry. The enzymatic removal of xylan from the fibre surface allows for increased success for chemical bleaching of lignin-derived material. One such commercially available xylanase is Pulpzyme HC that is produced by submerged fermentation of a selected strain of *Bacillus.* It catalyses the hydrolysis of deacetyled xylan substrates and contains endo-1,4-β-D-xylanase activity. The enzyme is stable at recommended working conditions at pH 6.5 - 9.5 and temperature 40 °C – 65 °C (Roncero *et al.,* 2000).

1.4. Classification of xylanases

Endoxylanases (EX) have been classified into families 5, 8, 10, 11 and 43 of glycosyl hydrolases, based on hydrophobic cluster analysis and similarities in their amino acid sequences (Coutinho and Henrissat, 1999). Henrissat and Bairoch (1993) suggest that from

sequence alignments, xylanases have evolutionary links from two ancestral proteins and can therefore be grouped into two large families, *viz*., F and G which are analogous to family 10 and 11 of glycosyl. Members of the two largest and best known families are the family F/10 and family G/11 xylanases (Jeffries, 1996). Withers (2001) has shown to link a common feature of both families of enzymes as their endo-acting characters. It is demonstrated that viscometrically and the double displacement mechanism of the hydrolysis of the glycosidic bond, means that both types of enzymes are retaining glycanases.

Harris *et al.* (1994) stated members of family 10 typically have a high molecular mass, acidic pI and display an $(\alpha/\beta)_8$ barrel fold structure. This structure has one face of the molecule having a large radius with the catalytic site near the narrower end, closest to the carboxyl terminus of the β-barrel. The glycoside family 11 is monospecific as it consists solely of 'true xylanases' that are exclusively on D-xylose containing substrates. They have a low molecular mass and a β-jelly roll fold structure. Their structure consists of β-pleated sheets formed into a two layered trough that surrounds the catalytic site. This structure has been likened to a palm and fingers of a right hand (Fig 1.2) (Torronen and Rouvinen, 1997). The xylanases from *R. marinus* and *B. halodurans* are family 10 while the xylanase from *T. lanuginosus* and Pulpzyme HC were included in family 11.

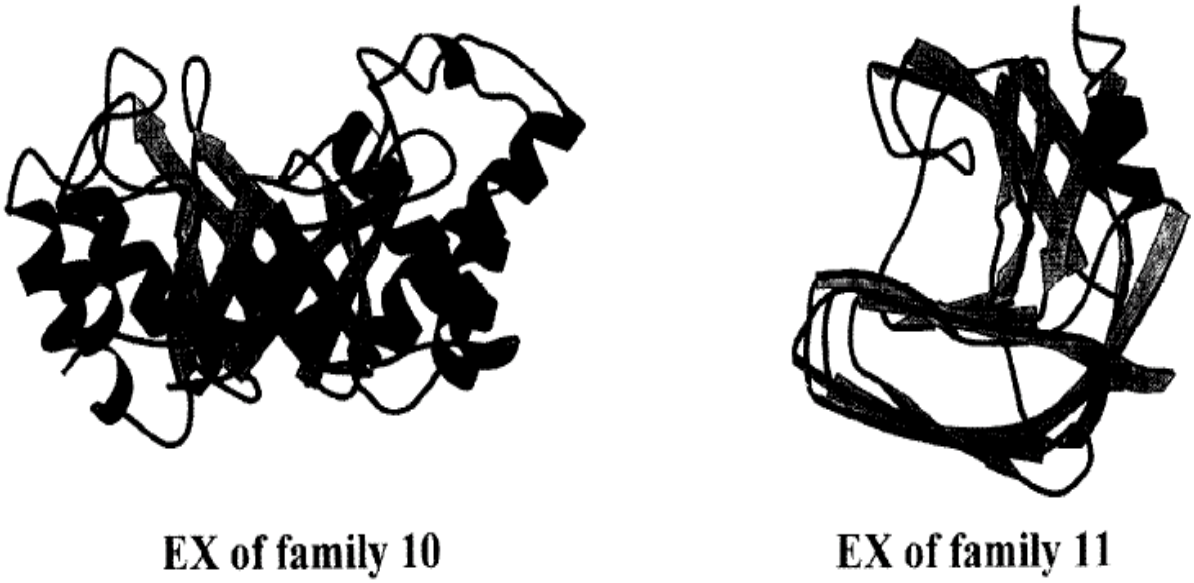

Fig. 1.2: Ribbon representations of the main fold of the catalytic domains of the endoxylanases (EX) of family 10 and 11 (Davies and Henrissat, 1995).

1.5 Structure of xylan

Lignocellulose is the most abundant and renewable biomass available on earth. It comprises three major groups of polymers, cellulose (a linear homopolymer of β-1,4 linked glucose units), hemicellulose (noncellulosic polymers including glucans, mannans, arabinans, galactans and xylans) and lignin (a complex polyphenol) (Kuhad and Singh, 1993). In plant cells, xylan is one of the three major structural polysaccharides and is localized in the cell wall matrix (Fig. 1.3). The relative distribution of lignocellulosic components in the cell walls is dependent on the plant species and on the stage of growth and development. Xylan, the second most abundant polysaccharide in nature, is the major component of hemicelluloses. It is a heterogeneous polysaccharide consisting of β-1,4-linked deoxy residues on the backbone but also contains arabinoses, glucuronic acids and arabinoglucuronic acids linked to the D-xylose backbone (Wong *et al.,* 1988). The xylopyranosyl backbone is substituted at positions C-2, C-3 and C-5 to varying degrees depending upon the plant and the stage of development of the plant when the polymer was obtained (Joseleau *et al*., 1992).

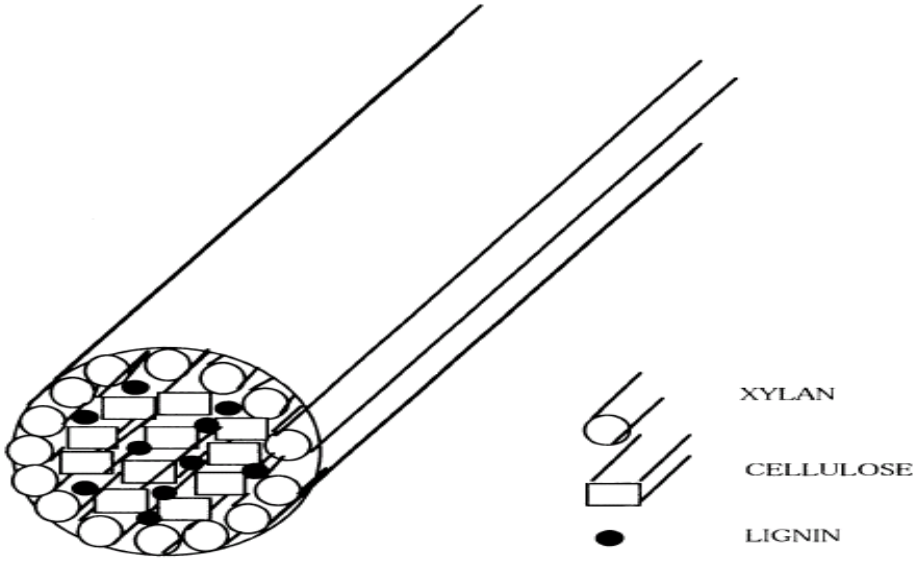

Fig. 1.3: A representation of a typical wood fibre and it's make up of xylan, cellulose and lignin. (Techapun *et al.,* 2003).

1.6. Xylan hydrolysis

Due to the heterogeneity nature of xylan, the enzymatic hydrolysis of xylan requires different activities. Two enzymes, β-1,4-endo-xylanase (EC 3.2.1.8) and β-xylosidase (EC 3.2.1.37), are responsible for hydrolysis of the main chain. The first group attacks the internal main-chain xylosidic linkages and the second releases xylosyl residues by endwise attack of xylooligosaccharides. Both of these enzymes are the major components of xylanolytic systems produced by biodegradative microorganisms such as *Trichoderma, Aspergillus, Schizophyllum, Bacillus, Clostridium and Streptomyces species* (Dekker, 1985). Due to its inherent heterogeneity it requires synergistic activities of different enzymes to achieve complete hydrolysis (Fig. 1.4).

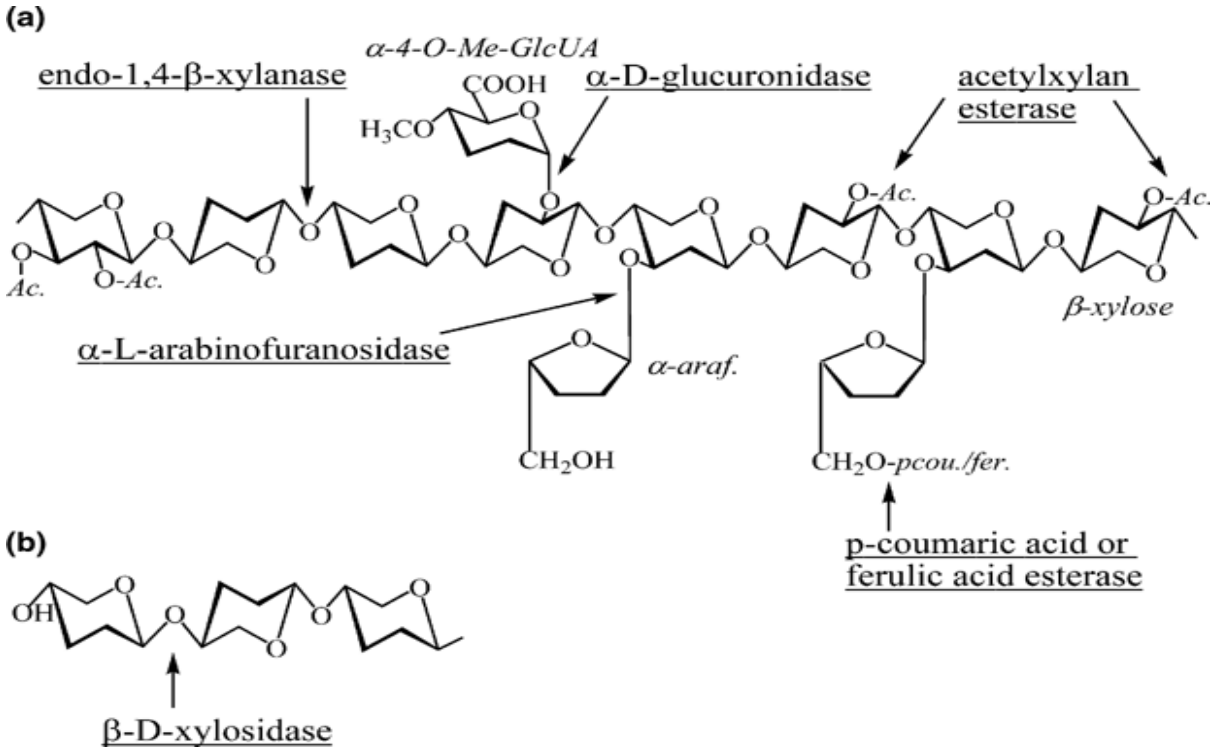

Fig. 1.4: a) Structure of xylan and the sites of its attack by xylanolytic enzymes. The backbone of the substrate is composed of 1,4- β-linked xylose residues. Ac., Acetyl group; α-araf., α-arabinofuranose; α-4-*O*-Me-GlcUA, α-4-*O*-methylglucuronic acid; pcou., *p*-coumaric acid; fer., ferulic acid. (Collins *et al.,* 2005). (b) Hydrolysis of xylo-oligosaccharide by β-xylosidase (Collins *et al.,* 2005).

Enzymatic cleavage of the glycosidic bond may follow two different mechanisms resulting either in overall retention or inversion of the anomeric configuration (McCarter and Withers, 1994). Different sites of attack by microbial xylanases can also occur on plant xylan structures (Fig. 1.5). In both cases, the reaction proceeds by general acid catalysis requiring a proton donor and a nucleophile. The first step in the reaction sequence consists of a protonation of the glycosidic oxygen. In the case of the inverting mechanism, a water molecule (activated by the nucleophile) attacks the anomeric carbon atom from the anterior, leading to inversion of the absolute configuration. The retaining mechanism, on the other hand, involves two consecutive inverting nucleophilic attacks. The first by the nucleophile and subsequently by a water molecule, resulting in overall retention of the anomeric

configuration. It is still an unclear as to whether the nucleophile forms a covalent bond to the anomeric carbon or if its negative charge only stabilizes the positive charge of the reaction

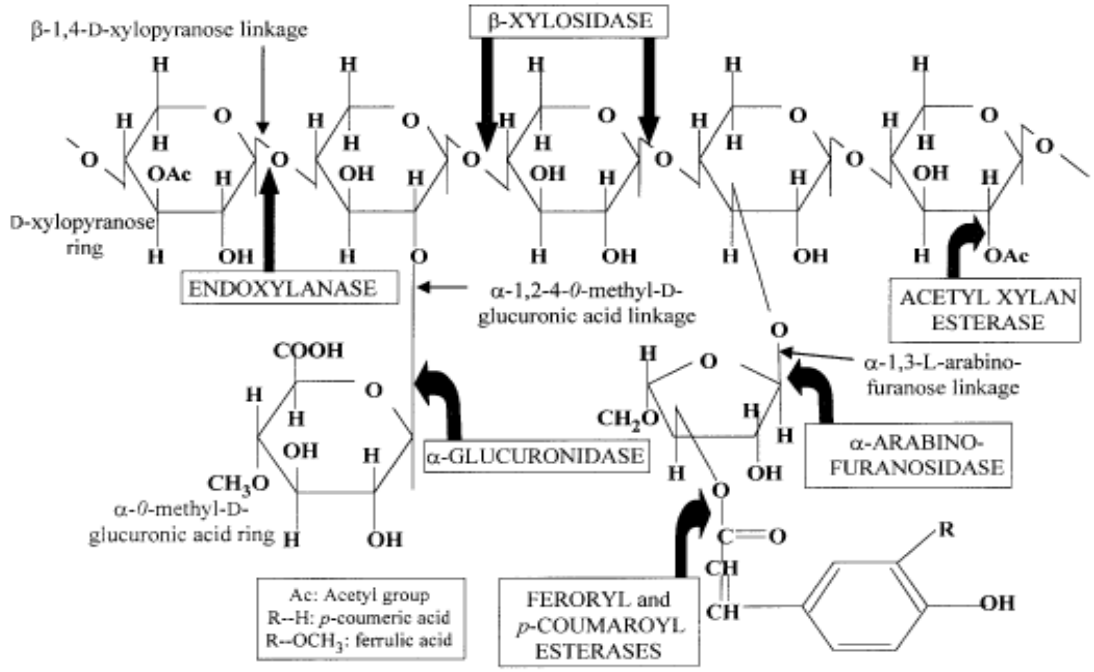

Fig. 1.5: Hypothetical plant xylan structure showing different substituent groups with sites of attack by microbial xylanases (Beg *et al.*, 2001).

intermediate (Sinnot, 1990) (Fig 1.6). At least three different types of active-site topologies are known to exist in glycosyl hydrolases (Davies and Henrissat, 1995). Pockets are optimal for monosaccharidases, and enzymes adapted to substrates with a large number of available chain ends. A tunnel was observed in cellobiohydrolases (Rouvinen *et al.*, 1990). This topology requires the polysaccharide chain to be threaded through, which is optimal for fibrous substrates such as native cellulose. The tunnel appears to be a special case of the third topology, the cleft or groove. Clefts allow the binding of several consecutive sugar units in linear or branched polymeric substrates, and they are commonly observed in endo-acting polysaccharidases (Gruber *et al.*, 1998).

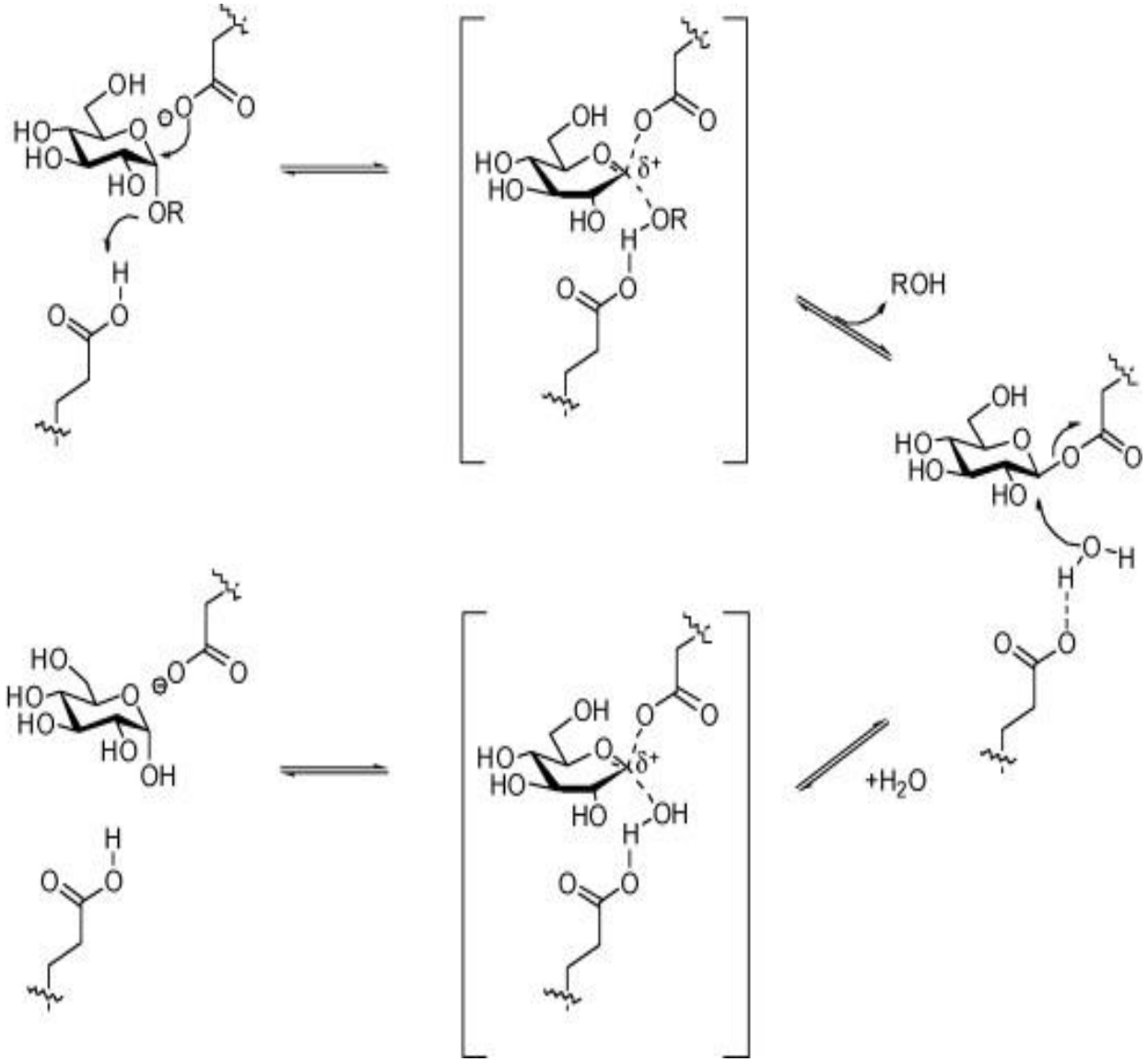

Fig. 1.6: Simplified scheme of the mechanism with nucleophilic attack of the glycosidic bond by the nucleophile, Glu or Asp, respectively, followed by the formation of an intermediate with a covalently bound glycosyl residue and its release by nucleophilic displacement by a water molecule).

1.7. Thermophilic xylanases

Previous xylanase applications were performed at pH 5 and 6, using a low concentration of enzyme. Producers of enzymes have made great strides in improving the properties of enzymes that are able to operate in the neutral pH range. Producers will continue to tailor the enzymes to conditions of industry such as mills in the paper and pulp industry that work at alkaline pH, high temperature and shorter retention times (Roncero *et al*., 2000). Interest in enzymes for industry has continued to grow with respect to their application in clarification of juices and wines, conversion of renewable biomass into liquid fuels and in development of environmentally sound pre-bleaching processes in the paper and pulp industry (Kulkarni *et al.*, 1999). Extensive studies with respect to industrial applications of xylanases exist but the far less information is available on molecular enzymology and clinical implications (Tarvainen *et al.*, 1991).

Properties of thermophilic xylanases in reviews have described characterization of xylanases from microbial systems (Kulkarni *et al.*, 1999; Sunna & Antranikian, 1997; Warren, 1996). Xylanases from *Thermoanaerobacterium* sp. (Shao *et al.*, 1995) and *Thermotoga thermarum* (Sunna *et al.*, 1996) showed higher molecular weights of 350 kDa and 266 kDa respectively. Few bacterial and fungal xylanases show maximal activities at temperatures between 60 °C – 80 °C (Khasin *et al.*, 1993; McCarthy *et al.*, 1985). The purified endoxylanases from various species belonging to the genus *Thermotoga* are optimally active at temperatures between 80 °C and 105 °C (Simpson *et al.*, 1991; Sunna *et al.*, 1996; Winterhalter & Liebl, 1995). Xylanases from *Dictyoglomus* sp. exhibited a half-life of 80 min at 90 °C (Mathrani & Ahring, 1991). *Clostridium stercorarium* xylanase exhibited a temperature optimum of 70 °C and a half-life of 90 min at 80 °C. The

thermophilic fungi include *Thermoascus aurantiacus* (Khandke *et al.,* 1989), which produces a thermostable xylanase reported to be stable at 70 °C for 24 h, *Paecilomyces variota* (Krishnamurthy *et al.,* 1989) and *Talaromyces byssochlamydoides* (Yoshioka *et al.,* 1981) with temperature optimum of 65 °C – 75 °C at pH 5 - 6.5. The xylanases that were used in this study also exhibited thermophilic properties and have adapted to their environment in novel ways (Table 1.2).

Table 1.2. Thermophilic xylanases of interest in this study, their optimum pH and temperature as well as their location of isolation.

Organism / Xylanase	Optimum temperature (°C)	Optimum pH	Source	Reference
R. marinus	90	6 - 7	Intertidal hot spring in Isafjardardjup, northwestern Iceland	Bjornsdottir *et al.,* 2011
B. halodurans	70	9 - 10	Soda Lake Ethiopian Rift Valley	Gashaw, 2006
T. lanuginosus	50 -70	6 - 7	Self-heating masses of organic debris	Singh, 2003
Pulpzyme HC	60	7	*Bacillus sp*	Csiszar *et al.* 2001

1.8. Fluorescence spectroscopic analyses

The relationship that exists between the structure and function of biological macromolecules including enzymes is an important issue that warrants study. An enzymes

ability to retain its conformational integrity, especially when subjected to different temperatures or pH, has a direct bearing on its stability and catalytic activity. Using the inherent fluorescent properties of Trp and Tyr residues present in enzymes, the loss of catalytic activity due to changing conditions can be studied (George, 2001).

Fluorescence is based upon a three stage process that occurs in certain molecules called fluorophores or fluorescent dyes. A fluorescent probe is a fluorophore that has been designed to link with a specific region of a specimen or that is set to react to a specific stimulus. The mechanics of the florescence of probes and other fluorophores is illustrated in the Jabolonski diagram (Fig. 1.7.)

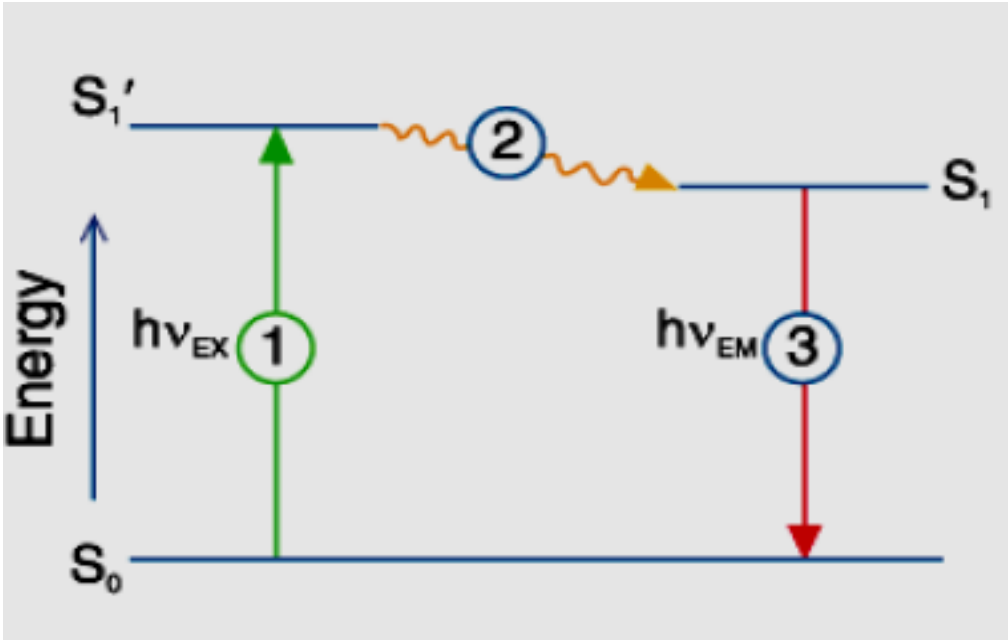

Fig. 1.7: Jablonski Diagram of a fluorescence event. The fluorescent molecule begins in its ground energy state, S_0, and is converted to an excited singlet state, S_1, by absorbing energy in a specific wavelength. The molecule will transition to the relaxed singlet state, S_1, by releasing some of the absorbed energy. Finally, the molecule will return to its ground energy state by releasing the remaining energy (Behlke *et al.*, 2005).

Most fluorophores are able to be repeatedly excited and detected unless they are irreversibly destroyed in the excited state. This is an important factor known as photobleaching. As the fluorescence is cyclical the ability of a single fluorophore to generate thousands of detectable photos is instrumental in the high sensitivity attributed to fluorescence detection techniques. Hv_{ex}, described as a photon of given energy (1), the molecule will transition to the relaxed singlet state by releasing some of the absorbed energy (2) and Hv_{em}, which is the emission energy of a fluorophore (3). Hv_{ex} and Hv_{em} are unsuitable for larger more complex molecules in solution (Fig. 1.7). As they are replaced by broad energy spectra called the fluorescence excitation spectrum and fluorescence emission spectrum respectively. The energy spectra of fluorescence excitation and emission are important when considered for applications involving the simultaneous detection of two or more different fluorophores. The fluorescence excitation spectrum of a single fluorophore in a dilute solution is usually identical to its absorption spectrum with very few exceptions. Under similar conditions, however, the emission spectrum is found to be independent of the excitation spectrum wavelength as a result of partial loss of the energy of excitation during the excited state lifetime (Behlke *et al.*, 2005).

Folding of proteins into its functional state occurs in several steps. From the native structure the formation of the secondary structure (2D) which is then followed by the tertiary structure (3D) arrangement. Often the protein will fold further to obtain a quaternary structure (4D) organisation. This is most often for oligomeric complex proteins. The reaction where proteins adopt their native 3D structure is termed protein folding (Fig. 1.8).

Phenylalanine (Phe), Tryptophan (Trp) and Tyrosine (Tyr) are three amino acids that possess intrinsic fluorescent properties. For experimental use, only Trp and Tyr are used due

to their excited and emission photons being of a high enough level to produce an adequate fluorescence signal. Though these residues are used to track protein folding and unfolding, such experiments are limited to proteins containing either Trp or Tyr residues. These amino acid residues are instrumental in following the folding and unfolding of proteins not only due to their high fluorescence signal but that they are sensitive to their environments as the protein folds and unfolds. When the protein is in its native folded state Trp and Tyr are usually found within the core of the protein. As the protein becomes partially folded or begins to unfold more completely the Trp and Tyr residues become exposed to the solvent.

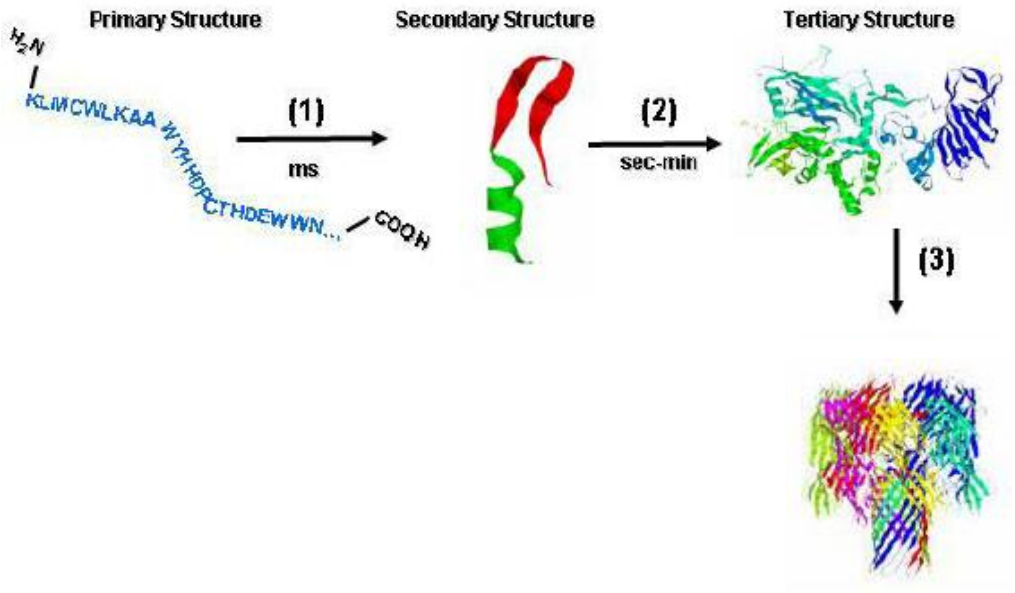

Fig. 1.8: Figure showing the process from primary structure to quaternary structure of proteins. After being synthesized, protein folds to acquire its functional 3-D shape. This reaction starts by secondary structure formation (1) and ends by formation of the tertiary structure (2) which is how the protein is organized in space. In some cases, the protein needs to assemble with either other protein chains or identical proteins to form a complex (3). This is the quaternary structure (4D) (www.physics.nus.edu.sg/~Biophysics/pc3267/Fluorescence %20Spectroscopy2007.pdf).

Within the protein core a hydrophobic environment exists where Trp and Tyr residues exhibit a high quantum yield and therefore release high fluorescence intensity. When Trp and Tyr

residues are exposed to a hydrophilic environment their quantum yields decrease releasing low fluorescence intensity. For Trp residues especially, there is a strong stoke shifts that is solvent dependant. Therefore the maximum emission wavelength will change depending on the environment of the residue. Protein unfolding can be achieved by disturbing the weak interactions that assist in the folding of proteins such as hydrophobic interactions and hydrogen bonding. Protein unfolding can be accomplished in many ways the most common of which are using chemical denaturants such as urea or guanidium hydrochloride, changing pH and the increase of temperature. It is possible to study either steady state or kinetics of protein unfolding. For example, the protein is unfolded by increasing temperature, so at each temperature the protein undergoes unfolding and reaches an equilibrium state which corresponds to a partially folded or fully unfolded state depending on the conditions. For each temperature, the fluorescence emission of Trp or Tyr is measured and compared to that of the native protein (Fig. 1.8).

The fluorescence properties of tryptophan (Trp) residues are sensitive to the microenvironment of the fluorophore in the protein structure. For this reason, fluorescence characteristics are widely used to study physico-chemical and dynamic properties of the tryptophan microenvironment in proteins and the structural transitions and behaviour of protein molecules as a whole (Lakowicz *et al.*,1983; Demchenko *et al.*, 1986). The overwhelming majority of proteins exhibit smooth, non-structured spectra of Trp fluorescence, which often contain more than one component. This multicomponent nature of protein spectra makes the unequivocal interpretation difficult and poses a task of development of methods for the decomposition of tryptophan fluorescence spectra into elementary components (Burstein *et al.*, 1973; Burstein, 1977).

1.9. Differential scanning fluorometry (DSF)

An enzymes ability to maintain its activity at different temperatures is often as result of its inherent structure and conformation. Methods that allow for the identification of an enzymes ability to function at high temperatures can provide important information whilst decressing the time when compared with conventional assay methods. DSF is a technique that is able to screen high numbers of stabilizing conditions for proteins as it only requires low protein concentrations and amounts. DSF can therefore be beneficial in other experiments that focus on analytical and biophysical processes that would need high protein concentrations as well as those that are susceptible to aggregation. Buffers, different salts and other nonspecific detergents have the ability to greatly increase the stability of proteins and DSF is able to screen high numbers of such ingredients to ensure a more stable protein structure. Site specific binding of ligands is another factor that is able to influence the stability of protein and as such, the protein-ligand interaction can help in elucidating information concerning function studies such as allosteric effectors and substrate specificity (Niesen *et al.*, 2007).

Currently, the dye with the most favourable properties for DSF is SYPRO orange, owing to its high signal-to-noise ratio. For example, with hen egg lysozyme, the increase in the fluorescence intensity of the dye bound to denatured protein compared to aqueous solution is almost 500% (Fig. 1.9 A.). The relatively high wavelength for excitation for SYPRO orange, near 500 nm (Fig. 1.9 B.), also decreases the likelihood that any small molecule would interfere with the optical properties of the dye and cause, for example, quenching of the fluorescence intensity. However, not all proteins can be analyzed using SYPRO orange.

Other dyes should be tested for cases where no unfolding transition is observed using SYPRO orange.

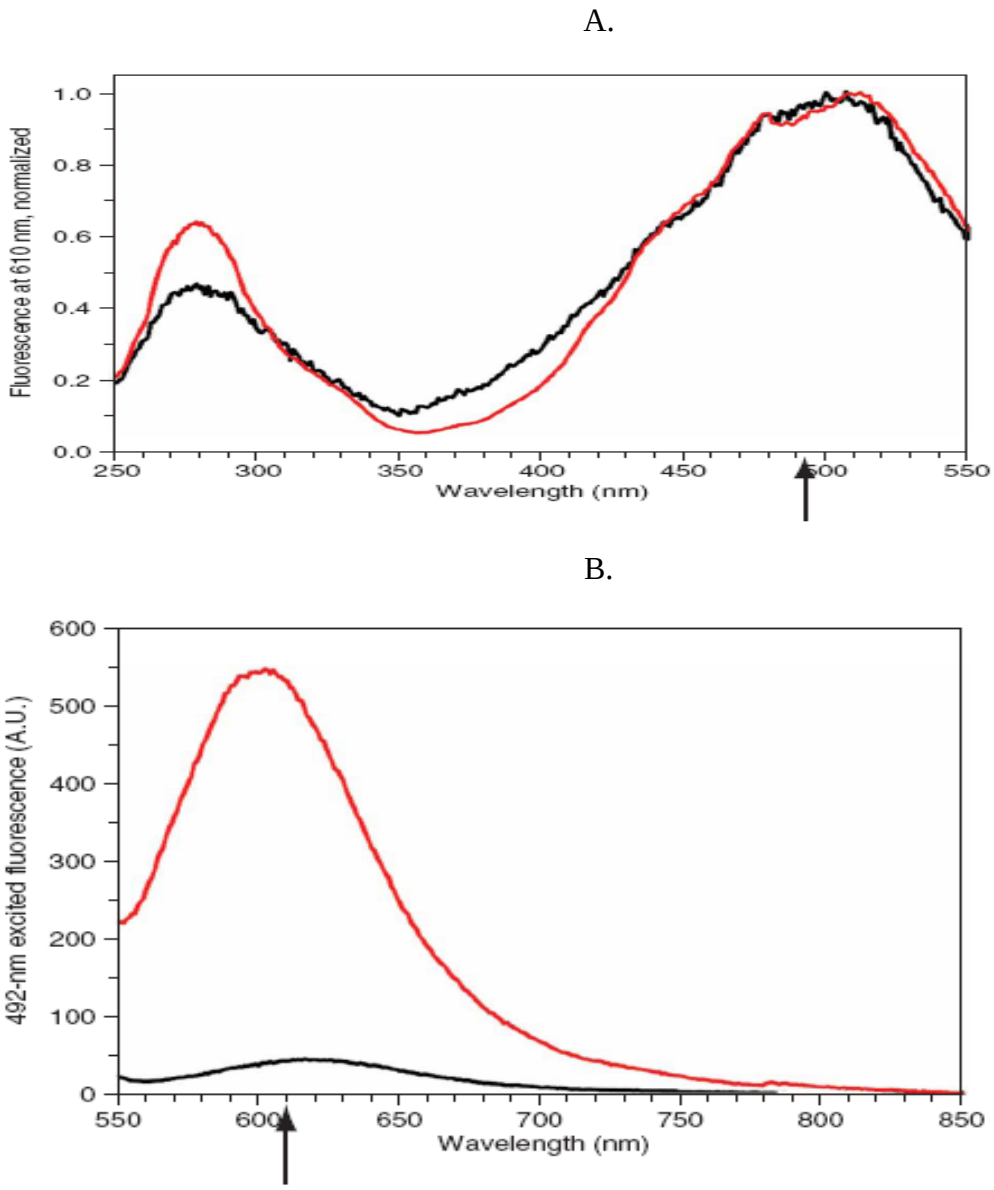

Fig 1.9: Optimum excitation of SYPRO orange in protein buffer and gain in fluorescence upon protein unfolding. Excitation/emission spectra of dye diluted 1:1,000 in a solution of 75 mg ml/1 hen egg lysozyme in buffer (10 mM 3-(cyclohexylamino)-1-propanesulfonic acid pH 9.0, 150 mM NaCl), before (black traces) and immediately after incubation for 5 min at 100 °C (red traces), are shown. Arrows depict position of the custom filters used in the Stratagene Mx3005p PCR instrument. (a) Normalized excitation spectra, recorded at a wavelength of 610 nm. (b) Non-normalized emission spectra upon excitation at 492 nm (Niesen *et al.*, 2007).

1.10. Circular Dichroism (CD)

All proteins are made up of a unique three-dimensional structure that is stabilized by multiple weak interactions, which include hydrophobic interactions, hydrogen bonds, and ionic interactions which in turn determine is function (Nelson and Cox, 2000; Rawn, 1989). Nelson and Cox (2000) describe treatments that disrupt such interactions and severely impact or destroy the three-dimensional structure of proteins with a subsequent loss of protein function. This demonstrates the relationship between the native protein structure and conformation and its function and activity.

CD measures unequal absorption of right- and left-handed circularly polarized light by the molecule. Although all amino acids except glycine contain at least one asymmetric carbon atom either in the L or D configuration, most amino acids display only small CD signals. The protein main chain assumes several principal conformations in aqueous solution: α-helix, extended β-structure (or β-sheet), turn, and so-called "random coil," which are non-regular structures (Fig. 1.10). The α-helix and β-sheet conformations are characterized by optimal hydrogen bonding between peptide groups in the polypeptide backbone and give rise to strong CD signals (Toniolo, 1970; Adler *et. al.*, 1973).

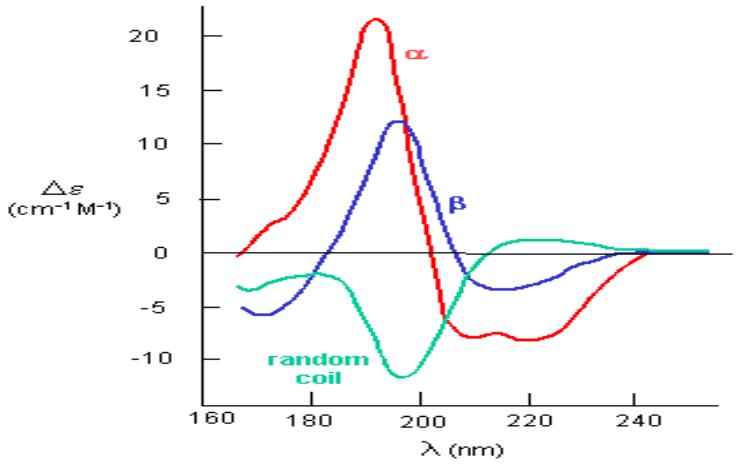

Fig 1.10: Graphical representation and comparison of α-helix, β-sheet and random coil as evaluated by circular dichroism.

1.11. Rationale of study

There are many uses for xylanases in industry at present. Animal feed, baking, surfactants, wines and biobleaching are just a few. The information on structure and function and their correlating relationship is still in need of further research. To ensure the varied needs of industry are met such studies have to continue to fill in the gap between what is presently available and what is needed. In a more focused field, enzymatic biobleaching has the potential to lighten the load of heavy and damaging chemical processes that are currently still being used. Global warming and the detrimental effects and burdens of humanity are highlighting 'greener' technologies more than ever before. To meet such demands and even surpass the requirements of industry to ensure such a paradigm shift occurs, further research is definitely necessary. Industries need xylanases that are both afordable to use and ensure productivity is not adversely affected. Xylanases that are, preferably, optimally active at high temperatures and varying pH values are necessary to suit different processes that demand different conditions. Further research into the relationship between structure and function of extremozymes such as xylanases from *Rhodothermus marinus,* (that are optimally active at 90ºC) and *Bacillus halodurans,* (active over a wide range of pH values as well as being an alkalophile and active at pH 8, 9 and 10) could yield interesting and important results. It could help uncover how the structure of the xylanases enables them to, not only be active, but flourish under such harsh conditions. Novel techniques, such as differential scanning fluorometry (DSF), circular dichroism (CD) and fluorometric analyses, help uncover important structural information of such xylanases. DSF can be used to quickly and efficiently assess the enzymatic stability in a vast amount of buffers, salt and glycerol conditions to achieve the most stable conditions. Fluorescence spectroscopy attempts to correlate Trp residue fluorescence with changes in temperature and the effect of GdnHCl on enzyme denaturation. CD elucidates the fraction of folded protein and the Gibbs free energy

from temperatures from 20 °C to 95 °C. Each technique offered unique insights into the structure-function relationships of xylanases that exhibit desirable qualities such as extreme thermostability and alkalophilic characteristics. Further engineering of other enzymes with the information gathered improves the chances of the creating enzymes that are tailor made for industrial processes.

The enzyme technology group at DUT have been involved in the biochemical characterisation of crude, purified and recombinant enzymes generated by directed evolution. It was thus appropriate that a more structural analytical approach be applied to accurately determine the structure – function relationship between enzymes. Therefore xylanases showing desirable traits such as *R. marinus* and *B. halodurans* were studied as well as commercially available *T. lanuginosus* and Pulpzyme HC to, not only further the structure - function relationship, but investigate this relationship in advantageous xylanases.

CHAPTER 2: BIOCHEMICAL CHARACTERISATION AND FLUORESCENCE SPECTROSCOPY OF XYLANASES

2.1 INTRODUCTION

Thermostable enzymes are defined by their ability to remain active above the maximum growth temperatures of the organism as well as those with increased stability above 50 °C over an extended time period (Gupta and Gupta, 1993). Enzymes with such stability and activity are often used in industrial applications. This leads to a need for characterisation of organisms and their enzymes in an attempt to find enzymes with suitable properties that will allow for their application in industry. As such xylanases that are produced and isolated from thermophilic fungi are usually found to have higher thermostability than those of mesophilic fungi (Steiner *et al.*, 1987). Dahlberg *et al.* (1993) further states that xylanases that have been produced by thermophilic eubacteria and archaebacteria have a longer half life at 80 °C and above than when compared with other thermophilic fungi. Strains of *T. lanuginosus* have shown high thermostability but have also found to be active over a wide range of pH values (Anand *et al.*, 1990). The xylanase isolated from *R. marinus* showed an optimum activity at 90 °C (Bjornsdottir *et al.*, 2011) and *B. halodurans* produces at xylanase that is not only active at 70 °C but is also highly alkophilic having stability from pH 7 to 10 (Gashaw, 2006). Biochemical characterisation is integral and often the first step in the understanding of enzyme properties both for further study as well as for industrial purposes.

In an attempt to understand the catalytic mechanism of an enzyme, it is essential to study the structural elements and the three-dimensional conformation of the active site.

Chemical modification of reactive amino acid side chains in the active site helps to identify residues that are important for catalysis (George, 2001).

Fluorescence spectroscopy has been widely used to study the conformation of xylanases. A red-shift of the emission wavelength can be caused by different solvent molecules that surround the fluorophore (Spampinato *et al.,* 2007) and blue-shift when the fluorescence intensity decreases (Vivian and Callis, 2001). Raja *et al.* (1999) explains red shifting as an emission maximum that is at a longer wavelength and lower energy then than that of the excitation and the energy difference between maximum excitation and emission is known as the Stokes Shift. All charged amino acid residues can significantly influence red-shifting but the residues Lys, Arg, Glu and N- or C terminal residues have the greatest effect on fluorescence shifts. Protein and water both effect the shift but their ratio of contribution is often hard to anticipate. Such charged groups that are located close to the Trp residues often dominate shift mechanisms and water often causes a blue shift in fluorescence (Vivian and Callis, 2001).

Nath *et al.* (2001) studied the structure and function analyses of xylanases from alkalophilic thermophilic *Bacillus* sp. and it has been shown how pH induces conformational and structural changes of xylanase using fluorescence spectroscopy. Tryptophan fluorescence quenching was found to be dependent on pH and exhibited unfolding above pH 8 as revealed by a red shift in the emission maximum of the enzyme as well as decreases in the fluorescence intensity. George *et al.* (2001) used fluorometry in an attempt to identify the residues involved in the active site of xylanase by subjecting them to modification with different group specific reagents such as *o*-phthalaldehyde (OPTA). OPTA reacts with lysine and histidine residues present in the active sites of the enzyme to form a fluorescent isoindole

derivative inactivating the xylanase. The formation of isoindole derivatives leads to an increase in fluorescence intensity at 415 nm confirming the formation of an isoindole derivative.

The present chapter describes the study of different temperatures and varying pH and its effects on the four separate xylanases. Temperature and pH optima are important in ensuring maximum xylanase activity and in selecting process applicable enzymes for industrial processes. Fluorescence spectroscopic analyses attempts to correlate the effects of temperature and chemical denaturation with GdnHCl on the structure of the xylanase.

2.2. MATERIALS AND METHODS

2.2.1. Materials

Crude xylanases from *Rhodothermus marinus* and *Bacillus halodurans* were obtained from the Department of Biotechnology, Lund University, Sweden. Commercial xylanases *Thermomyces lanuginosus* DSM 5826 and Pulpzyme HC were purchased from Sigma-Aldrich and Novozyme respectively. The xylanase from T. *lanuginosus* was expressed in *Aspergillus niger* and stabilized by the addition of wheatflower supplied by Sigma-Aldrich (Catalogue). All the xylanases were partially purified by gel filtration (Sephadex G75) before evaluation. DNS (dinitrosalicylic acid) and BSA (bovine serum albumin). Birchwood xylan were procured from Roth chemicals, Germany.

Fluorescence measurements were performed using quartz cuvettes on a Cary Eclipse Fluorescence Varian spectrophotometer. A single cell peltier was connected to the spectrophotometer which precisely controlled the temperature in the cuvette. Guanidine hydrochloride used for chemical denaturation was obtained from Sigma-Aldrich. All other chemicals were of analytical grade.

2.2.2. β-Xylanase assay

Endo-1,4-β-D-xylanase activity was assayed according to Bailey *et al.* (1992) by incubating the diluted enzyme solution at pH 7 and a temperature of 50 °C for 30 min by using a substrate solution of 1.0% (w/v) birchwood xylan. Reducing sugars were assayed by adding 3 ml of DNS reagent, boiling for 5 min, cooling, and measuring the absorbance at 540 nm. One unit of xylanase activity is defined as the release of one nmol of product per second.

2.2.3. Determination of pH and temperature optima of xylanases

The pH optima for β-xylanase activities were determined by measuring the enzyme activities at 50 °C in 50 mM sodium acetate (pH 4, 5), sodium phosphate (pH 6, 7), TrisCl (pH 8, 9) and bicarbonate buffer (pH 10). The optimum temperature for activity was determined by incubation of the activity assay at the pre-determined pH for *R. marinus* (pH 6), *B. halodurans* (pH 9), *T. lanuginosus* (pH 7) and Pulpzyme HC (pH 7) over a temperature range of 50°C to 90°C (10°C increments). Samples were evaluated for xylanase activity over 30 minutes as described in section 2.2.2.

2.2.4. Comparison of birchwood xylan hydrolysis by xylanase

A comparison of birchwood xylan hydrolysis was evaluated by applying 10 units/ml of each xylanase from *R. marinus, B. halodurans, T. lanuginosus* and Pulpzyme HC at their pre-determined pH optima and over a temperature range of 50 °C to 90 °C (10 °C increments) for 30 minutes. Samples were then evaluated for xylanase activity as described as in section 2.2.2.

2.2.5. Fluorescence spectra emissions at different temperatures

Emission spectra were captured for each xylanase (1 mg/ml) in a 3 ml reaction volume for *R. marinus* (pH 6), *B. halodurans* (pH 9), *T. lanuginosus* (pH 7) and Pulpzyme HC (pH 7). A Cary Eclipse Fluorescence Varian spectrophotometer with a single cell peltier connected, was used to accurately control the temperature in the cuvette for each reaction. The reaction mixtures were incubated for 10 min over a temperature range of 50 ºC to 90 ºC (10 °C increments). Fluorescence was excited at a wavelength of 295 nm and the emission was recorded from 300 nm to 500 nm. The slit widths on both excitation and emission were

set at 5nm and the spectra were obtained at 1 nm/min. Fluorescence data were corrected by running control samples of buffers and smoothed as described by Dash *et al.* (2002).

2.2.6. Fluorescence spectra emission at different GdnHCl concentrations

Emission spectra were captured for each of the xylanases as described as in section 2.2.5 with increasing guanidine hydrochloride (GdnHCl) concentrations of 0.5 M, 1.0 M, 2.0 M and 3 M, respectively, evaluated at each temperature (50 °C to 90 °C in 10 °C increments).

2.3. RESULTS AND DISCUSSION

2.3.1. Optimum temperature and pH for xylanases

The optimum conditions for hydrolysis of xylan by the xylanase from *R. marinus* was found to be at 80 °C to 90 °C (Fig. 2.1A) at pH 6 (Fig. 2.2A). Activity dropped sharply at 100 °C. Optimum activity at pH 6 was 20 % and 30 % than at pH 5 and pH 7, respectively. Previous studies on *R. marinus* have showed it to produce a xylanase that is optimally active at 90 °C and pH 6 (Bjornsdottir *et al.*, 2011).

The *B. halodurans* xylanase at pH 9 exhibited 100 % relative activity at 70 °C. Enzyme activity dropped to 10 % at 80 °C after 30 min with the total loss of all activity at 90 °C. The xylanase exhibited 80 % activity at 60°C (Fig. 2.1B) and showed optimum activity at pH 9 when assayed at 70 ºC (Fig. 2.2B) and exhibited pH stability from 7 to 10 retaining relative activity values of between 90 % and 100 %. At pH 8 the relative activity dropped to 90 % which could be attributed to the xylanase exhibiting less activity at a slightly basic pH. Gashaw (2006) stated that, when assayed at pH 10, the optimum temperature of the xylanase from *B. halodurans* was found to be 70 °C. These results are significant due to the fact that industrial xylanases need to have specific qualities to ensure maximum effectiveness such as pH stability and thermostability.

The xylanase from *T. lanuginosus* showed maximum activity at 50 °C but still retained over 90 % relative activity at 60°C and 80 % relative activity at 70 °C at pH 7 (Fig. 2.1D). The xylanase exhibited an optimum pH of 7 and retained 50 % relative activity at pH 4 while exhibiting a relative activity of 35 % at pH 10 (Fig. 2.2D). Cesar and Mrsa (1996) previously

reported that the xylanase from *T. lanuginosus* was found to have an optimum pH of 7 and an optimum temperature of 60 °C to 70 °C.

Pulpzyme HC displayed maximum activity at 60°C (Fig. 2.1D) and pH 7 with 94 % retention of activity at pH 8 (Fig. 2.2D). Reduced enzyme activity (25 % and 65 % relative activity) was evident at 40 °C and 50 °C, respectively. Pulpzyme HC exhibited only 18 % and 68 % activity at pH 4 and pH 5, respectively, confirming its inability to function in the acidic pH range. A similar pattern was evident beyond pH 8. Previous studied have found that Pulpzyme HC is optimally active at pH 7 to 8 and a temperature of 60 °C to 70 °C (Bhardwaj *et al.* 1996).

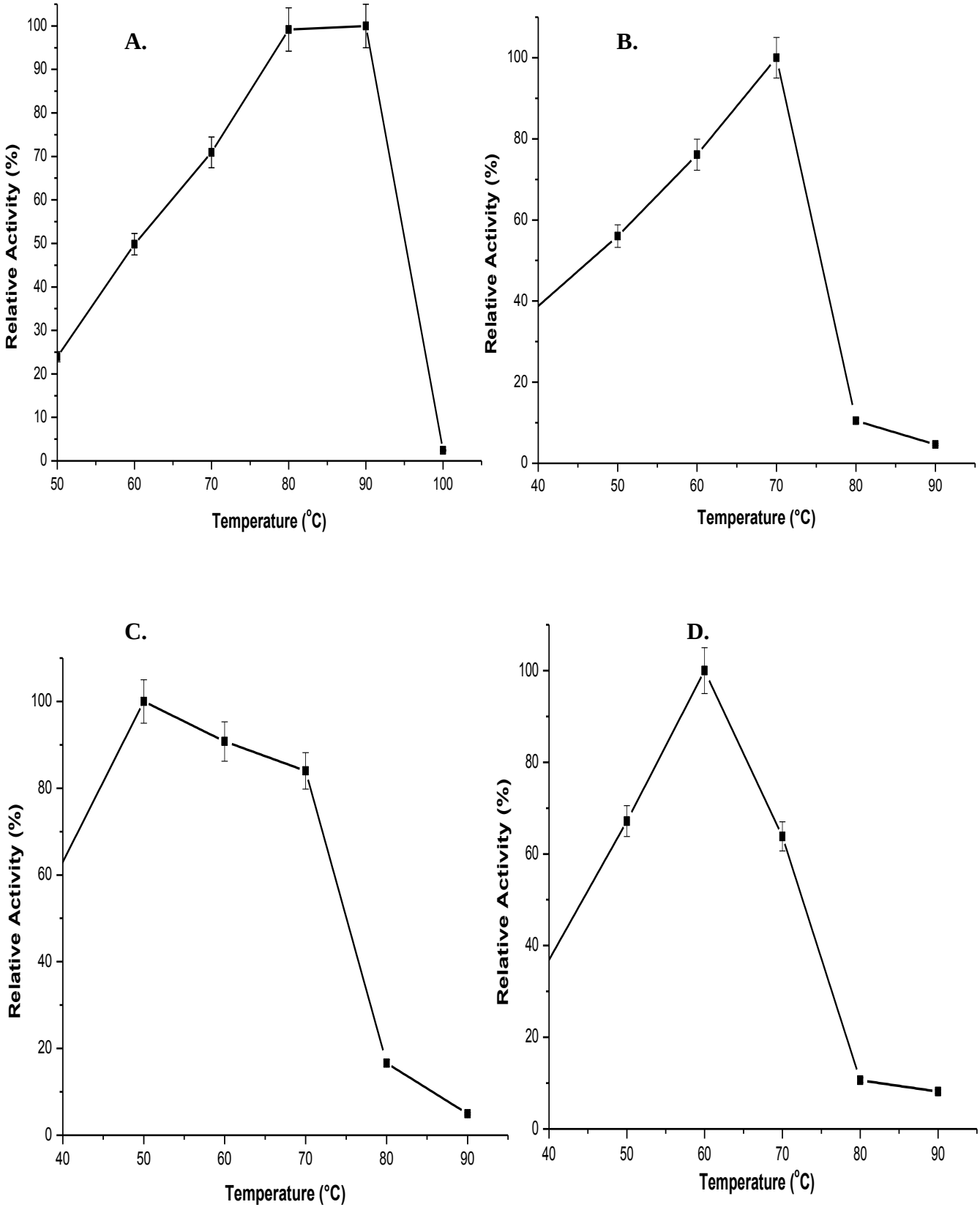

Fig. 2.1: Influence of incubation temperature over 30 min on the activity of β-xylanases from **A.** *R. marinus* (pH 6). **B.** *B. halodurans* (pH 9). **C.** *T. lanuginosus* (pH 7). **D.** Pulpzyme HC (pH 7). Each value is a mean of triplicate determinations with standard deviation (SD +/-).

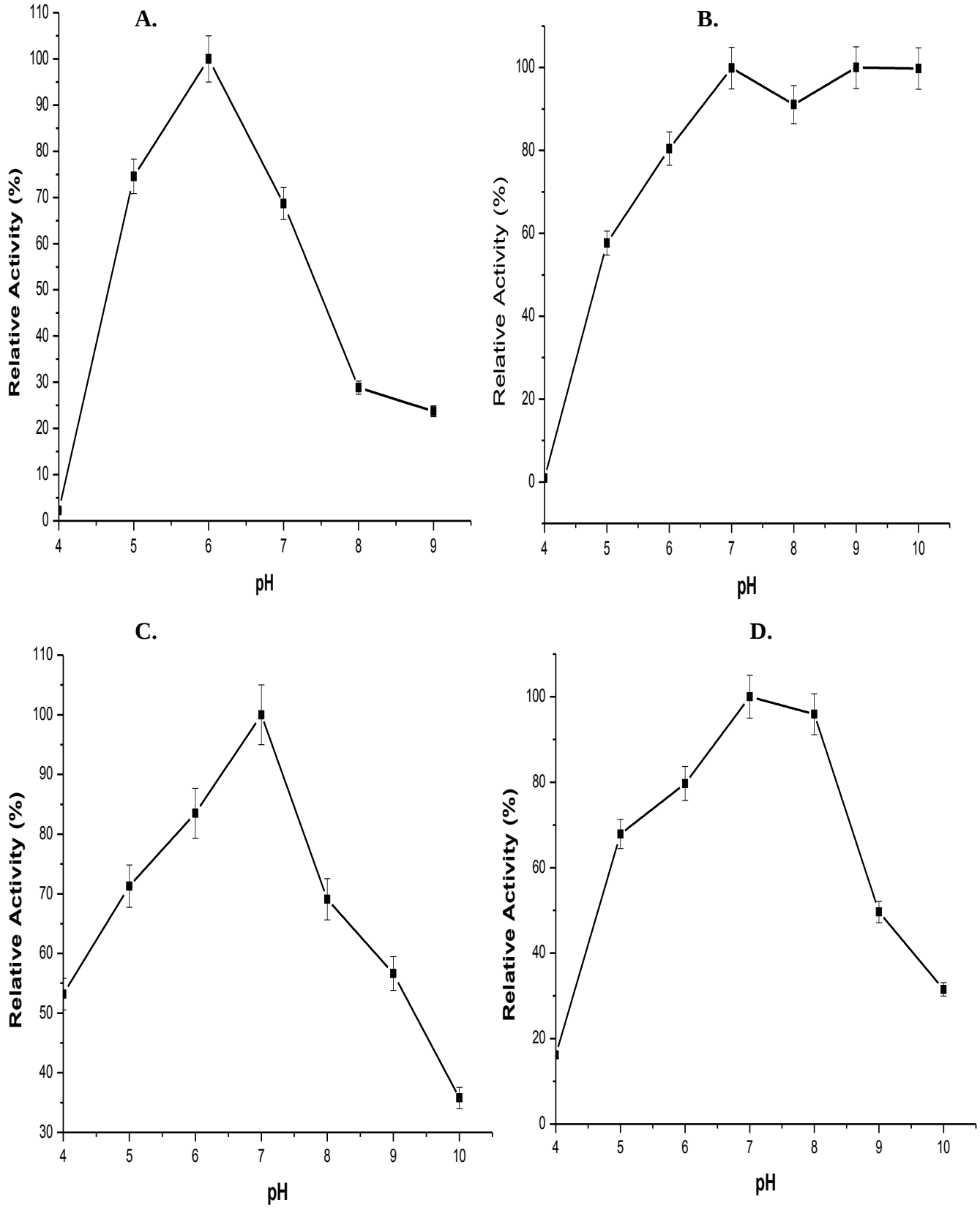

Fig. 2.2: Influence of incubation pH over 30 min on the activity of β-xylanases at optimum temperature. **A.** *R. marinus* (90 °C). **B.** *B. halodurans* (70 °C). **C.** *T. lanuginosus* (50 °C). **D.** Pulpzyme HC (50 °C). Each value is a mean of triplicate determinations with standard deviation (SD +/-).

2.3.2. Comparison of birchwood xylan hydrolysis by xylanases

The efficiency of birchwood xylan hydrolysis was compared using 10 units of the four xylanases. Percentage relative activity was calculated for each enzyme and measured against Pulpzyme HC which demonstrated the highest activity. All xylanases, other than the xylanase from *T. lanuginosus*, demonstrated optimum xylan hydrolysis at their respective temperature optima (Fig. 2.1). Pulpzyme HC when applied to birchwood xylan at 60 °C, its optimum temperature, displayed the greatest degree of hydrolysis in comparison to the remaining three xylanases tested at the same concentration. Furthermore this xylanase retained 92 % of its activity at 70 °C, however, rapid denaturation followed at higher temperatures. The xylanase from *R. marinus* showed a gradual increase in activity from 50 °C and displayed 86 % and 90 % relative activity at 80 °C and 90 °C, respectively. The *R. marinus* xylanase was shown to exhibit a maximum specific activity of 2670 nkat.mg^{-1} on oat spelts xylan with birchwood xylan and larchwood xylan showing almost two-fold less activity of 1320 nkat.mg^{-1} (Nordberg-Karlsson *et al.,* 1998). The xylanase from *R. marinus* confirmed its extremophilic properties with increasing activity at higher temperatures (80 °C and 90 °C), making it a desirable candidate for industrial application. The *T. lanuginosus* xylanase displayed similar activity for 50°C and 60 °C and only exhibited 76 % relative activity at 70 °C for 10 units. Yin *et al.* (2008) found optimum enzyme activity for *T. lanuginosus* on oat spelts xylan at 70 °C. The xylanase from *B. halodurans* displayed maximum activity at 70 °C with birchwood xylan as well as 95 % for beechwood xylan and 85 % for oat spelt xylan (Gashaw *et al.,* 2006). However, the *B. halodurans* xylanase demonstrated poor xylan hydrolysis at all temperatures from 50 °C to 90 °C when compared with the other three xylanases tested which indicated that although it displayed desirable alkalophilic properties and optimal activity at 70 °C its ability to hydrolyse xylan was inferior to the other three xylanases tested (Fig. 2.3). Substrate specificity experiments have been performed to ascertain optimum substrate

activity and kinetic parameters. One such is an endo-1, 4-beta-xylanase from *Trichoderma reesei*, that displayed 108 % activity for Birchwood xylan with oat spelts xylan (100 %) and cellulosic substrates including Gellan gum (11 %) and Avicel (1.9 %) showing significantly less activity (He *et al.*, 2009). Information pertaining to substrate specificity and thermostability is important when considering what enzymes can be utilized in industrial applications. The study of thermostable proteins is extensive and has been used as a tool in understanding mechanisms for achieving thermostability. Mesophilic, thermophilic and hyperthermophilic enzyme sequences have been compared in an attempt to elucidate the interactions that are responsible for enhanced thermostability (Kinjo and Nishikawa, 2001). Such proteins have already proven to be extremely useful for high temperature applications (Flores and Ellington, 2002).

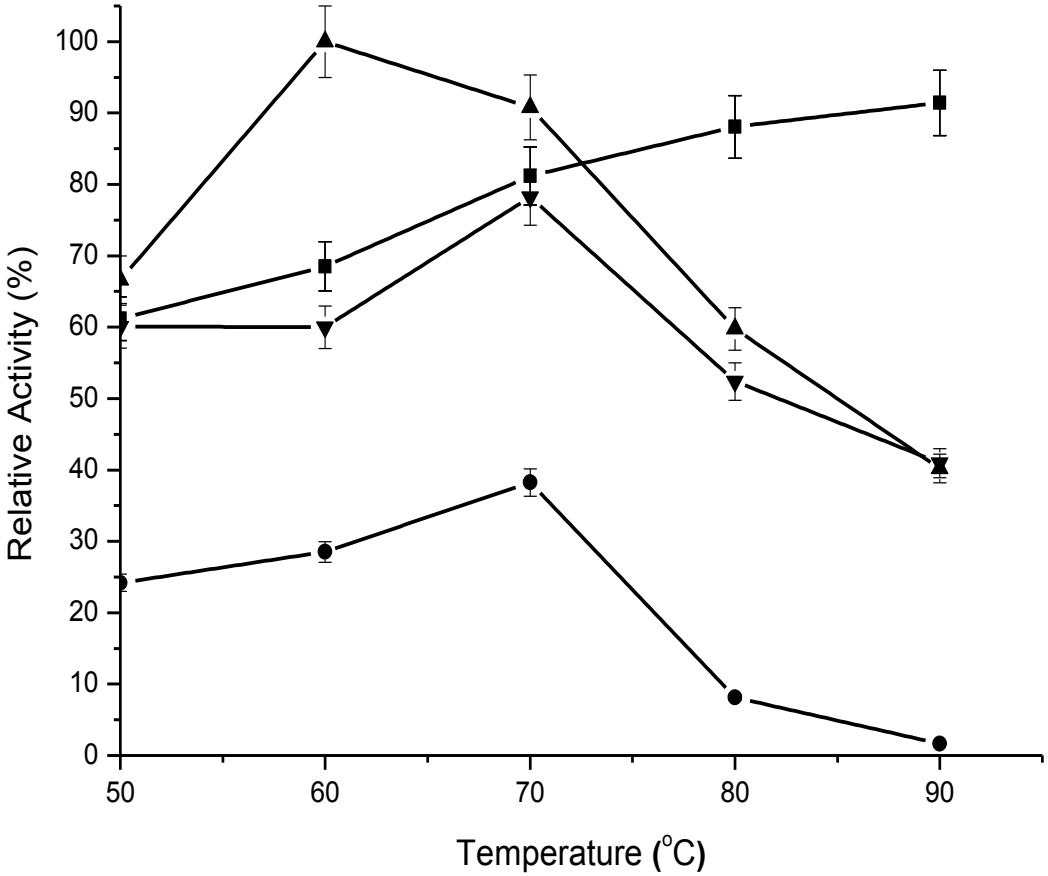

Fig. 2.3: Comparison of birchwood xylan hydrolysis using 10 units of each β-xylanase from *R. marinus* (pH 6) (■), *B. halodurans* (pH 9) (●), Pulpzyme HC (pH 7) (▲), *T. lanuginosus* (pH 7) (▼). Each xylanase was incubated for 30 min over a temperature range of 50 °C to 90 °C and percentage relative activity was calculated for each enzyme and measured against Pulpzyme HC.

2.3.3. Fluorescence spectra of xylanases at increasing temperatures

Fluorescent spectroscopy gives insight into the microenvironment of Trp residues in the protein. The structure and conformation of enzymes will change due to conditions of temperature, pH and changing salt concentrations. As the conformation of the enzymes changes the microenvironment of Trp residues will subsequently change. The temperature dependant fluorescence spectra of the thermostable *R. marinus* xylanase exhibited the lowest maximum fluorescence intensity with a maximum of 120 arbitrary units (a.u) (Fig. 2.4A) when compared to the other three xylanases. *R. marinus* which produces a highly thermophilic xylanase, exhibited its lowest fluorescent intensity at 90ºC with a relative activity of 100 % (Table 2.1). This could be due to the fact that, in its optimum conformation, the Trp residues are in an increased hydrophobic environment and therefore give off a lower fluorescence. It could also be attributed to non-radiated processes that deactivate the singlet-excited state as this trend is found in all four of the xylanases studied (Suresh Kumar, 2006). The *R. marinus* xylanase displayed an emission λ_{max} at around 340 nm from 50 °C to 70 °C which increased to 355 nm at its optimum temperature of 90 °C. The emission shift is due to tryptophan residues being further exposed to the solvent as native enzymes often display a fluorescence spectrum over 338 nm to 350 nm which indicated the Trp residues present in the differential environments (Favilla *et al.,* 2002; Shashidhara *et al.,* 2007).

The xylanase from *B. halodurans* also showed a low intensity with a maximum of 225 a.u. observed (Fig. 2.4A). The xylanase was thermo tolerant with 100% relative activity observed at 70 ºC and 76 % relative activity recorded at 60 ºC (Table 2.1). It is also highly alkalophilic displaying maximum activity between pH 7 to pH 10 (Fig 2.2B). Both *R. marinus* and *B. halodurans* xylanases showed low fluorescence intensity values and being thermophilic enzymes this could be attributed to the structure of enzymes that are able to

tolerate high temperatures and the positioning of Trp residues in hydrophobic microenvironments. The maximum emission was observed at 455 nm which is unusual after excitation at 295 nm. This emission could be explained by the addition of nicotinamide adenine dinucleotide phosphate-oxidase (NADPH) to the buffer to stabilize the enzyme solution. Therefore is could be the reason why the maximum emission was recorded at 455 nm rather than 350 nm. *The B. halodurans* xylanase showed minor λ_{max} deviation over the temperature range and similar results were evident from the work of Satyanarayana (2006) where studies on an alkaline thermophilic *Bacillus* xylanase displayed a constant λ_{max} at increasing temperatures. The two partially purified enzymes indicated low intensity values and as thermophilic enzymes, this could be attributed to the structure of enzymes that are able to tolerate high temperatures and the positioning of Trp residues in hydrophobic microenvironments.

The *T. lanuginosus* xylanase had an optimum temperature of 50ºC exhibiting 100 % relative activity and still exhibited 84 % relative activity at 70ºC (Table 2.1). In figure 2.4C, the control displayed a maximum fluorescence intensity of 750 a.u. and at 70 ºC an intensity of 250 a.u. was recorded. Shashidhara *et al*. (2010) indicated similar intensity values when subjecting α-mannosidase to thermal denaturation with a maximum fluorescence intensity of 760 a.u. at 30 °C with a subsequent decrease in fluorescence intensity as the temperature was increased. The xylanase from *B. halodurans* at 70 ºC showed similar emissions at the same temperature. Both *R. marinus* and *B. halodurans* xylanases showed high relative activities at 70ºC (71% and 100 %, respectively) but showed lower relative activities at 50ºC (24 % and 56 %, respectively). The emission λ_{max} of the xylanase from *T. lanuginosus* was approximately 341 nm for temperatures from 50 °C to 70 °C where maximum activity was observed and continued to increase to 348 nm at 80 °C and 350 nm at 90 °C. This could

indicate that enzymes able to function at higher temperatures having structural similarities at least with respect to Trp residue microenvironments and fluorescent emission. Similar results have been obtained by thermal denaturation of α-mannosidase where, from 30 °C to 60 °C, λ_{max} emission was 338 nm and at higher temperatures of 70 °C and 90 °C a red shift occurred and the λ_{max} increased to 350 and 353 nm, respectively (Shashidhara *et al*., 2010)

Pulpzyme HC is a commercially available enzyme with an optimum temperature for activity at 60 ºC. At 50 ºC and 70 ºC, the relative activity was found to be 64 % and 62 % respectively. The enzyme lost the majority of its activity at 80 ºC and 90 ºC retaining only 10 % and 8 % relative activity, at the respective temperatures (Table 2.1). Pulpzyme HC showed a high intensity of 500 a.u. and 300 a.u. at 50 ºC and 60 ºC, respectively (Fig. 2.4D). Pulpzyme HC also exhibited an emission λ_{max} of 346 nm at its optimum temperature of 60°C which increased sharply to 356 nm and 363 nm for 80 °C and 90 °C, respectively which indicate a red-shift in emission λ_{max} as the xylanase begins to unfold due to denaturation at high temperatures. Results from the thermal denaturation of bile salt hydrolase from *Bifidobacterium longum* displayed a similar trend whereby λ_{max} was 330 nm at temperatures up to 55 °C and at higher temperatures a red shift was observed where the λ_{max} increased to 350 nm which was presumed to be a result of Trp exposure to solvent (Suresh Kumar, 2006).

Table 2.1: Temperature and corresponding relative activity values (%) of different xylanases (1 mg/ml) assayed for 30 min from 50 °C to 90 °C using 1% birchwood xylan at their pH optima shown in parenthesis.

Organism / Xylanase	**Temperatures (°C)**				
	50	**60**	**70**	**80**	**90**
***R. marinus* (pH 6) Relative Activity (%)**	24	50	71	99	100
***B. halodurans (pH 9)* Relative Activity (%)**	56	76	100	11	5
***T. lanuginosus* (pH 7) Relative Activity (%)**	100	91	84	17	5
Pulpzyme HC (pH 7) Relative Activity (%)	64	100	62	10	8

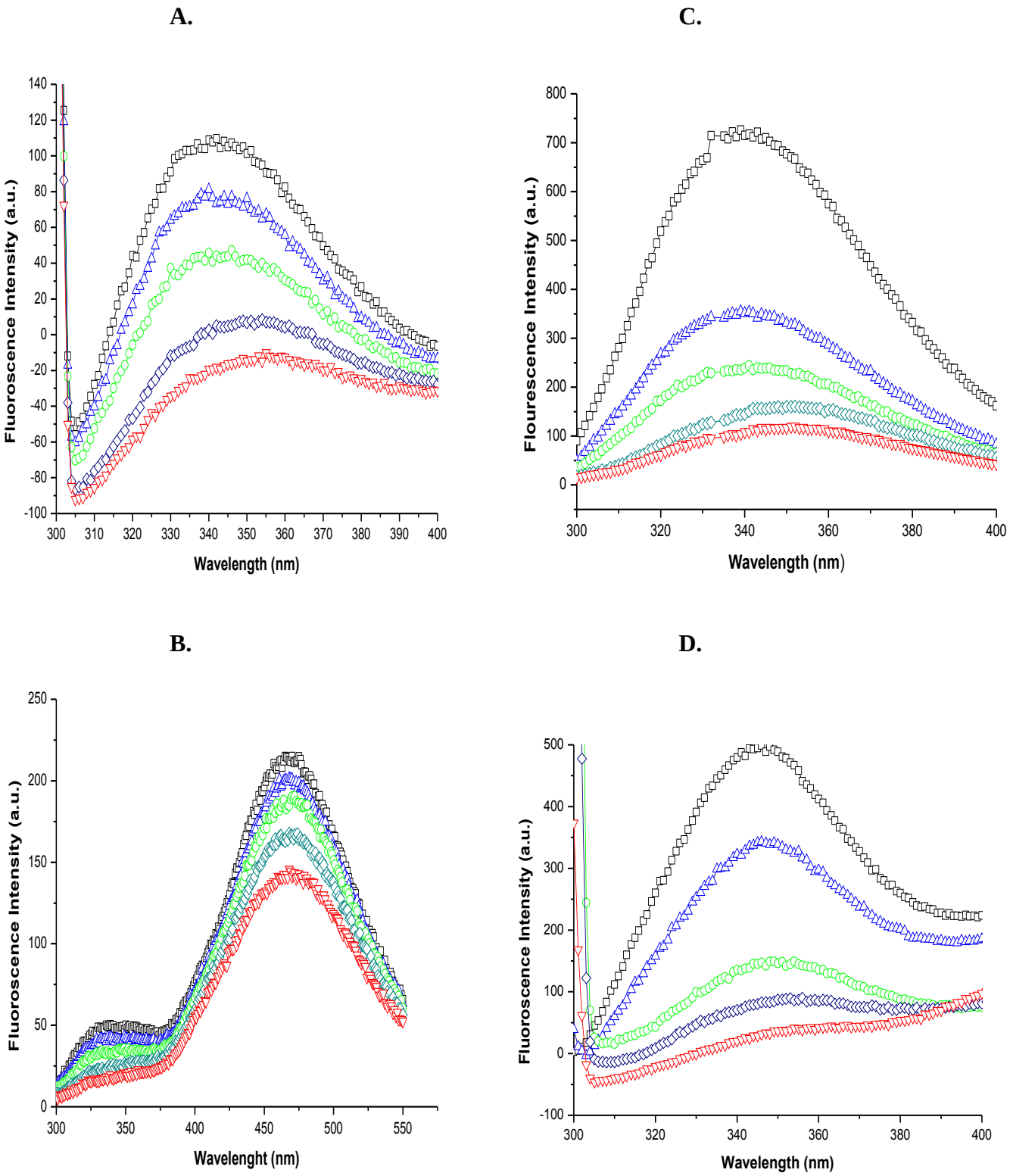

Fig. 2.4: Thermal emission spectra of xylanases (1 mg/ml) from **A.** *R. marinus* (pH 6). **B.** *B. halodurans* (pH 9). **C.** *T. lanuginosus* (pH 7). **D.** Pulpzyme HC (pH 7).excited at 295nm and recorded at a wavelength of 300 nm to 400 nm at various temperatures: 50ºC (□), 60ºC (Δ), 70ºC (○), 80ºC (◊) and 90ºC (▽).

2.3.4. Fluorescence spectra of xylanases subjected to chemical denaturation with GdnHCl at increasing temperatures

The current knowledge of the protein mechanism of folding and unfolding has come from concentrated and intense studies on protein denaturation using theoretical and biophysical methods (Ballery *et al.,* 1993; Wuthrich, 1994). The use of chemical denaturants such as GdnHCl and urea has assisted in the investigation of the role of the active sight in enzyme catalysis and which could also lead to stabilizing alternative states of conformation as well as in the study of the unfolding and refolding of protein conformation (Lopez *et al.,* 2011; Jiao *et al.,* 2010).

At 50 ºC the xylanase from *R. marinus* displayed a relative activity of 24 % (Table 2.1) and in the absence of GdnHCl displayed a maximum fluorescence intensity of 254 a.u., the xylanase with the addition of GdnHCl concentrations of 2.0 M and 3.0 M resulted in higher intensities when compared with concentrations of 0.5 M and 1.0 M that also exhibited a λ_{max} of 342 nm. The xylanases with higher concentrations of 2 M and 3 M GdnHCl displayed λ_{max} of 343 nm and 345 nm, respectively (Fig. 2.5A). At 70ºC a similar trend was observed but the maximum fluorescence intensity decreased by more than 50 % when GdnHCl concentrations of 0.5 M and 1 M were added to the *R. marinus* xylanase. It exhibited λ_{max} of 340 nm and high concentrations of 2 M and 3 M GdnHCl, added to the xylanase, showing a significant red-shift at 346 nm and 348 nm (Fig. 2.5B). Similar trends can be seen in other experiments, whereby there was no change in λ_{max} at lower concentrations whilst when higher GdnHCl concentrations were added to the *R. marinus* xylanase, a red-shift was observed which could indicate unfolding of the protein (Satyanarayana, 2006). At 90° C the maximum emission was 40 a.u. and the different GdnHCl concentrations applied to the xylanase had a minimal denaturation effect showing similar spectra values in the absence of GdnHCl but the λ_{max}, 354

nm in the absence of GdnHCl, 357 nm at 1 M and 363 nm at 3 M, exhibited an increase at each GdnHCl concentration (Fig. 2.5C). The *R. marinus* xylanase showed that it was only moderately susceptible to salt denaturation with GdnHCl, with respect to fluorescence intensity, where the control still gave the highest intensity but 3.0 M concentrations exhibited the second highest fluorescent intensity. At 90 ºC the control and increasing GdnHCl concentrations clustered together which could be due to the conformation of the xylanase in ensuring the Trp residues are unable to fluoresce. The *R. marinus* xylanase showed a similar trend in emission compared to that of TxyA-CBM where the control exhibits the highest intensity and as GdnHCl concentration is increased and a resulted decreased fluorescence emissions is observed (Okazaki *et al*., 2006)

The xylanase from *B. halodurans* exhibited a marked response to higher GdnHCl concentrations, especially at 3.0 M, and exhibited the highest fluorescence intensity at all three selected temperatures. At a concentration of 1.0 M GdnHCl, the xylanase displayed the lowest fluorescence intensity for the three temperatures tested. At 50 ºC, in the absence of GdnHCl and 3.0 M concentrations, the protein exhibited similar maximum fluorescence intensities of around 224 a.u. (Fig. 2.6A). At 70 °C, being the optimum temperature for activity, the xylanase displayed maximum spectral emission of 225 nm whilst in the absence of GdnHCl, the protein displayed lower intensities than at a concentration of 3.0 M GdnHCl (Fig. 2.6B). At 90 °C, 3.0 M GdnHCl resulted in the protein exhibiting a maximum emission of 190 a.u., with the absence of GdnHCl and 0.5 M showing similar fluorescence intensities for the protein of 150 a.u. (Fig. 2.6C). Rashid *et al.* (2005) confirmed similar findings in their investigation of the influence of GdnHCl on the denaturation of human placental cystatin (HPC) where chemical denaturation showed decreased fluorescence when at concentrations of up to 2 M, the fluorescence intensity decreased, but at higher concentrations of 3 M and

above, the fluorescence was found to be higher than when compared to the result obtained in the absence of GdnHCl.

The *T. lanuginosus* xylanase exhibited varying degrees of emission and intensity with GdnHCl denaturation together with a significant decrease in fluorescence intensity at higher temperatures from 70 °C and 90 °C. Okazaki *et al*. (2005) utilized fluorescence spectroscopy to study β-1,3-xylanase (TxyA) which displayed similar emission spectra with respect to GdnHCl denaturation and it was found to have similar fluorescence intensities. At 50 ºC, the protein in the absence of GdnHCl and in the presence of 2.0 M GdnHCl, exhibited identical intensities with a maximum fluorescence intensity of 700 a.u., whereas in 0.5 M GdnHCl it displayed the lowest fluorescence of 500 a.u. (Fig. 2.7A). At 70ºC, the intensities for all the recorded emissions were between 250a.u. and 300a.u., showing that at higher temperatures the effects of different salt concentrations was negated though there was an almost three-fold decrease in maximum emission. The *T. lanuginosus* xylanase exhibited a λ_{max} of 340 nm in the absence of GdnHCl to 1 M GdnHCl to the protein, which increased to 343 nm at 2 M that displayed a significant increase and red-shift at 3 M to 349 nm (Fig. 2.7B). At 90 °C all emissions were observed to have similar intensities with a maximum emission of 140 a.u., that represented a two-fold drop in maximum fluorescence intensity compared with 50 °C and displayed the same λ_{max} of 350 nm for the absence of GdnHCl to 1 M GdnHCl with an increase to 354 nm for 2 M and 3 M. (Fig. 2.7C). The *T. lanuginosus* xylanase displayed the least variance in fluorescence intensity due to chemical denaturation at higher concentrations the results clustered together showing only minor differences. However, a red-shift is observed when considering the λ_{max} for different temperatures and GdnHCl concentrations. Similar experiments conducted on streptomycin adenylyltransferase (SMATase) that showed a red-shift from 343 nm to 348 nm as the protein encounters the denaturation conditions of

the addition of GdnHCl. The denaturation conditions of GdnHCl increase the polar microenvironment of Trp residues and will produce conformations that are different from native conformations (Jana *et al.,* 2006).

Of the four xylanases tested, Pulpzyme HC displayed the greatest change in intensity due to GdnHCl denaturation and the xylanase, in the absence of GdnHCl exhibited the lowest intensity at all temperatures. Studies with HPC, using urea as a chemical denaturant, showed a similar relationship whereby, as the concentration of the chemical denaturant was increased so too did the fluorescence intensity (Rashid *et al.,* 2005). This could be attributed to GdnHCl affecting the conformation whereby the Trp residues are in the position to emit maximum fluorescence. Similar results were evident when α-mannosidase was treated with different concentrations of GdnHCl whereby an increased concentration of GdnHCl resulted in higher fluorescence intensity (Shashidhara *et al.,* 2010). At 50ºC, the addition of 1.0 M, 2.0 M and 3.0 M GdnHCl displayed intensities of 1400 a.u. In the absence of GdnHCl a fluorescence intensity of 500 a.u. was observed. Pulpzyme HC also showed a blue-shift where λ_{max}, in the absence of GdnHCl to 1 M of GdnHCl, was 340 nm and then decreased to 338 nm at 3 M GdnHCl (Fig. 2.8A). The fluorescence at 70ºC showed a similar trend when compared with the emissions at 50ºC but with a two-fold decrease in maximum fluorescence intensity. At higher temperatures a red shift was observed in the absence of GdnHCl, 0.5 M and 1 M GdnHCl (λ_{max} of 342) which showed a 3 nm increase at 2 M and 3 M GdnHCl up to 345 nm (Fig. 2.8B). At 90ºC, a similar GdnHCl induced trend continued at concentrations of 1.0 M, 2.0 M and 3.0 M displaying higher fluorescence intensities than in the absence of GdnHCl and 0.5 M GdnHCl. However, a major red-shift was observed in the absence of GdnHCl where by the protein exhibited florescence of 344 nm which increased to 349 nm at 0.5 M and 1 M, and then increased again to 356 nm with an increase to 2 M and 3 M GdnHCl. The

intensity dropped from over 1400 a.u. to a maximum of 260 a.u. for 3.0 M GdnHCl (Fig. 2.8C).

The four xylanases studied had both similarities and marked differences in emission spectra and intensities with respect to both thermal and GdnHCl denaturation as well λ_{max}. The xylanase that had the highest optimum temperature of 90ºC was from *R. marinus*. This enzyme exhibited the lowest intensities for both temperature and GdnHCl concentrations and displayed similar λ_{max} for lower concentrations of GdnHCl. This could be explained by the excited states of Trp interacting with molecules of water that form excited state complexes. This process then competes with the radiative relaxation and leads to a decreased in the intensity of fluorescence observed (Mc Guire and Feldman, 1973; Vetri and Militello, 2005; Stirpe *et al.*, 2005). The xylanase from *B. halodurans* showed a low intensity and was optimally active at 70ºC. The two crude enzymes therefore showed low intensity values and as thermophilic enzymes, this could be attributed to the structure of enzymes that are able to tolerate high temperatures and the positioning of Trp residues in hydrophobic microenvironments. The xylanase from *T. lanuginosus* had an optimum temperature of 50ºC and an intensity of 750 a.u. yet still exhibited 84% relative activity at 70ºC. The enzyme had a similar intensity at 70ºC, when compared with the *B. halodurans* xylanase. This could indicate that these enzymes are able to retain high relative activity at increased temperatures and will emit lower intensities as the structure of the enzyme is such that the Trp residue microenvironment allows for decreased fluorescence. The λ_{max} emission displayed minimal red shifts at higher temperatures and GdnHCl concentrations which could be attributed to a low number of Trp residues that are exposed to the solvent such as a xylanase, XynA, from *Thermotoga maritima* which exhibited only a small red shift from 346 nm to 349 nm at 7 M GdnHCl (Wassenburg *et al.*, 1997). Pulpzyme HC, a commercial xylanase, exhibited an optimum temperature at 60 ºC and showed high intensities at its optimum temperature of 500

a.u. and 300 a.u. for 50ºC and 60ºC respectively with a blue-shift recorded at 50 °C as the GdnHCl concentration was increased. A significant red-shift was observed at 90 °C from no GdnHCl to 0.5 M and from no GdnHCl to 2 M. Shashidhara *et al.* (2010) has explained however, that a loss in enzyme activity due to thermal and chemical denaturants can be exhibited without a significant change in the conformation and the irreversibility and denaturation of the enzyme could be attributed to adverse effects of the deficiency of the enzyme.

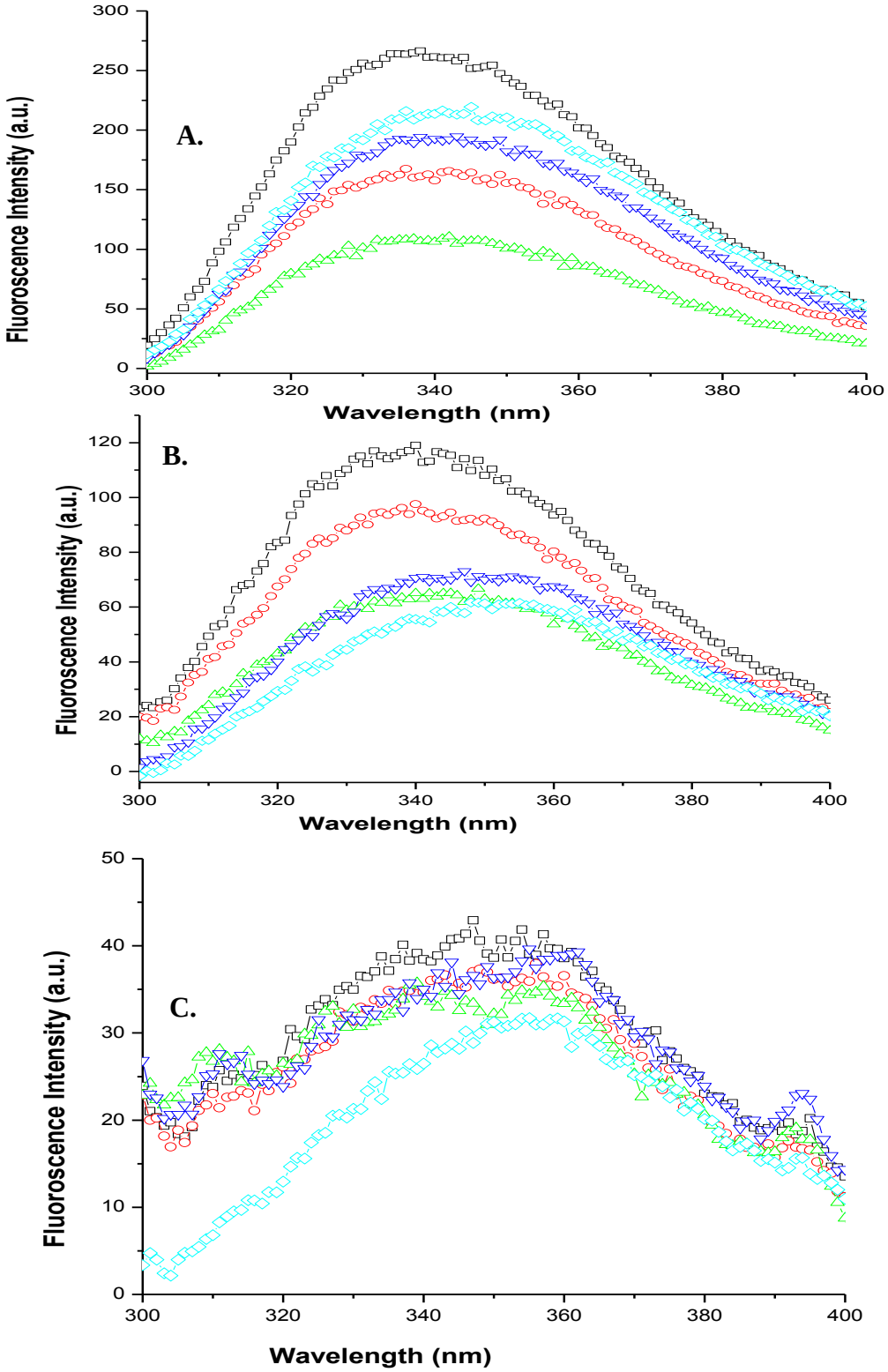

Fig. 2.5: Emission spectra of the *R. marinus* xylanase (1 mg/ml) at pH 6. Excitation at 295nm and emission were recorded at 300 nm to 400 nm after chemical denaturation with GdnHCl at various concentrations: No GdnHCl (□),0.5 M (○), 1.0 M (△), 2.0 M (▽), 3.0 M (◊) and temperatures: **A.** 50 °C. **B.** 70 °C. **C.** 90 °C.

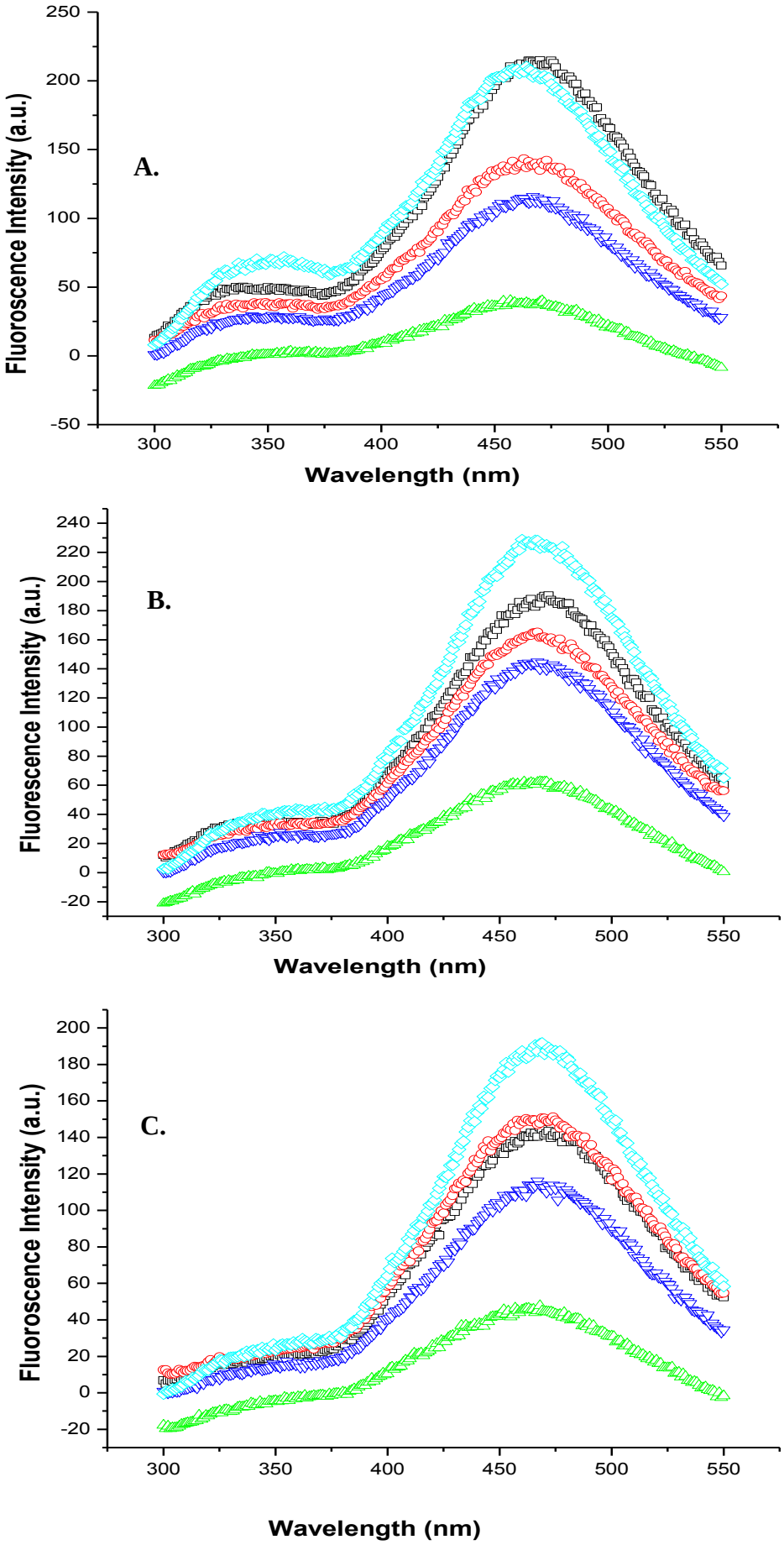

Fig. 2.6: Emission spectra of the *B. halodurans* xylanase (1 mg/ml) at pH 9. Excitation at 295nm and emission were recorded at 300 nm to 400 nm after chemical denaturation with GdnHCl at various concentrations: No GdnHCl (□),0.5 M (○), 1.0 M (△), 2.0 M (▽), 3.0 M (◊) and temperatures: **A.** 50 °C. **B.** 70 °C. **C.** 90 °C.

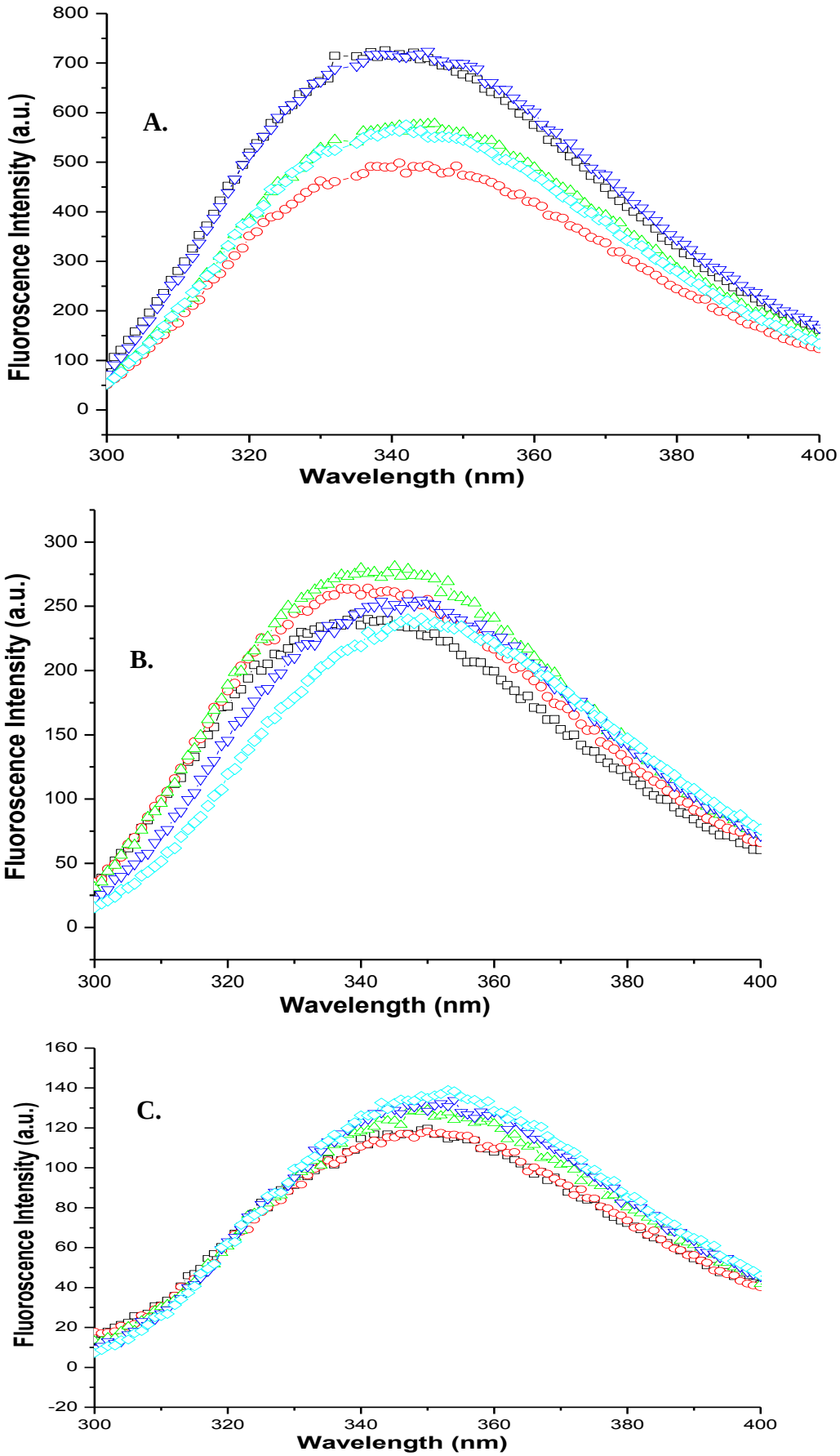

Fig. 2.7: Emission spectra of the *T. lanuginosus* xylanase (1 mg/ml) at pH 7. Excitation at 295nm and emission were recorded at 300 nm to 400 nm after chemical denaturation with GdnHCl at various concentrations: No GdnHCl (□),0.5 M (○), 1.0 M (△), 2.0 M (▽), 3.0 M (◊) and temperatures: **A.** 50 °C. **B.** 70 °C. **C.** 90 °C.

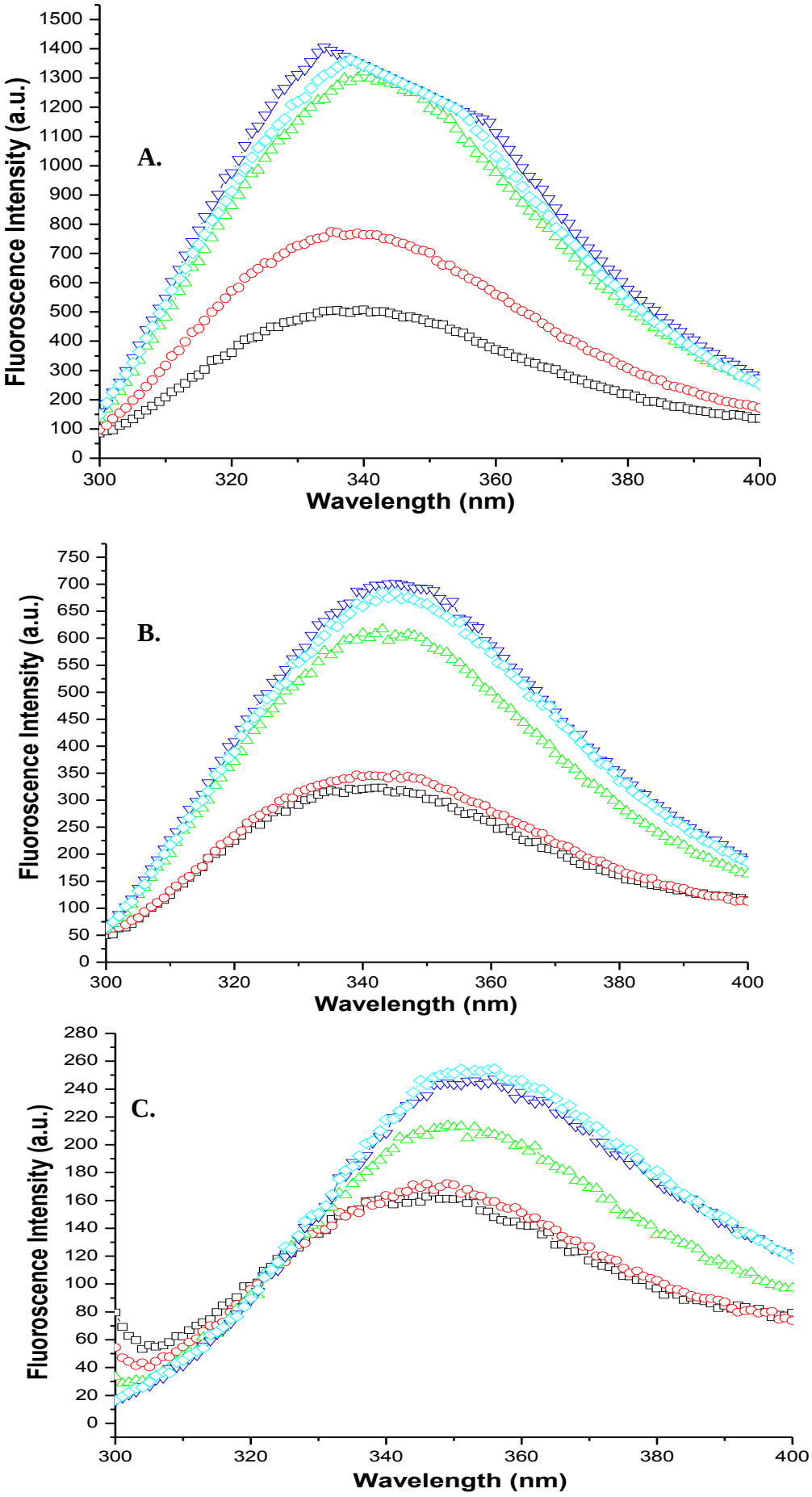

Fig. 2.8: Emission spectra of the Pulpzyme HC xylanase (1 mg/ml) at pH 7. Excitation at 295nm and emission were recorded at 300 nm to 400 nm after chemical denaturation with GdnHCl at various concentrations: No GdnHCl (□),0.5 M (○), 1.0 M (Δ), 2.0 M (▽), 3.0 M (◊) and temperatures: **A.** 50 °C. **B.** 70 °C. **C.** 90 °C.

2.4. Conclusions

The xylanase from *R. marinus* was optimally active at 90 °C, pH 6 and exhibited 94 % relative activity when compared with the other three xylanases. It also exhibited the lowest fluorescence intensity peak of 120 a.u. which decreased as the temperature was increased indicating a conformation that had the fluorescing Trp residues in a hydrophobic environment. The xylanase from *R. marinus* at 90 °C, when subjected to increasing GdnHCl concentrations, did exhibit a significant increase in λ_{max} from 354 nm in the absence of GdnHCl to 363 nm at 3 M GdnHCl which indicates a significant red-shift and change in conformation.

The *B. halodurans* xylanase was found to be highly alkalophilic showing an optimal activity at pH 8 to 10 and an optimum temperature of 70 °C. It did, however, perform poorly when compared with the other three xylanases, resulting in only 40 % relative activity at its optimum activity conditions. This xylanase also showed a low peak intensity of only 230 a.u. when compared with the commercially produced xylanases. The *B. halodurans* xylanase however, did not display a marked change when subjected to GdnHCl which could be attributed to its alkalophilic properties.

The xylanase from *T. lanuginosus* was found to be optimally active at pH 7 and 50 °C but was found to have 84 % relative activity at 70°C but when compared with the other three xylanases it only achieved 78 % relative activity. The commercial *T. lanuginosus* showed the highest peak fluorescence peak intensity of 750 a.u. Due to its high activity from 50 °C to 70 °C, even when subjected to GdnHCl, it was expected that a minor red-shift occurred with a λ_{max} of 341 nm. However, as the temperature was further increased, a red shift took place and at 90 °C it was recorded at 350 nm which could be attributed to denaturation of the enzyme.

The commercial Pulpzyme HC xylanase showed an optimum activity at 60 °C and pH 7 and displayed the highest relative activity of 100 % when compared with the three other xylanases. It showed a peak intensity of 500 a.u. but was the most susceptible to the addition of GdnHCl as the control of 0 M GdnHCl was found to be the lowest intensity at all three temperatures. It also displayed a significant red-shift from 346 nm at its optimum temperature of 60 °C to 363 nm at 90 °C.

Chapter two focused upon four interesting xylanases with different desirable characteristics such as thermophilic and alkalophilic activity. Structural studies were then done to assess the change in fluorescence due to thermal stress as well as under chemical denaturation conditions with the use of GdnHCl. The structures of the xylanases that give rise to their function under such harsh conditions was further studied using differential scanning fluorometry (DSF) and circular dichroism (CD) in an attempt to further understand the relationship between structure and function.

CHAPTER 3: CONFORMATIONAL STUDIES OF XYLANASES USING DIFFERENTIAL SCANNING FLUOROMETRY AND CIRCULAR DICHROISM

3.1. INTRODUCTION

The mechanisms of protein folding is an important topic of research that has continued to go unresolved. Structural experiments such as crystallography or nuclear magnetic resonance (NMR) spectroscopy has elucidated structural data that could be used to model three dimensional structure of most proteins (Wei and Song, 2005). However, the fundamental principles regarding the folding and stability of proteins is still largely unknown whereby it is difficult to distinguish between thermophilic and mesophilic counterparts despite their 3D structures already being known. There are now many tools available for the investigation of protein folding including NMR, circular dichroism (CD), protein intrinsic fluorescence decay and resonance energy transfer and the measuring of fluorescence decay which allows for the direct observation of the dynamics of protein structural changes (Eftink, 1994).

Vedadi *et al.* (2006) states that differential scanning fluorometry (DSF) is a platform that excels at screening for stabilizing conditions for proteins due to the fact of small amount and low concentrations of the protein are required and therefore this method can be applied to samples for which low stability or aggregation will complicate purification. DSF monitors thermal unfolding of proteins in the presence of a fluorescent dye (Poklar *et al.,* 1997; Pantoliano *et al.,* 2001) and is applicable to a wide range of proteins (Vedadi *et al.,* 2006; Ericsson *et al.,* 2006). DSF is most often used in conjunction with a real-time PCR instrument (Lo *et al.,* 2004). The fluorescent dyes that are most commonly used in DSF are those that are

highly fluorescent in non-polar environments where as in aqueous solutions the fluorescence is often quenched. The hydrophobic sites on unfolded proteins provide a good non-polar environment for fluorescence of dyes. Epps *et al.* (2001) concludes that different dyes are found to be useful as they possess different inherent optical properties, particularly in the fluorescence quantum yield caused by binding to denatured protein.

The stability of a protein is related to its Gibbs free energy of unfolding, ΔG_u, which is temperature-dependent (Schellman, 1997; Privalov, 1979). The stability of most proteins decreases with temperature; as the temperature increases, the ΔG_u decreases and becomes zero at equilibrium where the concentrations of folded and unfolded protein are equal. At this point, the temperature is considered as melting temperature (T_m). If the protein unfolds in a reversible two-state manner, the equilibrium thermodynamics models will apply (Brandts, 1990). If a compound binds to a protein, the free energy contribution of ligand binding in most cases results in an increase in ΔG_u, which may cause an increase in the T_m. It has been shown that the stabilizing effect of compounds upon binding is proportional to the concentration and affinity of the ligands (Matulis *et al.*, 2005 and Vedadi *et al.*, 2006). Although for many proteins unfolding is not a reversible (equilibrium) monomolecular two state reaction as described, assuming equilibrium conditions allows one to approach protein stability reasonably well and compare it under different conditions.

Thermal stability can be assessed using CD by following changes in the spectrum with increasing temperature. A single wavelength can be chosen which monitors a specific feature of the protein structure, and the signal at that wavelength is then recorded continuously as the temperature is raised. If the protein precipitates or aggregates as it is unfolded, the melting reaction will be irreversible, and the melting temperature will reflect the kinetics of aggregation and the solubility of the unfolded form of the molecule as well as

the intrinsic conformational stability. The co-operativity of the unfolding reaction is measured qualitatively by the width and shape of the unfolding transition. A highly cooperative unfolding reaction indicates that the protein existed initially as a compact, well-folded structure, while a very gradual, non-cooperative melting reaction indicates that the protein existed initially as a very flexible, partially unfolded protein or as a heterogeneous population of folded structures (www.ap-lab.com).

This chapter focuses on the effects of different buffer conditions and temperature on the conformation of the xylanases. The application of DSF assesses the effects of different buffers including the addition of NaCl and glycerol on the melting temperature of the xylanases. The secondary structure of the proteins were further investigated using CD, and the folded fraction and gibbs free energy were calculated.

3.2. MATERIALS AND METHODS

3.2.1. Materials:

SYPRO Orange was purchased from Invitrogen (cat. no. S6650). Adhesive aluminium seals were from ABgene, (cat. no. AB-0626) and U-bottom 96-well microplates were from Corning (cat. no. 3355). All DSF and CD experiments were performed in Prof. Eva Nordberg-Karlsson's laboratory (Department of Biotechnology, Lund University, Sweden).

3.2.2. Differential Scanning Fluorometry (DSF)

DSF monitors thermal unfolding of proteins in the presence of a fluorescent dye SYPRO orange and is typically performed by using a real-time PCR instrument according to the protocol by Vedadi *et al.* (2006). A Tecan Freedom Evo 200 Robot was used to dispense buffers in a 96 well PCR plate. A volume of 700 µl was used for each well with a xylanase concentration of 100 mg/ml. 1 µl of the fluorescent dye SPYRO orange was added and the solution was mixed using a pipette. The solution was then centrifuged at 200 g for 1 minute to collect all of the solution at the bottom and to remove bubbles. The PCR plate was then sealed with optical foil and placed into a RT-PCR instrument and the temperature scan was run from 25 ºC to 95 °C, at 1 °C min^{-1}. SYBR green software was used to analyse data and to display selected curves. In DSF, the fluorescence intensity is plotted as a function of temperature; this generates a sigmoidal curve that can be described by a two-state transition. The inflection point of the transition curve (Tm) is calculated using a Boltzmann equation,

$$y = LL + \frac{(UL - LL)}{1 + \exp\frac{(Tm - x)}{\alpha}}$$

where LL and UL are the values of minimum and maximum intensities, respectively, and α denotes the slope of the curve within T_m. T_m values were calculated by determining the maximum of the first derivative using the SYBR green software.

3.2.3. Circular dichroism (CD)

The CD spectra of the three xylanase proteins were obtained using a JASCO J-815 CD spectrophotometer in a reaction volume of 300 µl at a concentration of 0.3 mg/ml to 0.5 mg/ml. The normalization of spectra was performed using the software provided by the instrument manufacturer. Temperature spectra scans were recorded from 20 °C to 95 °C for the xylanases from *B. halodurans* and *T. lanuginosus* and 20 °C to 98 °C for the xylanase from *R. marinus.* Buffer/Blank CD (mdeg) signal was substituted from the sample. Spectra in the near UV region were measured in a 0.01 mm pathlength cylindrical quartz cell in 20mM phosphate buffer at 220 nm (Davoodi, 1996).

The CD signal (θ, in milli degrees) was converted to mean residual ellipticity units ([θ] in deg.cm^2/dmol) using the following equation (Labhardt, 1986):

$$[\theta] = \frac{\theta \text{ x MRW}}{10 \text{ x C x l}}$$

Where MRW is the mean residue weight of the protein in g/mol, *C* is the concentration in mg/ml and *l* is the path length of the cuvette in cm. The mean residue weight of the protein was calculated by the equation:

$$MRW = \frac{MW}{n}$$

Where MW is the molecular weight of the protein and *n* was the number of residues.

Further analysis was conducted from CD data and the fraction of folded protein (1), constant of folding (2) and the free energy of unfolding (3) were calculated using the following equations:

1. The fractions of folded protein at any temperature (α) was calculated as:

$$\alpha = {(\theta_{Obs} - \theta_u)}\Big/{(\theta_f - \theta_u)}$$

Where θ_{Obs} is the observed ellipticity at any point, θ_u is the ellipticity of the unfolded protein and θ_f is the ellipticity of the fully folded form.

2. The constant of folding was determined from the equation:

$$K = {(F)}\Big/{(U)}$$

Where F is the fluorescence observed in the folded state and U is the fluorescence observed in the unfolded state.

3. The free energy of unfolding ($\boldsymbol{\Delta G}$) determined as:

$\Delta G = -RT ln k$

Where R is the gas constant (1.987 $cal.mol^{-1}.K^{-1}$), T is the absolute temperature.

3.3. RESULTS AND DISCUSSION

3.3.1. Differential scanning fluorometry for *R. marinus* xylanase

The different temperatures obtained at which the *R. marinus* xylanase denatures in different buffers are detailed in Table 3.1. The PCR software package Mx3005p created a graphical representation for each of the temperatures. The *R. marinus* xylanase showed two maximum denaturation points at 89 °C for 50 mM Na_2HPO_4 at pH 7.2 and 1 M NaHepes at pH 7.6: This means that the *R. marinus* xylanase is stable until 89 ºC in 50 mM Na_2HPO_4 at pH 7.2 (Fig 3.1A) and 1M NaHepes at pH 7.6 (Fig. 3.1B). Similar melting temperatures (T_m) were displayed utilizing differential scanning calorimetry where the xylanase from *R. marinus* displayed a T_m of 91.9 °C (Abou-Hachem *et al.*, 2003). The amplification graph represented the fluorescent emission captured by the PCR machine. Starting at 20 °C at cycle one the temperature increased by increments of 1 °C for every cycle. As the enzyme unfolds the fluorescence increases. When the enzyme was incubated with 50 mM Na_2HPO_4 at pH 7.2 it showed the highest fluorescence emission and denaturation point (Fig. 3.2A). The dissociation curve displaying fluorescence against temperature, clearly shows (50 mM Na_2HPO_4at pH 7.2) maintained the highest fluorescent emission for the protein (Fig. 3.2B). DSF allows for the expression of T_m for a large number of different buffer conditions (Niesen *et al.*, 2007). T_m shows the optimum temperature for activity before denaturation occurs. The *R. marinus* xylanase, further confirmed results as reported in Chapter 2, with a T_m of 89ºC for two separate buffers, the highest optimum activity of the three xylanases.

Table 3.1: Influence of different buffer conditions on the DSF melting temperature (T_m) for *R. marinus* xylanase (100 mg/ml) using the fluorescent dye Spyro Orange (1 ul) over a temperature range of 25 ºC to 95 °C, at 1 °C min^{-1}.

Well Number	Buffer	Buffer Volume (ml)	3 M NaCl (ml)	Glycerol (ml)	H_2O (ml)	T_m (°C)
A1	1M NaOAc pH 5.1	0.4	0.2	0	0.4	64
A2	0.5M MES pH 6	0.8	0.2	0	0	66
A3	1 M AmAc pH 6	0.4	0.2	0	0.4	82
A4	0.73M Bis Tris pH 6.5	0.4	0.2	0	0.4	82
A5	2M Nakako pH 6.7	0.2	0.2	0	0.6	82
A6	0.5M Imidazole pH 7	0.8	0.2	0	0	82
A7	0.5M MOPS pH 7.2	0.8	0.2	0	0	82
A8	10x PBS pH 7.3	0.4	-	0	0.6	85
A9	1M AmAc pH 7.5	0.4	0.2	0	0.4	82
A10	1M Hepes-Ac pH 7.5	0.4	0.2	0	0.4	82
A11	**1M Na-Hepes pH 7.6**	**0.4**	**0.2**	**0**	**0.4**	**89**
A12	1M Na-Hepes pH 8	0.4	0.2	0	0.4	82
B1	1M Tris/HCl pH 8	0.4	0.2	0	0.4	82
B2	1M Bicin pH 14	0.4	0.2	0	0.4	82
B3	1M PCTP pH 9.5	0.4	0.2	0	0.4	82
B4	0.5 Fosfat pH 10 (Insulin)	0.8	0.2	0	0	82
B5	1M NaHepes pH 7.6	0.4	0.2	0	0.6	81
B6	1M NaHepes pH 7.6	0.4	0.0668	0	0.533	80
B7	1M NaHepes pH 7.6	0.4	0.2	0	0.4	82
B8	1M NaHepes pH 7.6	0.4	0.2	0	0.4	82
B9	**1M NaHepes pH 7.6**	**0.4**	**0.2**	**0**	**0**	**89**
B10	1M NaHepes pH 7.6	0.4	0.2	0.2	0.2	64
B11	1M NaHepes pH 7.6	0.4	0.2	0.4	0	82
B12	1M NaHepes pH 7.6	0.4	0.2	0.2	0	82

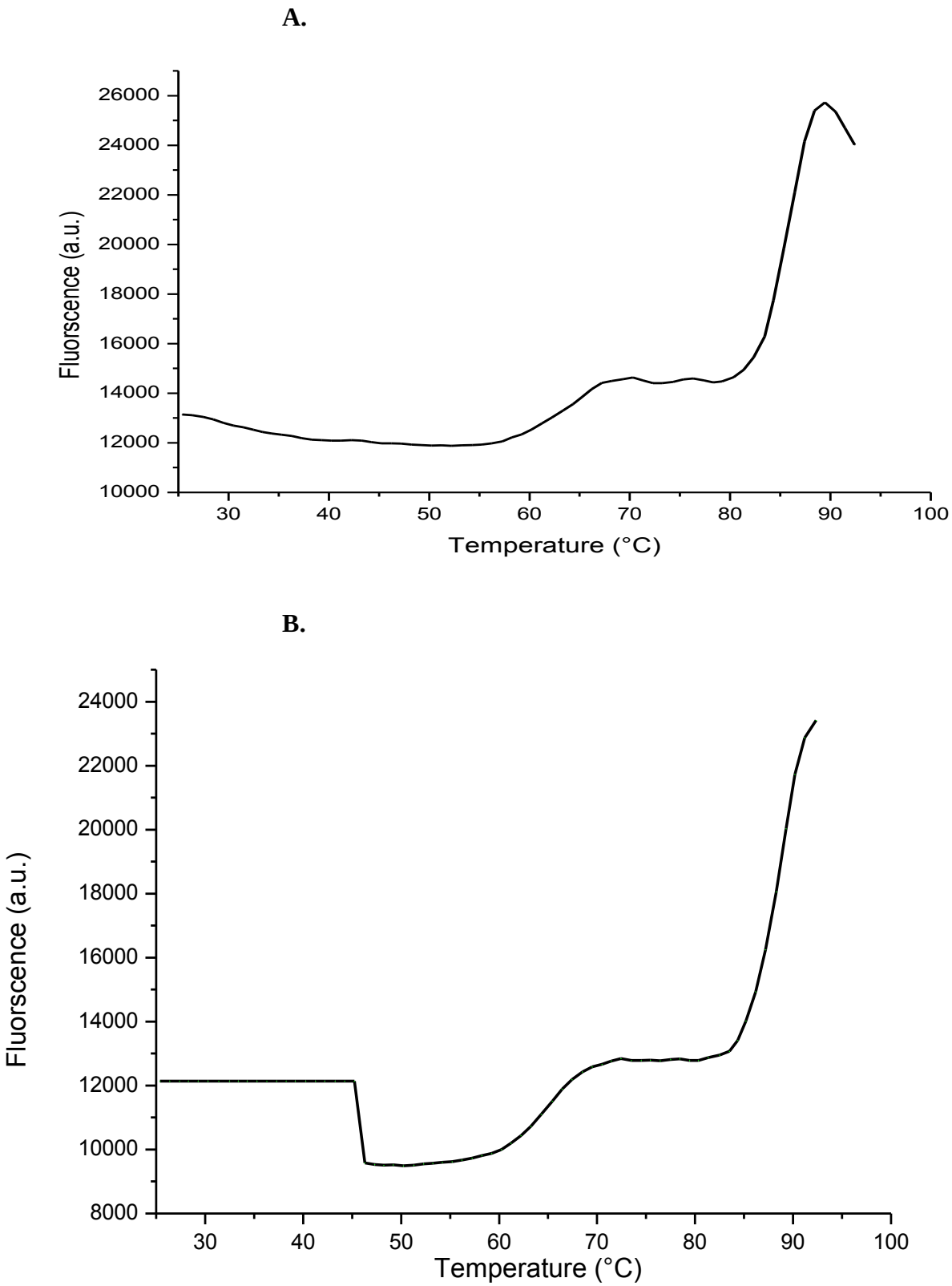

Fig. 3.1: Xylanase from *R. marinus* (100 mg/ml) with Spyro Orange (1 µl) from 25 ºC to 95 °C, at 1°C min^{-1} with **A.** 1M NaHepes (pH 7.6) showing a maximum denaturation temperature at 89 °C. **B.** 50 mM $NaPO_4$ (pH 7.2) showing a maximum denaturation temperature at 89 °C.

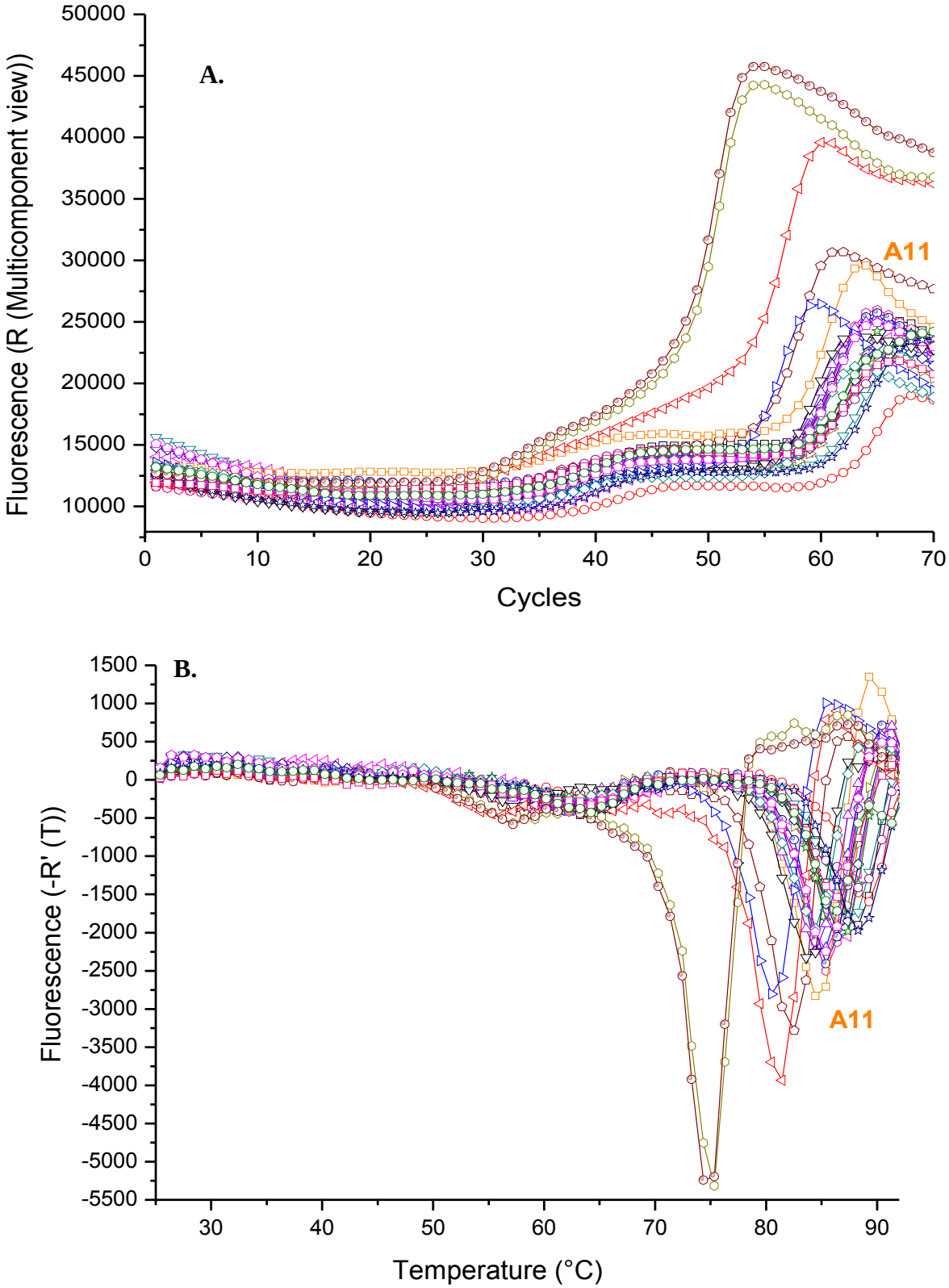

Fig. 3.2: Xylanase from *R. marinus* (100 mg/ml) with Spyro Orange (1 µl) from 25 ºC to 95 °C, at 1 °C min^{-1}. **A.** Amplification curve showing fluorescence against the number of PCR cycles and **B.** Dissociation curve showing fluorescence against temperature using various buffers (Table 3.1): A1 (□), A2 (○), A3 (△), A4 (▽), A5 (◁),A6 (▷), A7 (◊), A8 (⌂), A9 (○),A10 (☆), A11 (□), A12 (○), B1 (○),B2 (△), B3 (▽), B4 (◁), B5 (▷), B6, B7 (◊), B8 (⌂), B9 (○), B10 (☆), B11 (○), B12 (□).

3.3.2. Differential scanning fluorometry for *B. halodurans* xylanase

The xylanase from *B. halodurans* showed a much wider range of pH stability and its maximum denaturation point in four different buffers was 77°C (Table 3.2). Utilizing differential scanning calorimetry, the T_m for a *B. circulans* xylanase was calculated with the wild type exhibiting a T_m 59.7 °C while mutants of the same enzyme exhibiting a T_m as high as 72 °C (Davoodi, 1996). With a minimum denaturation temperature of 74 °C, this confirmed that the xylanase is active in a wide variety of buffers and over a wide range of pH values as there is only a two degree difference between its highest and lowest temperature of denaturation. Two buffer's where the xylanase showed a maximum denaturation point are 1 M NaOAc at pH 5.1 (Fig. 3.4A) and 1 M NaHepes at pH 7.6 (Fig. 3.4B) again highlighting good pH stability. The *B. halodurans* xylanase exhibited a marked pH tolerance and the amplification curve confirmed this. With only a 2 °C difference between the highest and lowest temperatures obtained, the graphs all peak in a very similar area, from about 54 to 58 cycles (Fig. 3.5A). The dissociation curve for the *B. halodurans* xylanase clearly illustrates its pH tolerance (Fig. 3.5B) with visible peaks at 75 °C and 77 °C. The close grouping of peaks and the similar fluorescence values confirm that the xylanase from *B. halodurans* has a high pH tolerance. *B. halodurans* produces a highly alkalophilic enzyme that has an optimum pH of 9 but exhibits high relative activity from pH 7 to pH 10 (Gashaw, 2006). The recorded DSF data reinforced that the xylanase is optimum over such a relatively wide pH range, as the recorded T_m for the different buffers ranged from 74 ºC to 77 ºC with a clustering of the T_m curves in both the amplification and dissociation curves. The xylanase was found to have optimum activity at 70 ºC, so further investigations into stabilizing conditions could be done to enhance its thermostability.

Table 3.2: Influence of different buffer conditions on the DSF melting temperature (T_m) for *B. halodurans* xylanase (100 mg/ml) using the fluorescent dye Spyro Orange (1 ul) over a temperature range of 25 ºC to 95 °C, at 1 °C min^{-1}.

Well Number	Buffer	Buffer Volume (ml)	3 M NaCl (ml)	Glycerol (ml)	H_2O (ml)	T_m (°C)
A1	**1M NaOAc pH 5.1**	**0.4**	**0.2**	**0**	**0.4**	**77**
A2	0.5M MES pH 6	0.8	0.2	0	0	76
A3	1 M AmAc pH 6	0.4	0.2	0	0.4	75
A4	0.73M Bis Tris pH 6.5	0.4	0.2	0	0.4	75
A5	2M Nakako pH 6.7	0.2	0.2	0	0.6	77
A6	0.5M Imidazole pH 7	0.8	0.2	0	0	75
A7	0.5M MOPS pH 7.2	0.8	0.2	0	0	77
A8	10x PBS pH 7.3	0.4	-	0	0.6	75
A9	1M AmAc pH 7.5	0.4	0.2	0	0.4	75
A10	1M Hepes-Ac pH 7.5	0.4	0.2	0	0.4	77
A11	1M Na-Hepes pH 7.6	0.4	0.2	0	0.4	75
A12	1M Na-Hepes pH 8	0.4	0.2	0	0.4	75
B1	1M Tris/HCl pH 8	0.4	0.2	0	0.4	75
B2	1M Bicin pH 14	0.4	0.2	0	0.4	74
B3	1M PCTP pH 9.5	0.4	0.2	0	0.4	74
B4	0.5 Fosfat pH 10 (Insulin)	0.8	0.2	0	0	75
B5	1M NaHepes pH 7.6	0.4	0.2	0	0.6	75
B6	1M NaHepes pH 7.6	0.4	0.0668	0	0.533	75
B7	1M NaHepes pH 7.6	0.4	0.2	0	0.4	75
B8	1M NaHepes pH 7.6	0.4	0.2	0	0.4	75
B9	**1M NaHepes pH 7.6**	**0.4**	**0.2**	**0**	**0**	**77**
B10	1M NaHepes pH 7.6	0.4	0.2	0.2	0.2	75
B11	1M NaHepes pH 7.6	0.4	0.2	0.4	0	75
B12	1M NaHepes pH 7.6	0.4	0.2	0.2	0	76

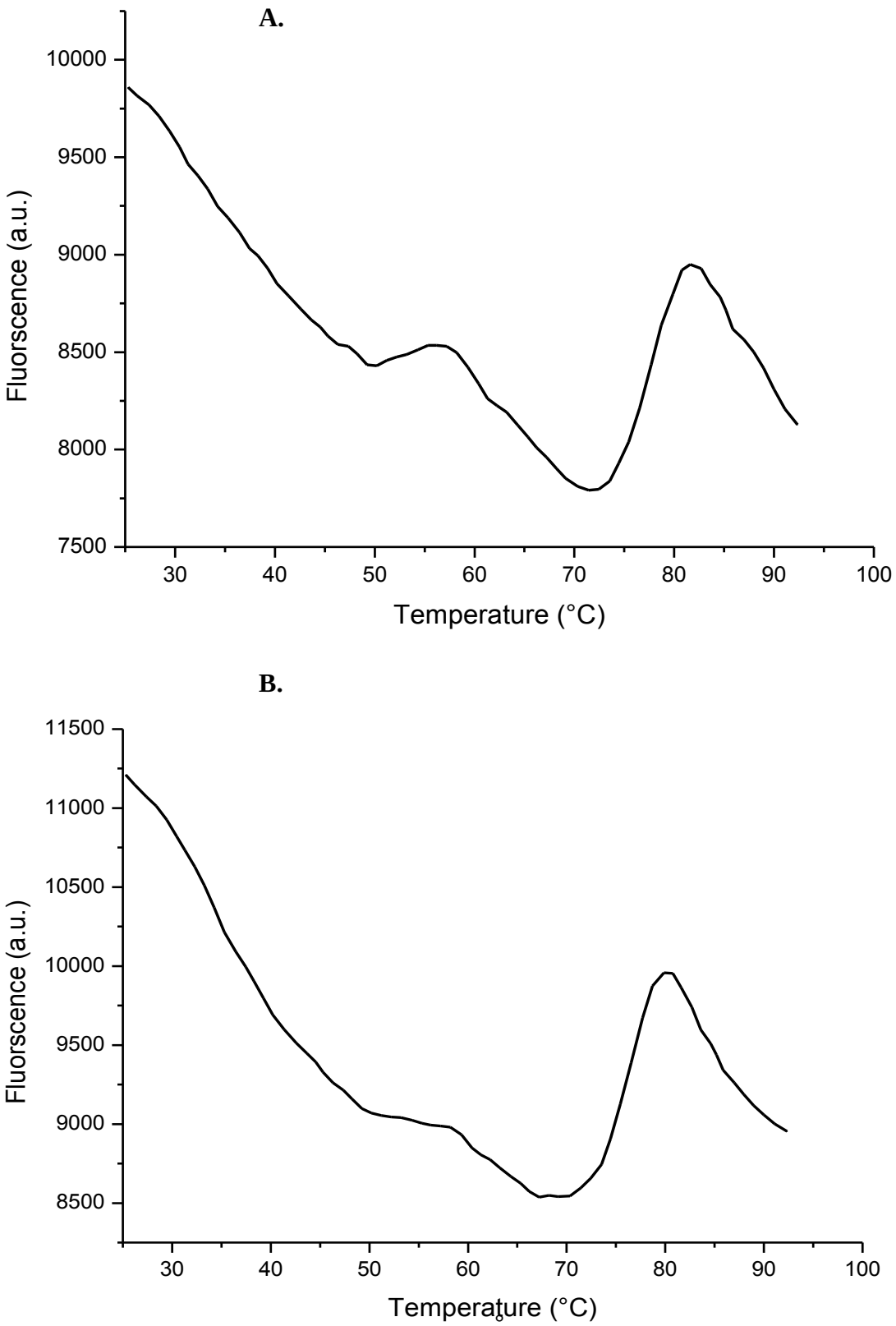

Fig. 3.3: Xylanase from *B. halodurans* (100 mg/ml) with Spyro Orange (1 µl) from 25 ºC to 95 °C, at 1 °C min^{-1} with **A.** 1 M NaOAc (pH 5.1) showing a maximum denaturation temperature at 77 °C. **B.** 1 M NaHepes (pH 7.6) showing a maximum denaturation temperature at 77 °C.

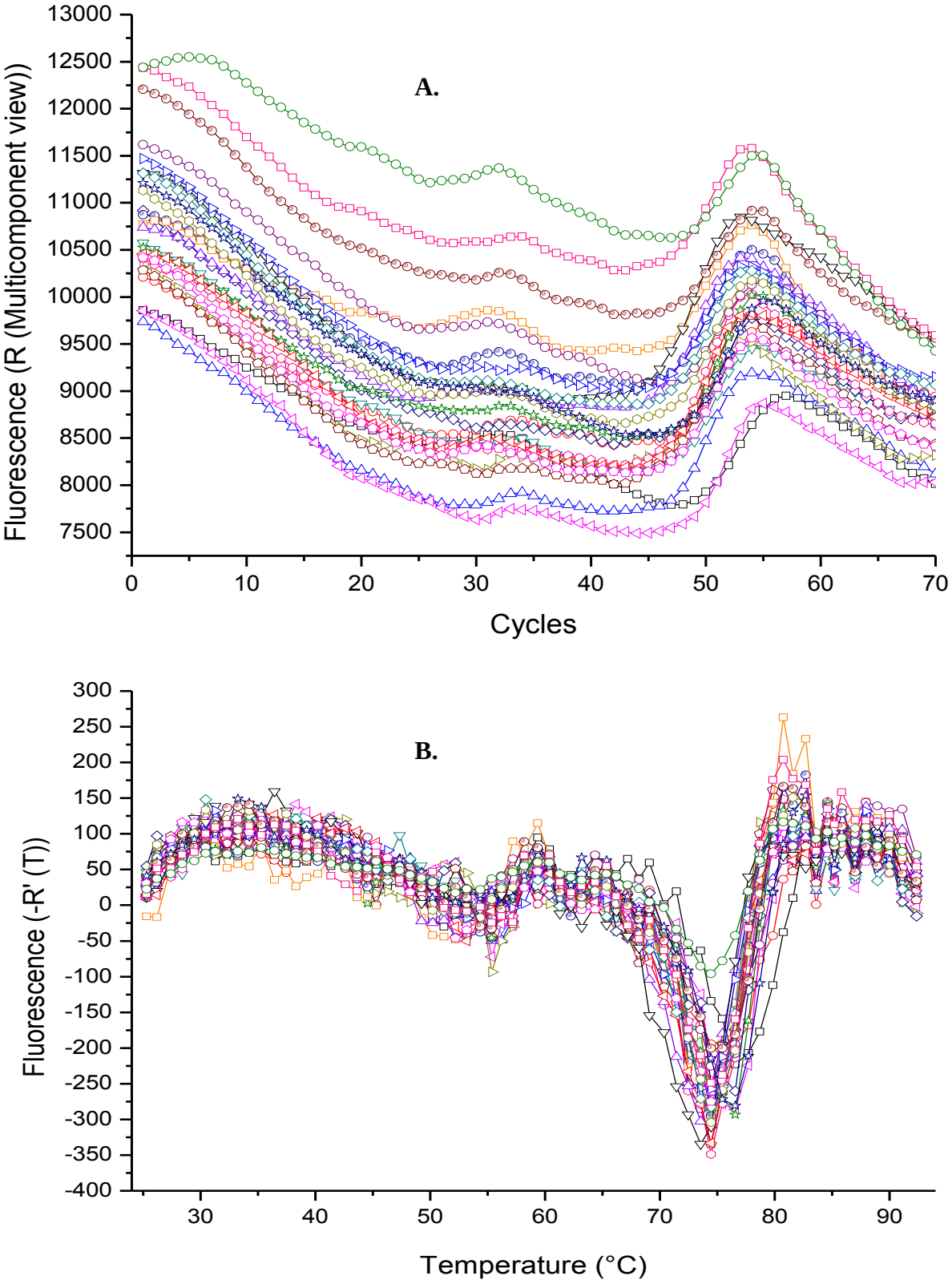

Fig. 3.4: Xylanase from *B. halodurans* (100 mg/ml) with Spyro Orange (1 µl) from 25 ºC to 95 °C, at 1 °C min^{-1}. **A.** Amplification curve showing fluorescence against the number of PCR cycles and **B.** Dissociation curve showing fluorescence against temperature using various buffers (Table 3.2): A1 (□), A2 (○), A3 (△), A4 (▽), A5 (◁),A6 (▷), A7 (◊), A8 (⌂), A9 (○),A10 (☆), A11 (□), A12 (○), B1 (○),B2 (△), B3 (▽), B4 (◁), B5 (▷), B6, B7 (◊), B8 (⌂), B9 (○), B10 (☆), B11 (○), B12 (□).

3.3.3. Differential scanning fluorometry for *T. lanuginosus* xylanase

The xylanase from *T. lanuginosus*, when compared to the *B. halodurans* xylanase, was not as tolerant for the buffers tested. The maximum temperature was 78°C, with a minimum of 67 °C, showing a 12 °C difference (Table 3.3). The buffer yielding the optimum temperature was 0.73 M Bis Tris pH at 6.5 (Fig. 3.6A) with 0.5 M MES at pH 6 (Fig. 3.6B) and 1 M AmAc at pH 6, both showing a denaturation point of 76 °C. The amplification curve clearly achieved the highest peak at 78°C with 0.73 M Bis Tris at pH 6.5, while the 0.5 M MES at pH 6 and 1 M AmAc at pH 6 both peaked at 76 °C despite the difference in fluorescent emissions (Fig.3.7A). Differential scanning calorimetry results for a phytase produced by *T. lanuginosus* exhibited T_m of 69 °C (Berka *et al.,* 1998 and Maheshwari *et al.,* 2000). Several other buffers tested exhibited similar results confirming the three buffers were by far the most suitable. The dissociation curve again clearly shows the ideal buffers for thermal protection against denaturation. Well A4, 0.73 M Bis Tris at pH 6.5, showed maximum emission at 78 °C (Fig. 3.7B). The xylanase from *T. lanuginosus* showed the greatest increase with regards to DSF results with a maximum T_m at 78 ºC.

Table 3.3: Influence of different buffer conditions on the DSF melting temperature (T_m) for *T. lanuginosus* xylanase (100 mg/ml) using the fluorescent dye Spyro Orange (1 ul) over a temperature range of 25 ºC to 95 °C, at 1 °C min^{-1}.

Well Number	Buffer	Buffer Volume (ml)	3 M NaCl (ml)	Glycerol (ml)	H_2O (ml)	T_m (°C)
A1	1M NaOAc pH 5.1	0.4	0.2	0	0.4	74
A2	**0.5M MES pH 6**	**0.8**	**0.2**	**0**	**0**	**76**
A3	1 M AmAc pH 6	0.4	0.2	0	0.4	76
A4	**0.73M Bis Tris pH 6.5**	**0.4**	**0.2**	**0**	**0.4**	**78**
A5	2M Nakako pH 6.7	0.2	0.2	0	0.6	73
A6	0.5M Imidazole pH 7	0.8	0.2	0	0	75
A7	0.5M MOPS pH 7.2	0.8	0.2	0	0	73
A8	10x PBS pH 7.3	0.4	-	0	0.6	72
A9	1M AmAc pH 7.5	0.4	0.2	0	0.4	73
A10	1M Hepes-Ac pH 7.5	0.4	0.2	0	0.4	70
A11	1M Na-Hepes pH 7.6	0.4	0.2	0	0.4	71
A12	1M Na-Hepes pH 8	0.4	0.2	0	0.4	69
B1	1M Tris/HCl pH 8	0.4	0.2	0	0.4	73
B2	1M Bicin pH 14	0.4	0.2	0	0.4	71
B3	1M PCTP pH 9.5	0.4	0.2	0	0.4	69
B4	0.5 Fosfat pH 10 (Insulin)	0.8	0.2	0	0	67
B5	1M NaHepes pH 7.6	0.4	0.2	0	0.6	69
B6	1M NaHepes pH 7.6	0.4	0.0668	0	0.533	73
B7	1M NaHepes pH 7.6	0.4	0.2	0	0.4	70
B8	1M NaHepes pH 7.6	0.4	0.2	0	0.4	71
B9	1M NaHepes pH 7.6	0.4	0.2	0	0	73
B10	1M NaHepes pH 7.6	0.4	0.2	0.2	0.2	73
B11	1M NaHepes pH 7.6	0.4	0.2	0.4	0	69
B12	1M NaHepes pH 7.6	0.4	0.2	0.2	0	70

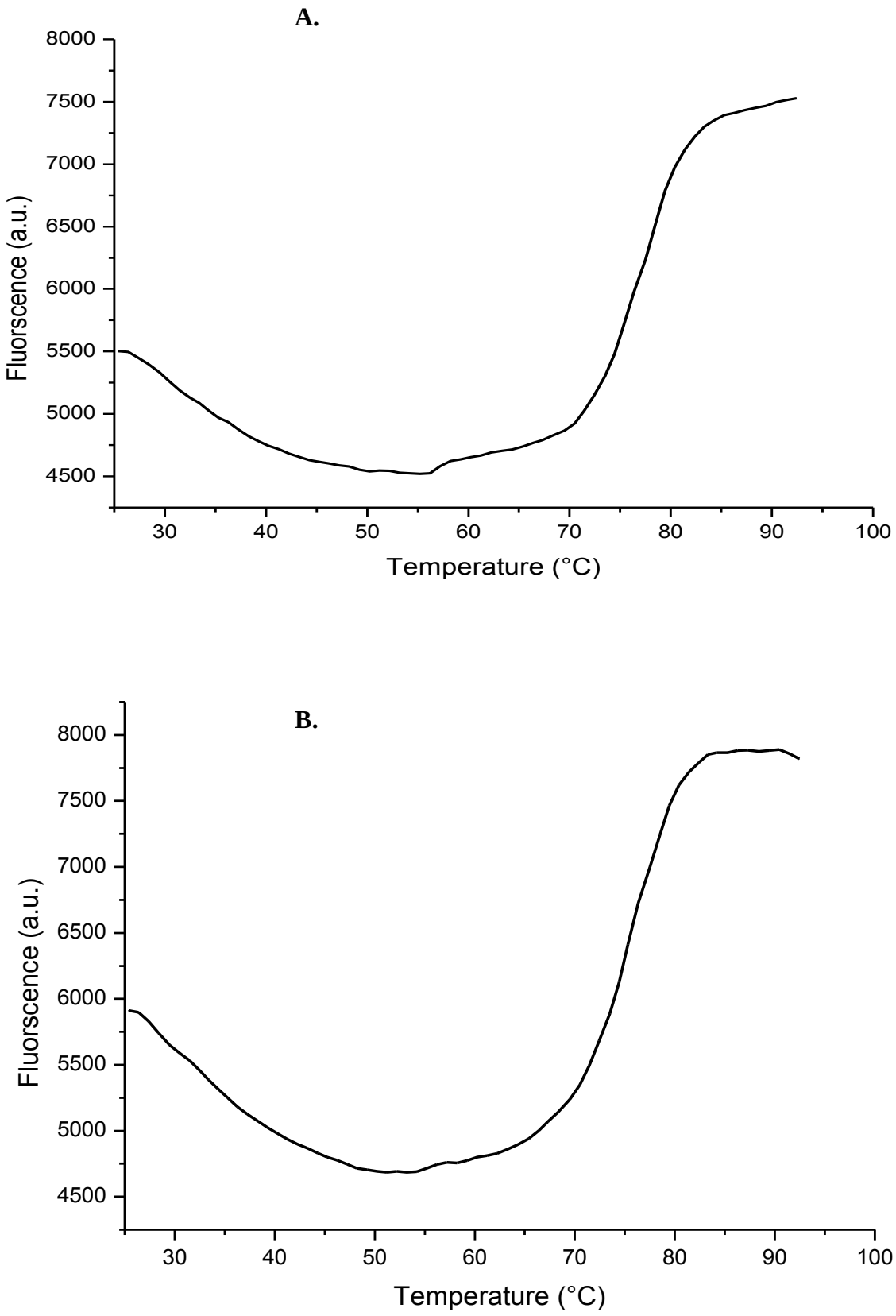

Fig. 3.5: Xylanase from *T. lanuginosus* (100 mg/ml) with Spyro Orange (1 µl) from 25 ºC to 95 °C, at 1 °C min^{-1} with **A.** 0.73 M Bis Tris (pH 6.5) showing a maximum denaturation temperature at 78 °C. **B.** 0.5 M MES (pH 6) showing a maximum denaturation temperature at 76 °C.

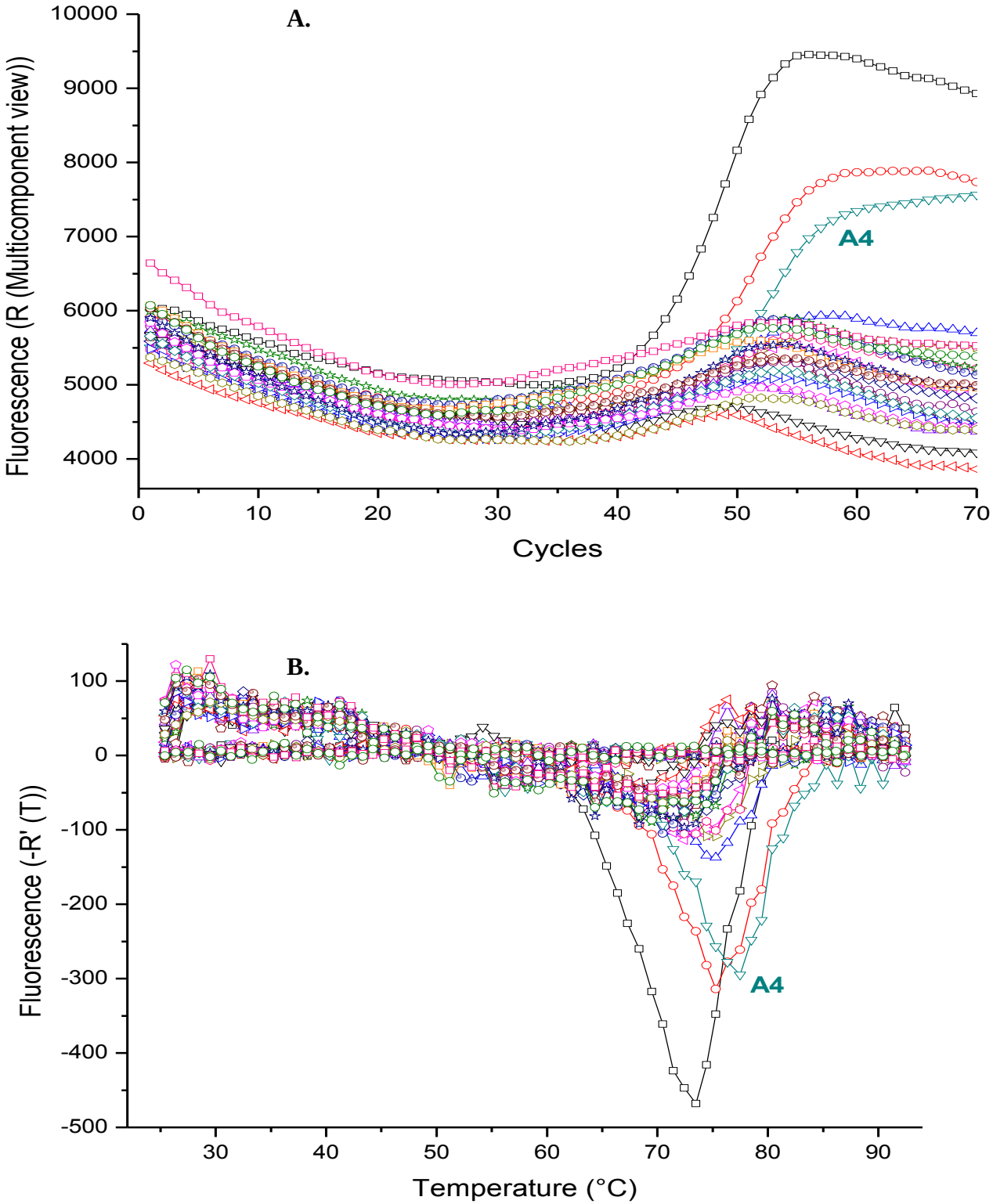

Fig. 3.6: Xylanase from *T. lanuginosus* (100 mg/ml) with Spyro Orange (1 µl) from 25 ºC to 95 °C, at 1 °C min^{-1}. **A.** Amplification curve showing fluorescence against the number of PCR cycles and **B.** Dissociation curve showing fluorescence against temperature using various buffers (Table 3.1): A1 (□), A2 (○), A3 (△), A4 (▽), A5 (◁),A6 (▷), A7 (◊), A8 (⌂), A9 (○),A10 (☆), A11 (□), A12 (○), B1 (○),B2 (△), B3 (▽), B4 (◁), B5 (▷), B6, B7 (◊), B8 (⌂), B9 (○), B10 (☆), B11 (○), B12 (□).

3.3.4. Circular dichroism for *R. marinus* xylanase

R. marinus produces a highly thermostable xylanase that has an optimum activity at 90 °C. The enzyme depicts a 50 % β-sheet conformation comprised of 12 strands and 85 residues along with 3 % α-helical structure comprised of 2 helices and 6 residues (PDB accession no. 1K42). Fig. 3.8A shows an emission at $[\theta]_{240nm}$ of -320 deg.cm^2/dmol at 20 °C. The emission for $[\theta]_{240nm}$ at 20 °C to 60 °C shows similar mean residual ellipticity which indicates no change in conformation over higher temperatures.. The emission increased steadily from around 70 °C to 90 °C as the enzyme would have taken on its optimal conformation as it reaches its optimum temperature for activity. This indicates the onset of changes in the enzyme structure and it can be concluded that the enzyme starts denaturing at this temperature. CD experiments on an α-mannosidase displayed a similar temperature profile where a gradual decrease in ellipiticity was observed with an increase in temperature. Although fluorescence indicated basic unfolding, far UV CD spectra indicated that major unfolding did not take place even at 9 0°C (Shashidhara *et al.*, 2010). The midpoint of the denaturation curve shows the T_m value of 82 °C, which is comparable to the data from DSF. Sazuki *et al.* (2001) reported similar melting profiles for 3-isopropylmalatede hydrogenases that exhibited similar residual activity at thermophilic temperatures. For $[\theta]_{240nm}$, the reverse from 98 °C to 20 °C showed evidence that the xylanase from *R. marinus* is unable to regain its conformation, however, after the temperature was raised to 98 °C giving a [θ] of -220 deg.cm^2/dmol and showing a vast increase from original $[\theta]_{240nm}$, of -290 deg.cm^2/dmol at 20 °C compared with -210 deg.cm^2/dmol . A steady baseline of just over 400 V for both 20 °C to 90 °C and the reverse indicating the signal was of an acceptable level with no interference indicated is shown in Fig. 3.8B.

The fraction of the folded protein (α) for the *R. marinus* xylanase is shown in Table 3.4. From 25 °C to 50 °C (Fig. 3.8A) a minimal change in conformation occurred and at 50 °C an α value of 0.9137 was recorded. At 60 °C, slightly more unfolding was observed with an α value of 0.8633. At 70 °C more than 50 % of the *R. marinus* xylanase remained folded with an α value of 0.615 recorded. The α value at 90 °C, was 0.1383 and this could be attributed to this conformation of the enzyme that allows for optimum activity. All three xylanases exhibited negative ΔG values indicating exothermic reactions that do not need an input of energy. The *R. marinus* xylanase exhibited the same ΔG value of -296.24 kcal.mol^{-1} for 30°C and 40 °C. At 80 °C, a ΔG value of -126.59 kcal.mol^{-1} was exhibited which was a substantial increase from 70 °C, and at 90 °C, ΔG again increased to -34.71 kcal.mol^{-1}. The xylanase from *R. marinus* exhibited the lowest ΔG of -34.71 kJ at 90 °C which was expected as it was optimally active at that temperature.

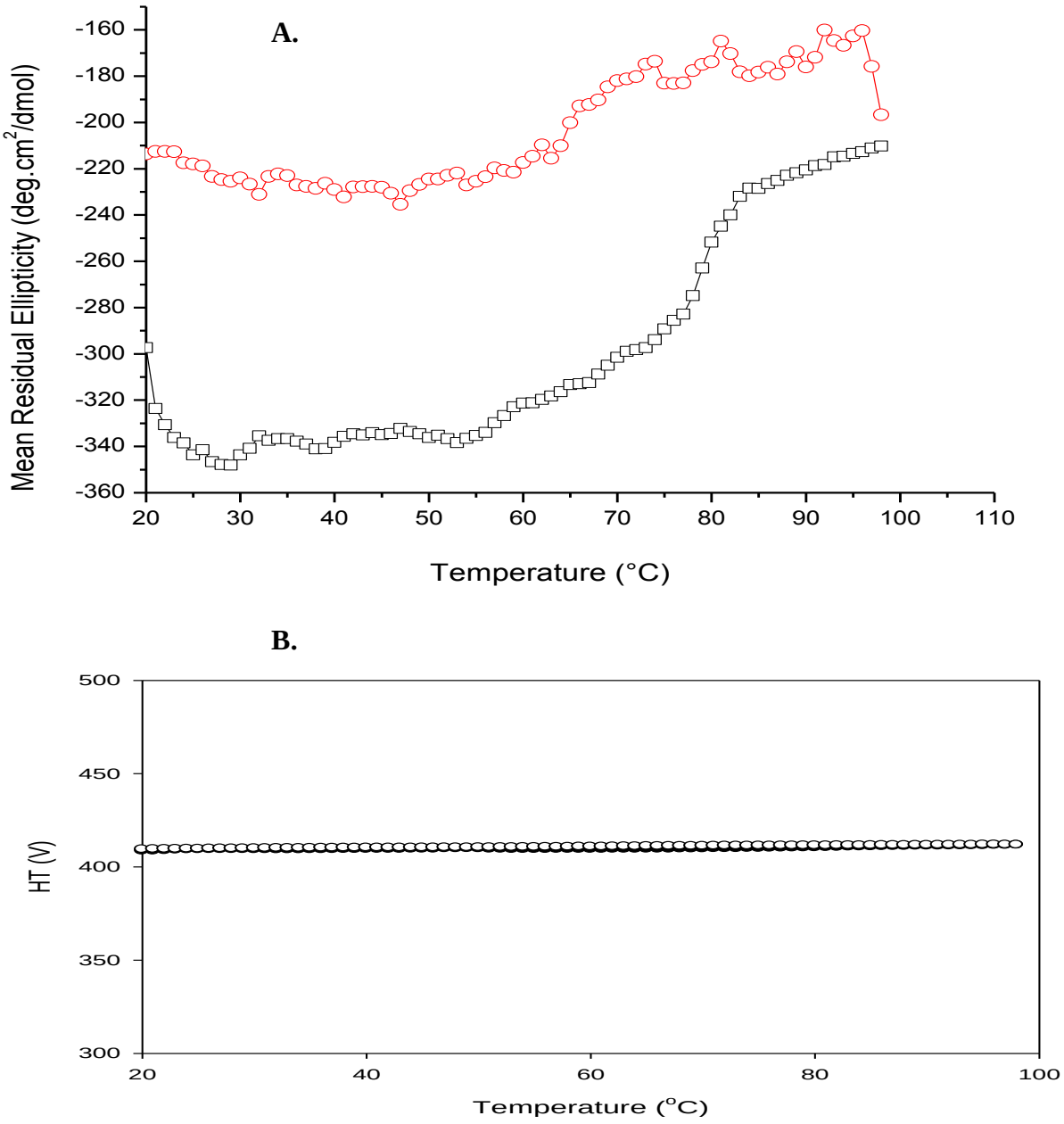

Fig. 3.7: A. Analysis of *R. marinus* xylanase (0.5 mg/ml in 20 mM phosphate buffer) recorded at 220 nm from 20 ºC – 98 ºC (□) and 98 ºC – 20 ºC (○). **B.** Monitoring of CD interference (voltage) from 20 ºC – 98 ºC (●) and 98 ºC – 20 ºC (○).

Table 3.4: Fraction of folded protein (α) and Gibbs free energy of unfolding (ΔG) at increasing temperatures for the *R. marinus* xylanase.

Temperature (°C)	α	ΔG (kcal.mol^{-1})
25	1	-
30	0.9676	-296.2402
40	0.9287	-296.2402
50	0.9137	-301.7223
60	0.8633	-281.0059
70	0.6153	-246.0075
80	0.3007	-126.5883
90	0.1383	-34.7081

3.3.5. Circular Dichroism for *B. halodurans* xylanase

The xylanase from *B. halodurans* has an optimum activity at 70 °C, but is highly alkophilic being stable over a pH range from 7 to 10. The enzyme shows 44 % α-helix conformation comprised of 18 helices and 160 residues along with 16 % β-sheet structure comprised of 19 strands 60 residues (PDB accession no. 2UWF). Fig. 3.9A showed a marked increase in mean residual ellipticity for the xylanase starting at 50 °C tailing off at around 80°C. The $[\theta]_{240nm}$, from 20 °C to 50 °C showed similar values of -370 deg.cm^2/dmol. After 50°C the mean residual ellipticity increased to 80 °C of $[\theta]_{240nm}$ -260 deg.cm^2/dmol. At 80 °C to 95 °C although the results were not smooth there was no significant increase in mean residual ellipticity. As with the xylanase from *R. marinus* (Fig. 3.8A), the xylanase from *B. halodurans* was unable to regain its conformation after the reverse run ending at around –230 deg.cm^2/dmol at 20 °C compared to -340deg.cm^2/dmol at the beginning of the experiment. The midpoint of the denaturation curve shows the T_m value of 68 °C which is comparable to the data from DSF. Hontzeas *et al.* (2004) reported melting curves for 1-

aminocyclopropane-1-carboxylate deaminase that exhibited similarities with the *B. halodurans* xylanase as well as a strong signal at 222 nm which is found to be a characteristic for α helical protein such as the xylanase from *B. halodurans*. Fig. 3.9B showed a voltage of around 480 V for both 20 °C to 95 °C and the reverse with steady baselines showing there was minimal interference and adequate signal.

When compared with the fraction of folded protein, the xylanase from *B. halodurans* showed a larger fraction of unfolding (Table 3.5) when compared with the more thermal active *R. marinus* xylanase. At 30 °C the *B. halodurans* xylanase exhibited an α value of 0.9015 where at 40 °C and 50 °C the enzyme displayed similar α values of 0.8339 and 0.8235 respectively. At 60 °C the fraction of folded protein was 0.4929 which showed a large decrease over 10 °C. At 70 °C the fraction of folded protein was 0.3514 and continued to drop as the temperature was increased. The *B. halodurans* xylanase showed similar ΔG values at lower temperatures. 30 °C, 40 °C, and 50 °C exhibited -262.80 kcal.mol^{-1}, -270.11 kcal.mol^{-1} and -247.02 kcal.mol^{-1} respectively. When compared with the xylanase from *R. marinus, the B. halodurans* xylanase had an increase in free energy at lower temperatures (164.70 kcal.mol^{-1}) at 60 °C and further increasing to -52.71 kcal.mol^{-1} at 70 °C. Higher ΔG values were exhibited for 80 °C and 90 °C of -25.68 kcal.mol^{-1} and -6.21 kcal.mol^{-1} respectively.

The *B. halodurans* xylanase, as expected, displayed an increased unfolding of protein when compared with the more robust xylanase from *R. marinus* as well as higher ΔG values especially at higher temperatures of 80 °C and 90 °C. At 70 °C, the optimum temperature of the *B. halodurans* xylanase, it exhibited 0.3514 folded protein and a ΔG of -52.71 kcal.mol^{-1} which was far lower than both the xylanases from *R. marinus* and *T. lanuginosus*. This could

be explained from chapter II where even though the *B. halodurans* xylanase was optimally active at 70 °C it expressed far lower activity then both the xylanases from *R. marinus* and *T. lanuginosus*.

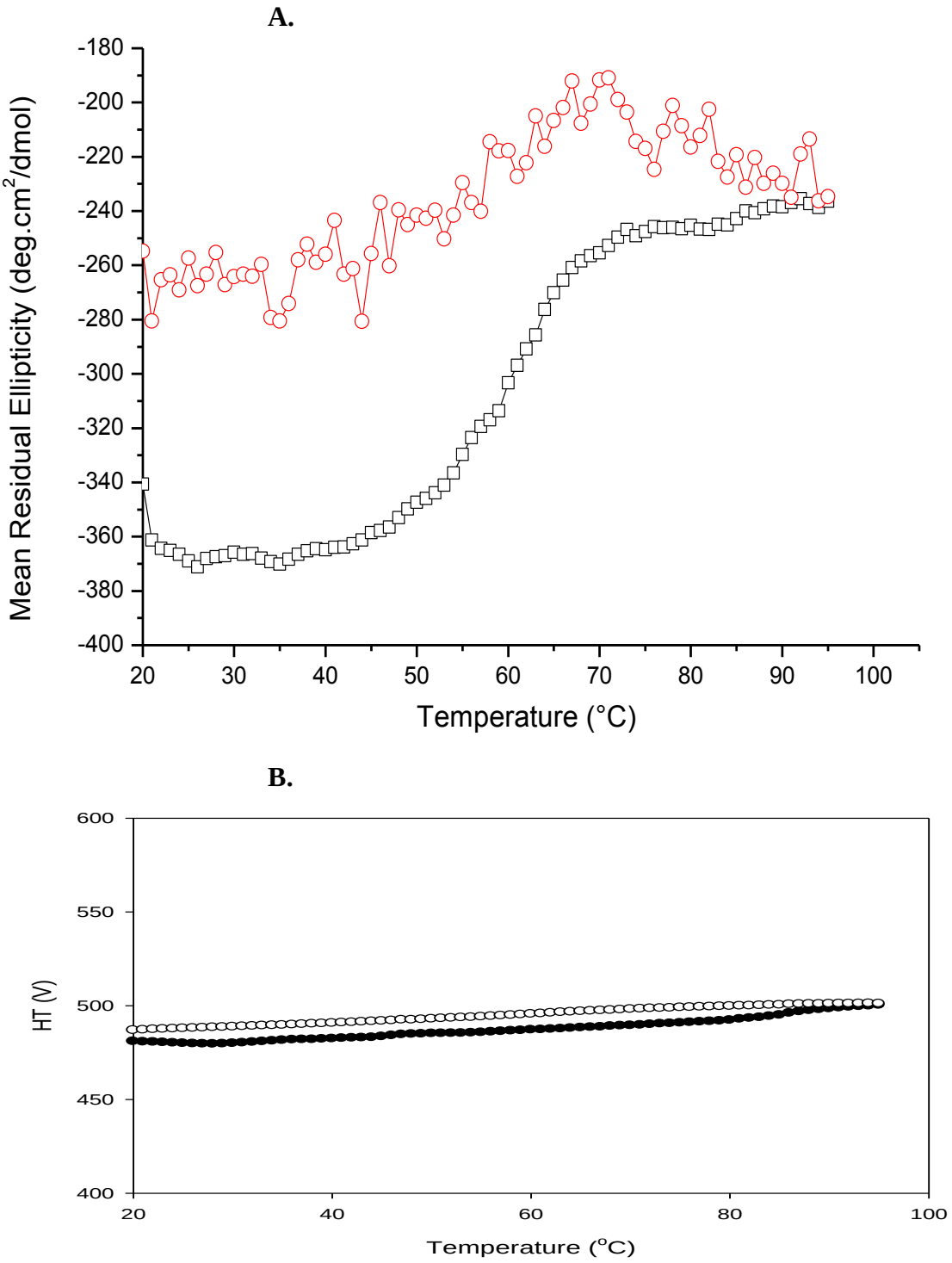

Fig. 3.8: A. Analysis of *B. halodurans* xylanase (0.5 mg/ml in 20 mM phosphate buffer) recorded at 220 nm from 20 ºC – 98 ºC (□) and 98 ºC – 20 ºC (○). **B.** Monitoring of CD interference (voltage) from 20 ºC – 98 ºC (●) and 98 ºC – 20 ºC (○).

Table 3.5: Fraction of folded protein (α) and Gibbs free energy of unfolding (ΔG) at increasing temperatures for the *B. halodurans* xylanase.

Temperature (°C)	α	ΔG (kcal.mol^{-1})
25	1	-
30	0.9015	-262.8093
40	0.8339	-270.1096
50	0.8235	-247.0155
60	0.4929	-164.8965
70	0.3514	-52.7062
80	0.2417	-25.6825
90	0.1738	-6.2056

3.3.6. Circular Dichroism for *T. lanuginosus* xylanase

The xylanase isolated from *T. lanuginosus* has an optimum activity at 70 °C and a β-sheet conformation. The enzyme shows 63% β-sheet conformation comprised of 15 strands and 123 residues along with 5% α-helix structure comprised of 1 helix and 10 residues (PDB accession no. 1YNA). Fig 3.10A shows a slow increase in mean residual ellipticity at 60 °C to 70 °C followed by a steep increase to 80 °C which then remained constant until 95 °C. Similar ellipticity where exhibited for protease subtilisin S41 mutants 3-2G7 and 8-4A9 where the melting curves indicate a substantial structural stabilization in its folded state (Wintrode *et al.*, 2001). The $[\theta]_{240nm}$ at 50 °C was -360 deg.cm^2/dmol and remained so until around 60 °C. The *R. marinus* xylanase showed a similar pattern for the reverse spectra but at 80 °C the increased from -340 deg.cm^2/dmol to -240 deg.cm^2/dmol. The xylanase from *T. lanuginosus* as well as those from *R. marinus* and *B. halodurans*, were unable to regain its confirmation as for the reverse 20 °C the $[\theta]_{240nm}$ was found to be -290 deg.cm^2/dmol compared with -360 deg.cm^2/dmol at the start of the experiment. The midpoint of the

denaturation curve shows the T_m value of 75 °C which is comparable to the data from DSF. Fig 3.10B showed a constant voltage of around 390 V for both 20 °C to 95 °C and the reverse showing an adequate signal and no interference.

The fraction of folded protein for the xylanase from *T. lanuginosus* (Table 3.6) showed minimal unfolding at 30 °C, 40 °C and 50 °C with α values of 0.9805, 0.9738 and 0.9738, respectively. At 60 °C, an α value of 0.8639 was observed showing that from 30 °C to 60 °C very little unfolding of the protein occurred. The optimum temperature for the *T. lanuginosus* xylanase was 50 °C but the enzyme exhibited 91% and 84% relative activity for 60 °C and 70 °C respectively. Being a xylanase that is active at such high temperatures, a lack of unfolding at these temperatures was expected. After 70°C the *T. lanuginosus* xylanase exhibited less than 20 % relative activity and this can be compared with the extremely low α values observed from circular dichroism data, as at 80°C and 90°C the corresponding α values were 0.0260 and 0.0640 respectively, the lowest observed fraction of folded protein for the three xylanases studied. The ΔG at 30°C for the *T. lanuginosus* xylanase was observed to be -313.05 kcal.mol^{-1} which decreased to -322.69 kcal.mol^{-1} and -331.32 kcal.mol^{-1} for 40 °C and 50°C respectively. These were the lowest recorded ΔG values for all three xylanases. At 60 °C, the ΔG value was still very low at -309.01 kcal.mol^{-1} but started to increase at 70 °C, the optimum temperature of the xylanase from *T. lanuginosus*, to -240.96 kcal.mol^{-1}. It showed a dramatic increase in ΔG at 80 °C and 90° C only exhibiting -3.72 kcal.mol^{-1} and -3.03 kcal.mol^{-1} respectively at such high temperatures.

The *T. lanuginosus* xylanase showed the least unfolding and the lowest ΔG values from 30 °C to 70 °C which was as expected due to retaining high relative activity from 50 °C to 70 °C which could suggest robustness under such conditions. As the temperature was increased

to 80 °C and 90 °C, however, the xylanase quickly lost viability exhibiting 0.0260 folded protein and a ΔG of -3.7190 kcal.mol^{-1}.

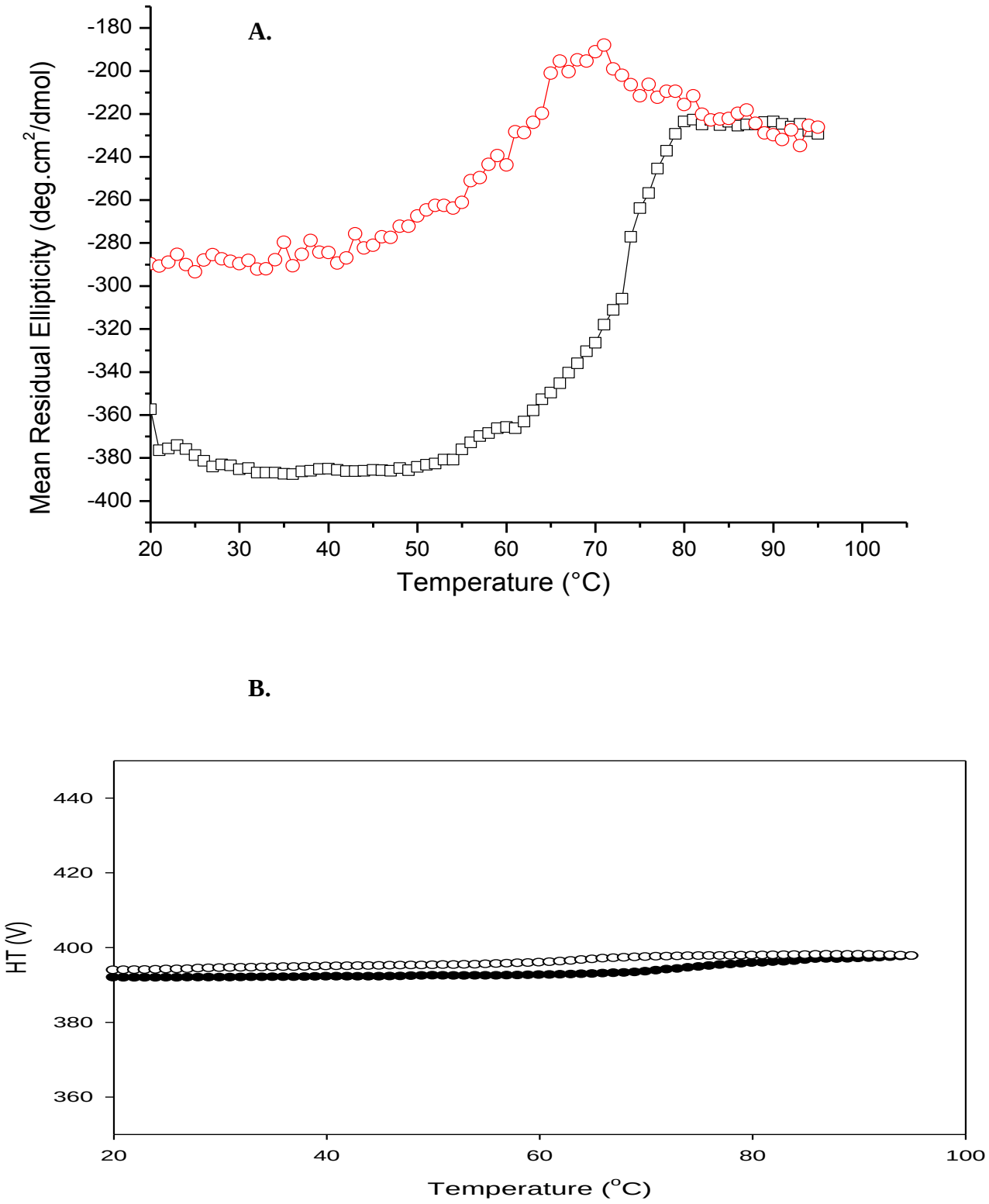

Fig: 3.9. A. Analysis of *T. lanuginosus* xylanase (0.5 mg/ml in 20 mM phosphate buffer) recorded at 220 nm from 20 ºC – 98 ºC (□) and 98 ºC – 20 ºC (○). **B.** Monitoring of CD interference (voltage) from 20 ºC – 98 ºC (●) and 98 ºC – 20 ºC (○).

Table 3.6: Fraction of folded protein (α) and Gibbs free energy of unfolding (ΔG) at increasing temperatures for the *T. lanuginosus* xylanase.

Temperature (°C)	α	ΔG (kcal.mol^{-1})
25	1	-
30	0.9805	-313.0456
40	0.9738	-322.6880
50	0.9738	-331.3231
60	0.8639	-309.0072
70	0.6313	-240.9619
80	0.0260	-3.7190
90	0.0640	-3.0306

3.4. Conclusions

The *R. marinus* xylanase exhibited a fluorescence that indicated a T_m of 89 °C which was comparable to water bath assays in chapter 2. The fraction of folded protein was calculated and although fluorescence indicated basic unfolding, major unfolding did not take place. At 70 °C still over 50 % of fraction folded protein was indicated and at 80 °C and 90 °C negative ΔG of -126.59 kcal.mol^{-1} and -34.71 kcal.mol^{-1}, respectively were exhibited. The xylanase from *R. marinus* displayed the lowest ΔG at 80 °C and 90 °C which was to be expected due to its thermophilic nature and optimum activity at 90 °C.

Results expressed by DSF again reiterated the *B. halodurans* xylanase pH stability as all the T_m were located between 74 °C and 77 °C where it's optimum temperature for activity was 70 °C. However, at 70 °C the fraction of folded protein was recorded as 0.3514 and a ΔG value of -52.71 kcal.mol^{-1} which was far higher than that of the *R. marinus* and *T.*

lanuginosus xylanase. This could be due to the fact that although the *B. halodurans* xylanase was optimally active at 70 °C when compared with the three other xylanases it showed significantly lower activity exhibiting a relative activity of 40 % at its optimum temperature.

The xylanase from *T. lanuginosus* displayed a peak T_m of 78 °C for 0.73 M Bis Tris at a pH of 6.5 which was the highest increase in T_m for the three xylanases tested. The xylanase exhibited 84 % relative activity at 70 °C. The *T. lanuginosus* xylanase exhibited the least decrease in the fraction of folded protein displaying values of 0.9805, 0.9738 and 0.9738 for 30 °C, 40 °C and 50 °C, respectively. At 60 °C a folded fraction of 0.8639 and the lowest ΔG value of -309.01 kcal.mol^{-1}. At 70 °C the ΔG increased to -240.96 kcal.mol^{-1} but the enzyme quickly began to denature at higher temperatures of 80 °C and 90 °C exhibiting a ΔG of -3.72 kcal.mol^{-1} and -3.03 kcal.mol^{-1} and a folded fraction of 0.0260 and 0.0640, respectively. As the xylanase from *T. lanuginosus* exhibited 20 % and 10 % relative activity at 80 °C and 90 °C, these results are to be expected as the enzyme would be undergoing denaturation.

CHAPTER 4: GENERAL DISCUSSION

4.1 The research in perspective

Biotechnology is rapidly entrenching itself into industrial applications in an effort to produce greener, cleaner and more efficient processes. Industries are looking for replacements to harsher chemical processes and biotechnological applications are attempting to fill the niche created by over production and over pollution. The pulp and paper industry is such an industry. Bleaching of the pulp used in the process of creating paper is often accomplished by the addition of liberal amounts chlorine where by biotechnology now offers the alternative of biobleaching, the addition of xylanases to accomplish the same ends and enzymes that exhibit thermostable characteristics have been utilized as a suitable substitute for chlorine chemicals in pulp bleaching (Kulkarni *et al.,* 1999). Biotechnology has played a major role in the advancement of the paper and pulp industry and has attracted considerable interest as a way to overcome many ecological and economical problems related to conventional industrial technologies (Shatalov and Pereira, 2007). There are still challenges facing biobleaching, namely the necessity of tailored enzymes for the process that are able to withstand high temperatures and the alkaline pH's that are prevalent in the biobleaching process as well as the activity at such diverse conditions. Such enzymes are being discovered or in fact created it will lead to more efficient processes and decrease the use of harsher chemicals in the pulp and paper industry as well as other industrial processes (Johannes & Zhao, 2006) and thermostable proteins have been studied extensively to gain insight into the adaptive mechanisms for achieving thermostability (Kinjo and Nishikawa, 2001).

The main focus of this study was to attempt to characterise xylanases possessing thermophilic and alkalophilic traits that would be of use in industrial processes. Their

structures and how they relate to function and activity was also assessed in an attempt to correlate their structure and specific desirable traits to function. Information that has been collected pertaining to the sequence, structure and mutagenesis of enzymes has, however, shown that there is no single mechanism that is responsible for the stability of thermophilic proteins (Vieille and Zeikus, 2001).

The second chapter involved biochemical characterisation and fluorescence spectroscopic analyses at increasing temperatures and the results of salt denaturation with GdnHCl of the four selected xylanases from organisms. Two crude xylanases, one from *R. marinus* a hyperthermophile, a second, *B. halodurans* an alkalophile and *T. lanuginosus* and Pulpzyme HC two commercially available enzymes. The xylanases studied possessed desirable characteristics for study and to be used in industrial processes and such thermostable proteins have been studied extensively to gain insight into the adaptive mechanisms for achieving thermostability (Kinjo and Nishikawa, 2001). The xylanase from *R. marinus* was found to be optimally active at 90 °C, the *B. halodurans* xylanase was found to be optimally active at 70 ºC and active over a wide pH range having a relative activity of over 90 % from pH 7 to 10. The commercially xylanase from *T. lanuginosus* was found to retain over 90 % and 84 % relative activity at 60 ºC and 70 ºC, respectively while Pulpzyme HC had an optimum temperature at 60 ºC and pH 7. Although stability is an important consideration when determining the economic feasibility of introducing an enzyme into an industrial process, some enzymes have genuine temperature optima that are not dictated by conformational stability (Farinas *et al*., 2001 and Daniel *et al*., 2001).

The xylanases activity was then compared using 10 units of the enzyme at their optimum pH. Pulpzyme HC exhibited the highest relative activity even retaining 90 % at 70 ºC. The

xylanases from *B. halodurans* and *T. lanuginosus* were out performed by Pulpzyme HC and the *R. marinus* xylanases. The xylanase from *B. halodurans* only exhibited 40 % relative activity and its optimum temperature. The xylanase from *T. lanuginosus* exhibited superior results having a relative activity of around 75 % at its optimum. The xylanase from *R. marinus* showed approximately 90 % and 95 % at 80 ºC and 90ºC, respectively which when compared with the commercially available xylanase from *T. lanuginosus* and Pulpzyme HC at such high temperatures would suggest it as a desirable enzyme.

Fluorescence spectroscopic analyses of the four xylanases was then performed at increasing temperatures as well as using GdnHCl denaturation. The studies did show similarities in emission spectra and intensities for thermal studies. The denaturation of proteins is the unfolding from a structured native state to an unstructured state with a decreased residual structure which tends toward random coil but proteins rarely exhibiting spontaneous unfolding as the native state exhibits the most stability (Graaf, 2000). The xylanase from *T. lanuginosus* at 70ºC gave off similar emissions when compared with that of the *B. halodurans* xylanase at its optimum temperature of 70ºC. This could show a relationship that both enzymes have a similar conformation with respect to Trp residue position when active at higher temperatures. Consalvi *et al.* (2000) suggested that upon heating, specifically at higher temperatures, the local tryptophan microenvironment is not identical to that of the native state. The *R. marinus* xylanase exhibited the lowest emission intensity which could be due to its structure and the Trp microenvironment that allows it to achieve optimal activity at such high temperatures such as 80ºC and 90ºC and under denaturing conditions the energy transfer from Tyr or Trp residues does not occur anymore and frequently results in increased tyrosine emission in the fluorescence spectra with Tyr

residues fluorescing at 280 nm (Froelich and Yeates, 1976**)**. Pulpzyme HC exhibited a high intensity for 50ºC and 60ºC respectively.

Due to the native state of proteins exhibiting the most stability unfolding is typically studied using chemical denaturants such as GdnHCl and urea which induces varying degrees of unfolding in the domains and loses its residual structure and then increases in size (Vazquez., *et al.,* 1999; Dill and Shortle, 1991). The xylanases from *R. marinus* and *T. lanuginosus* showed only moderate to low susceptibility to chemical denaturation with GdnHCl especially at high temperatures, the conformation due to increasing concentrations of GdnHCl was similar to that of the control. The xylanase from *B. halodurans* showed more of a marked response to GdnHCl as 3.0 M GdnHCl influenced the xylanase the most showing its highest intensity as the structure of the enzyme reacts to increased temperature and salt concentration as the Trp residues are able to fluoresce at a higher rate. Chemical denaturation had the largest effect of Pulpzyme HC as the control always showed the lowest intensity in all three selected temperatures by some degree. At 50ºC the control emissions intensity was around 500 a.u. whereas at a concentration 3.0M the intensity was recorded at over 1400 a.u. Even at its optimum temperature of 50ºC its conformation was vastly changed due to the addition of GdnHCl. This trend continued for 70ºC and 90ºC and can be attributed to conformation becoming increasingly that of a random coil at the highest concentrations of denaturant (Shortle and Ackerman, 2001)

This investigation into fluorescence spectroscopy helped in elucidating information concerning the structural and functional relationship. The enzymes with high levels of activity at high temperatures showed similar low emission intensities and it was shown that Pulpzyme HC, although the best xylan degrader, underwent significant conformational

changes due to the addition of even small amounts of GdnHCl. The xylanase from *B. halodurans*, despite being highly alkalophilic, also exhibited conformational change due to chemical denaturation specifically at high salt concentrations. The xylanases from *R. marinus* and *T. lanuginosus* exhibited only minor changes to the addition of GdnHCl.

Conformational studies were further investigated in chapter four which dealt with differential scanning fluorometry and melting temperatures due to a variety of different buffers and additives as well as conformational circular dichroism studies. The xylanases from *R. marinus* and *B. halodurans* displayed thermo tolerance exhibiting a T_m of 90 °C and pH stability, respectively as was to be expected from earlier studies. The proteins stability is linked to the ΔG which is temperature dependant (Schellman, 1997 and Privalov, 1979) and as the temperature increases so too does the stability and ΔG which indicates that concentrations of folded and unfolded proteins are equal. This point of zero ΔG is considered the melting temperature (T_m) (Brandts, 1990). The *R. marinus* xylanase exhibited a melting temperature (T_m) of 89 ºC where as the alkalophilic xylanase from *B. halodurans* exhibited T_m ranging from only 74 ºC to 77 ºC which highlighted both its pH stability and its thermophilic nature. The xylanase from *T. lanuginosus* displayed the greatest increase in T_m from the buffer mixture. Its optimum temperature for xylan hydrolysis was found to be 50ºC although it did exhibit up to 84% relative activity for 70 ºC. A T_m of 78 ºC is an 8 °C increase using 0.73 M Bis Tris pH 6.5. The use of 0.5 M MES pH 6 buffer also gave a good increase in T_m to 76 ºC.

All three xylanases investigated exhibited thermophilic properties, the *R. marinus* xylanase, a hyperthermophile with an optimum activity at 90 ºC, the *B. halodurans* xylanase having an optimum temperature for activity at 70 ºC and the xylanase from *T. lanuginosus*

retaining over 84 % relative activity at 70 ºC. All three enzymes lost conformation and were unable to regain it after such high temperatures, but all three xylanases exhibited negative ΔG values indicating exothermic reactions that do not need an input of energy. Afzal *et al.* (2005) suggests that lower ΔG values indicate the action of transition complex into products as increasingly spontaneous and due to lower changes of free energy would translate to more feasible and spontaneous reactions. The *R. marinus* xylanase exhibited the highest temperature for optimum activity also showed the lowest ΔG, -34.71 kcal.mol^{-1}, at 90 °C which was expected. The xylanase from *B. halodurans* with an optimum activity at 70 °C exhibited 0.3514 of folded protein and a ΔG of -52.71 kcal.mol^{-1} with when compared with the 0.6153 and -246.01 kcal.mol^{-1} of the *R. marinus* xylanase and 0.6313 and -240.96 kcal.mol^{-1} for the xylanase from *T. lanuginosus*, is low in comparison. An explanation can be found when compared in terms of relative activity however from fig. 2.3 where the *B. halodurans* was found to have significantly lower relative activity. The *T. lanuginosus* showed the highest values for all three enzymes from 30 °C to 60 °C. At 60 °C the fraction of folded protein was still 0.8639 and it still retained a ΔG of -309.01 kcal.mol^{-1}. Even at 70 °C the fraction of folded protein for the *T. lanuginosus* xylanase was found to be 0.6313 and -240.96 kcal.mol^{-1} for ΔG. From fig. 2.8 it can be seen that the xylanase from *T. lanuginosus*, although showing an optimum temperature of 50 °C, 84 % relative activity and the majority of conformation was still retained at 70 °C.

Evolution of this study confirms that the action on xylan hydrolysis among the four different xylanases as well as increasing the knowledge of the structural and functional relationships of the enzymes. It demonstrated the importance of understanding the structure and function relationship of enzymes and the further work that is still necessary. The majority of current studies only investigate typical pH and temperature data during incubation if water

baths, which are often found not to be accurate or reveal sufficient information pertaining to the structure-function relationship of enzymes. This study was able to demonstrate this and helps pave the way to apply similar methods to enzymes that are rapidly evolving as a result of directed evolution. Through fluorescence spectroscopy, structural similarities were seen between the three more thermophilic enzymes where as the commercially available Pulpzyme HC showed a susceptibility to chemical denaturation. DSF was particularly beneficial for the xylanase from *T. lanuginosus* where it obtained a melting temperature of 78ºC. Assessing diverse enzymes such as the hyperthermophilic xylanase from *R. marinus* and the alkalophilic xylanase from *B. halodurans* provided further insight into the structure-function relationship and how these desirable traits could best be used for industrial processes.

4.2 Future prospects for research

Further work into the structure and function relationship of not only xylanases but other enzymes will lead to accumulating data and increasing the understanding of what exactly it is that gives thermopiles the ability and conformation to remain active at such high temperatures. Enzymes isolated from thermophilic organisms most often tend to retain activity at their high temperature optima whilst their mesophilic counterparts are optimally active at their own temperature optima (Jaenicke and Bohm, 1998) and while enzymes such as some fungal strains have genuine temperature optima that are not always dictated and reliant on conformational stability (Daniel *et al*., 2001) most enzyme activity at high temperatures, pH and other conditions are based upon its conformation.

Thermal adaptation, however, cannot be completely attributed to any specific characteristic but rather is an amalgamation of various changes and processes that contribute

to the overall stability of an organism. Characteristics including membrane lipid composition, protein structure and synthesis or thermostabilizing substances found in the cytoplasm could all contribute to overall stability (Rizzatti and Sandrim, 2004).

Therefore further study in an organisms ability to perform and remain active under different stressful conditions is needed. With respect to conformation further work involving CD can be done with chemical denaturants to assess how the conformation changes. Other enzymes can be studies that posses inherent characterises that valued in industry such as thermo and pH stability, high activities, or even pyscrophiles to assess their conformations at ranging conditions. Studies into the ability of chaperonins that are responsible for assisting in protein refolding in their active form could also be important to further understanding (Everly and Alberto, 2000). The effect of the conformation of the enzymes and the relationship which allows the enzyme to retain function and activity would be crucial in further understanding the structure-function relationship. Molecular techniques could also be of great assistance is isolating and even reproducing the valued characteristics of different enzymes in an attempt to create more robust enzymes that are tailored to suit specific processes.

5. REFERENCES

Abou-Hachem, M., Olsson, E. and Nordberg-Karlsson, E. 2003. Probing the stability of the modular family 10 xylanase from *Rhodothermus marinus*. *Extremophiles*, **7**: 483-491.

Adler, J., Hazelbauer, G.L. and Dahl, M.M. 1973. Chemotaxis toward sugars in *Escherichia coli*. *Journal of Bacteriology*, **115:** 824-847.

Afzal, A.J., Ali, S., Latif, F., Rajoka, M.I. and Siddiqui, K.S. 2005. Innovative kinetic and thermodynamic analysis of a purified superactive xylanase from *Scopulariopsis* sp. *Applied Biochemistry and Biotechnology*, **120:** 51–70.

Anand, L., Krishnamurthy, S. and Vithayathil, P.J. 1990. Purification and properties of xylanase from thermophilic fungus, *Humicola lanuginose*. *Archives of Biochemistry and Biophysics*. **276:** 546–553.

Arai, M. and Kuwajima, K. 2000. Role of the molten globule state in protein folding. *Advanced Protein Chemistry*, **53:** 209-82.

Bailey, M.J., Biely, P. and Poutanen, K. 1992. Interlaboratory testing of methods for assay of xylanase activity. *Journal of Biotechnology*, **23:** 257–270.

Bajpai, P. 1999. Application of enzymes in the pulp and paper industry. *Biotechnology Progress*, **15:** 147–157.

Bajpai, P., Bhardwaj, N.K., Bajpai, P.K., Jauhri, M.B. 1994. The impact of xylanases on bleaching of eucalyptus Kraft pulp. *Journal of Biotechnology*, **38:** 1–6.

Ballery, N., Desmadril, M., Minard, P. and Yon, J. M. 1993. Characterization of an intermediate in the folding pathway of phosphoglycerate kinase: chemical reactivity of genetically introduced cysteinyl residues during the folding process. *Biochemistry*. **32**: 708 - 714.

Behlke, M.A., Huang, L., Bogh, L., Scott Rose, S. Devor, E.J. 2005. Fluorescence and Fluorescence Applications. *Integrated DNA Technologies*, 1-13 http://www.idtdna.com/support/technical/TechnicalBulletinPDF/fluorescence_and_fluorescence_applications.pdf

Becker, P., Abu-Reesh, I., Markossian, S., Antranikian, G. and Ma¨rkl, H. 1997. Determination of the kinetic parameters duringcontinuous cultivation of the lipase-producing thermophile *Bacillus* sp. IHI-91 on olive oil. Applied Microbiology and Biotechnology, **48:** 184–90.

Bedford M.R., Classen H.L. 1992. The influence of dietary xylanase on intestinal viscosity and molecular weight distribution of carbohydrates in rye-fed broiler chick. Xylans and xylanases. In: Visser, J, Beldman, G, van Someren, M.A.K., Voragen, A.G.J. (eds). Xylans and xylanases. *Elsevier, Amsterdam*, 361–370

Beg, Q.K., Kapoor, M., Mahajan, L., Hoondal, G.S. 2001. Microbial xylanase and their industrial application: a review. *Applied Microbiololgy and Biotechnology*, **56:** 326–338.

Berka, R. M., Rey, M.W., Brown, K.M., Byun, T. and Klotz, A.V. 1998 Molecular Characterization and Expression of a Phytase Gene from the Thermophilic Fungus *Thermomyces lanuginosus***.** *Applied and Environmental Microbiology*, **64:** 4423-4427.

Bhat, M.K. 2000. Cellulases and related enzymes in biotechnology. *Biotechnology advances*, **18:** 355-383.

Bhardwaj, N. K., Bajpai, P. and Bajpai, P. K. 1996. Use of enzymes in the modification of fibres for improved beatability. *Journal of Biotechnology*, **51:** 21-26.

Biely, P. 1985 Microbial xylanolytic systems. *Trends in Biotechnology*, **3:** 286–290

Blanchard, J.E. and Withers, S.G. 2001. Rapid screening of the aglycone specificity of glycosidases: Applications to enzymatic synthesis of oligosaccharides. *Chemistry and Biology*, **8***:* 627-633.

Bjornsdottir, S.H., Fridjonsson, O.H., Hreggvidsson, G.O. and Eggertsson, G. 2011. Generation of targeted deletions in the genome of *Rhodothermus marinus*. *Applied and Environmental Microbiology*, **77:** 5505-5512.

Bradford, M. M. 1976. *Analytical Biochemistry*, **72:** 248–254.

Brandts, J.F. 1990. Study of strong to ultratight protein interactions using differential scanning calorimetry. *Biochemistry,* **29:** 6927–6940.

Bray, M. R. and Clarke, A. J. 1990. Essential carboxy groups in xylanase A. *Biochemical Journal*, **270:** 91-96.

Buchholz, K. and Seibel, J. 2008. Industrial carbohydrate biotransformations. *Carbohydrate Research,* **343:** 1966-1979.

Burstein, E. A. 1977. Intrinsic protein luminescence. The nature and application. *Advances in Science and Technology*, **7.**

Burstein, E. A., Vedenkina, N. S. and Ivkova M. N. 1973. Fluorescence and the location of tryptophan residues in protein molecules. *Photochemistry* and *Photobiololgy,* **18:** 263–279.

Cesar, T. and Mrsa, V. 1996. Purification and properties of the xylanase produced by *Thermomyces lanuginosus*. *Enzyme and Microbial Technology*, **19:** 289-296.

Chauthaiwale, J. and Rao, M. 1994. Chemical modification of xylanase from alkalothermophilic Bacillus species: evidence for essential carboxyl group. *Biochimica et Biophysica Acta*, **1204:** 164-168.

Cherry J.R. and Fidantstef, A.L. 2003. Directed evolution of industrial enzymes: an update. *Current Opinion in Biotechonology,* **14:** 438-433.

Collins, T., Gerday, C. and Fellar G. 2005. Xylanases, xylanase families and extremophilic xylanases. *FEMS Microbiology Reviews,* **29:** 3-23.

Consalvi, V., Chiaraluce, R., Giangiacomo, L., Scandurra, R., Christova, P., Karshikoff, A., Knapp, S. and Ladenstein, R. 2000. Thermal unfolding and conformational stability of the recombinant domain II of glutamate dehydrogenase from the hyperthermophile *Thermotoga maritima. Protein Engineering,* **13:** 501-507.

Cooney, D.G. and Emerson, R. 1964. Thermophilic Fungi: An Account of their Biology, Activities and Classification. Freeman, San Francisco, CA. 80-88.

Coutinho, P.M. and Henrissat, B. 1999. Carbohydrate-active enzyme server (CAZY) at URL: http://afmb.cnrsmrs.fr/~cazy/CAZY/.

Covarrubias, R. 2006. Fiber modification through biotechnology. *Pulp & Paper,* **80.**

Csiszar, M., Losonczi, A., Szakacs,G, Rusznak, I., Bezur, L. and Reicher, J. 2001. Enzymes and chelating agent in cotton pretreatment. *Journal of Biotechnology,* **89:** 271-279.

Dahlberg, L., Holst, O. and Anker, L. 1995. United States Patent. Patent number 5,395,765.

Daniel, R.M., Danson, M.J. and Eisenthal, R. 2001. The temperature optima of enzymes: a new perspective on an old phenomenon. *Trends in Biochemical Science,* **26**: 223-225.

Danson, M.J., Hough, P.L., Russel, D.W. and Taylor, G.L. 1996. Enzyme thermo stability and thermo activity. *Protein Engineering,* **9:** 629-630.

Dash, C., Vathipadiekal, V., George, S.P. and Rao, M. 2002. Slow-tight binding inhibition of xylanase by an aspartic protease inhibitor. *Journal of Biological Chemistry,* **277:** 17978-17986.

Davies, G. and Henrissat, B. 1995. Structures and mechansism of glycosyl hyrdrolases *Structure,* **3:** 853-859.

Davoodi, J. 1996. *Bacillus circulans* xylanase: Stability and mechanism of action. Ph. D. Thesis. University of Ottawa, Canada.

Dekker, R. 1985. Biodegradation of the hemicelluloses. Biosynthesis and biodegradation of wood components. *Orlando Florida: Academic Press*, 505–533.

Demchenko, A. P. 1986. Ultraviolet Spectroscopy of Proteins. *Springer-Verlag. Berlim Heidelberg New York.*

Deshpande, V., Hinge, J. and Rao, M. 1990. Chemical modification of xylanases: evidence for essential tryptophan and cysteine residues at the active site. Biochimica et Biophysica Acta, **1041:** 172-177.

Dib, J.R., Weiss, A., Neumann, A., Ordonez, O., Estevez, M. C. and Farias, E. 2009. Isolation of bacteria from remote high altitude Andean Lakes able to grow in the presence of antibiotics. *Recent patents on anti-infective drug discovery*, **4:** 66-76.

Dill, K. A. and Shortle, D. 1991. Denatured state of proteins. Annual *Review of Biochemistry*, **60:** 795–825.

Edward, V.A., Pillay, V.L, Swart, P. and Singh, S. 2002. Localisation of *Thermomyces lanuginosus* SSBP Xylanase on polysulphone membranes using immunogold labelling and environmental scanning electron microscopy (ESEM). *Process Biochemistry*, **38:** 939-943

Eftink, M. R. 1994. The use of fluorescence methods to monitor unfolding transitions in proteins. *Biophysical Journal*, **66:** 482-502

Eichler, J. 2001. Biotechnological uses of archaeal extremozymes. *Biotechnology Advances*, **19:** 261-278.

Emerson, R. 1968. Thermophiles. In: The Fungi - An Advanced Treatise (Answorth, G.C. and Sussman, A.S., Eds. *Academic Press, London*, 105-128.

Epps, D.E., Sarver, R.W., Rogers, J.M., Herberg, J.T. and Tomich, P.K. 2001. The ligand affinity of proteins measured by isothermal denaturation kinetics. *Analytical Biochemistry*, **292:** 40–50.

Ericsson, U.B., Hallberg, M.B., DeTitta, G.T., Dekker, N. and Nordlund, P. 2006. Thermofluor based high-throughput stability optimization of proteins for structural studies. *Analytical Biochemistry*, **357:** 289–298.

Everly, C. and Alberto, J. 2000. Stressors, stress and survival: overview. *Frontiers in Bioscience*, **5:** 780-786.

Farinas, E.T., Bulter, T. and Arnold, F.H. 2001. Directed enzyme evolution. *Current Opinion in Biotechnology*, **12**: 545-551.

Favilla, R., Goldoni, M., Mazzini, A., Muro, P. D., Salvato, B. and Beltramini, M. 2002. Guanidinium chloride induced unfolding of hemocyanin subunit from *Carcinus aestuarii* I. Apo form. *Biochimica et Biophysica Acta*, **1597:** 42-50

Fittera, J., Herrmannb, R., Hau, T., Lechnerd, R.E. and Dencherb, N.A. 2001. Dynamical properties of α-amylase in the folded and unfolded state: the role of thermal equilibrium fluctuations for conformational entropy and protein stabilisation. *Physica B*, **301:** 1–7.

Flores, H. and Ellington, A.D. 2002. Increasing the thermal stability of an Oligomeric protein, Beta-glucuronidase. *Journal of Molecular Biology*, **315**: 325-337.

Froelich P.M. and Yeates, M. 1976 The effect of mixed aqueous solvent systems on the fluorescence of indoles and aromatic amino acids and their metabolites. *Analytica Chimica Acta*, **87:** 185–191.

Gashaw, M. 2006. An alkaline active endo-xylanase from *Bacillus halodurans* S7: Molecular and structural aspects. Doctoral dissertation. Lund University.

Gashaw, M., Hatti-Kaul, R. and Mattiasson, B. 2006. A thermostable alkaline active endo-β-xylanase from *Bacillus halodurans* S7: Purification and characterization. *Enzyme and Microbial Technology,* **39:** 1492-1498.

George, S.P. 2001. *Molecular and biochemical aspects of extremophilic actinomycete*. Ph. D Thesis. University of Poona, India.

Gilkes, N. R., Henrissat, D. G., Kilburn, R. C., Miller, Jr., and Warren, R. A. J. 1991. Structural and functional relationships in two families of beta-1,4-glycanases. *Microbiology and Molecularbiology Reviews,* **55:** 303-315.

Glazer, A. N., Delange, R. J. and Sigman, D. S. 1975. In Chemical Modification of Proteins: Selected Methods and Analytical Procedures. *Elsevier Medical Press, Amsterdam.*

Graaf, L. A. D. 2000. Denaturation of proteins from a non-food perspective. *Journal of Biotechnology*, **79:** 299-306

Gruber, K., Klintschar, G., Hayn, M., Schlacher, A., Steiner, W. and Kratky, C. 1998. Thermophilic Xylanase from *Thermomyces lanuginosus*: High-Resolution X-ray Structure and Modeling Studies. *Biochemistry,* **37:** 13475-13485.

Gupta, S and Gupta, M.N. 1993. Mechanisms of irreversible thermo-inactivation and medium engineering. *Thermostability of enzymes*, 114-122. Gupta, M.N. (ed.) Narosa Publishing House, New Delhi.

Hardy, L. A. W. and Poteete, A. R. 1991. Reexamination of the role of Asp20 in catalysis by bacteriophage T4 lysozyme. *Biochemistry.* **30:** 9457-9463.

Harris, G.W., Jenkins, J.A., Connerton, I., Cummings, N., Lo Leggio, L., Scott, M., Hazlewood, G.P., Laurie, J.I., Gilbert, H.J. and Pickersgill, R.W. 1994. Structure of the catalytic core of the family F xylanase from *Pseudomonas fluorescens* and identification of the xylopentaose-binding sites. *Structure*, **2:** 1107–1116.

Hashimoto S, Muramatsu T. and Funatsu M. 1971. Studies on xylanase from Trichoderma viride. Part I: Isolation and some properties of crystalline xylanase. *Agricultural and Biological Chemistry,* **35:** 501–508.

He, J., Yu, B., Zhang, K., Ding, X. and Chen, D. 2009. Expression of endo-1, 4-beta-xylanase from *Trichoderma reesei* in *Pichia pastoris* and functional characterization of the produced enzyme. *BMC Biotechnology*, **9:** 56-66.

Henrissat, B. 1991. A classification of glycosyl hydrolases based on amino acid sequence similarities. *Biochemical Journal*, **280:** 309-316

Henrissat, B. and Bairoch, A. 1993. New families in the classification of glycosyl hydrolases based on amino acid sequence similarities. *Biochemical Journal*, **293:** 781-788.

Hibbert, E.G. and Dalby, P.A. 2005. Directed evolution strategies for improved enzymatic performance. *Microbial Cell Factories*, **4:** 29.

Hoebler, C. and Brillouet, J. M. 1984. Purification and properties of an endo-(1->4)-β-d-xylanase from *Irpex lacteus* (*Polyporus tulipiferae)*. *Carbohydrate Research*, **128:** 141-155.

Hontzeas, N., Zoidakis, J., Glick, B.R. and Abu-Omar, M.M. 2004. Expression and characterization of 1-aminocyclopropane-1-carboxylate deaminase from the rhizobacterium *Pseudomonas putida* UW4: a key enzyme in bacterial plant growth promotion. *Biochimica et Biophysica Acta*, **1703:** 11 –19

Huang, L. Hseu, T.Z. and Wey, T. 1991. Purification and characterization of an endoxylanase from *Trichoderma koningii* G-39. *Journal of Biochemistry,* **278:** 329- 333.

Jaenicke, R. and Bohm, G. 1998. The stability of proteins in extreme environments. *Current Opinion in Structural Biology* **8**: 738-748.

Jaenicke, R., Schurig, H., Beaucamp, N. and Ostendorp, R. 1996. Structure and stability of hyperstable proteins. Glycolytic enzymes from hyoerthermophilic bacterium *Thermotoga maritime. Advances in Protein Chemistry*, **48:** 181-269.

Jaenicke, R. 1987. Folding and association of proteins. *Progress in Biophysics and Molecular Biology,* **49:** 117-237.

Jagannathan, V., Singh, K. and Damodaran, M. 1956. Carbohydrate metabolism in citric acid fermentation. 4. Purification and properties of aldolase from *Aspergillus niger Biochemical Journal,* **63:** 94-105.

Jagtap, S and Rao, M. 2009. Fluorscence study on interactions of α-Crystallin with the molten globule state of 1,4-β-D-Glucan Glucanohydrolase from *Thermomonospora* sp. induced by guanidine hydrochloride. *Journal of Fluorescence*. **19:** 967-973.

Jana, S., Kumar Chaudhuri, T. and Deb, J.K. 2006. Effects of Guanidine Hydrochloride on the Conformation and Enzyme Activity of *Streptomycin Adenylyltransferase* Monitored by Circular Dichroism and Fluorescence Spectroscopy. *Biochemistry (Moscow),* **71:** 1230-1237.

Janardhnan, S. and Sain, M. M. 2006. Isolation of cellulose microfibrils-An enzymatic Approach. *Bioresources,* **1:** 176-188

Jeffries, T.W. 1996. Biochemistry and genetics of microbial xylanases. *Current Opinions in Biotechnology*, **7:** 337–342.

Jiao, M., Zhou, Y., Li, H., Zhang, D., Chen, J. and Liang, Y. 2010. Structural and functional alterations of two multidomain oxidoreductases induced by guanidine hydrochloride. *Acta Biochimica et Biophysica Sinica*, **42:** 30–38

Johannes, T.W. and Zhao, H. 2006. Evolution of enzymes and biosynthetic pathways. *Directed Current Opinion in Microbiology,* **9:** 1-7.

Joseleau, J. P., Comtat, J. and Ruel, K. 1992. *Xylan and Xylanases. Biotechnology Progress,* **7:** 1-15

Kaur, R., Dikshit, K.L. and Raje, M. 2002. Optimization of immunogold labeling TEM: An elisa-based method for evaluation of blocking agents for quantitative detection of antigen. *Histochemistry & Cytochemistry,* **50:** 863-873.

Kapoor, M., Beg, Q.K., Bhushan, B,, Singh, K., Dadhich, K.S. and Hoondal, G.S. 2001. Application of an alkaline and thermostable polygalacturonase from Bacillus *sp.* MG-cp-2 in degumming of ramie (*Boehmeria nivea*) and sunn hemp (Crotalaria juncea) bast fibers. *Process Biochemistry,* **36:** 803–807

Keskar, S. S., Srinivasan, M. C. and Deshpande, V. V. 1989. Chemical modification of a xylanase from a thermotolerant *Streptomyces*. Evidence for essential tryptophan and cysteine residues at the active site. *Biochemical Journal,* **261:** 49-55.

Khandke, K.M., Vithayathil, P.J. and Murthy, S.K. 1989. Purification and characterization of an alpha-D-glucuronidase from a thermophilic fungus, *Thermoascus aurantiacus*. *Archives of Biochemistry and Biophysics,* **274:** 491-500.

Khasin, A., Alchanti, I. and Shoham, Y. 1993. Purification and characterization of a thermostable xylanase from *Bacillus stearothermophilus* T-6. *Applied Environmental Microbiololgy,* **59:** 1725-1730.

Kinjo, A.R. and Nishikawa, K. 2001. Comparison of energy components of proteins from thermophilic and mesophilic organisms. *European Biophysics Journal,* **30**: 378-384.

Kirk, O., Borchert, T.V. and Fuglsang, C.C. 2002. Industrial enzyme applications. *Current Opinions in Biotechnology*, **13:** 345- 351.

Kolarova, N. and Farkas V. 1983. Laminarinases, xylanases and amylases in the crude cellulolytic enzyme complex from Trichoderma reseei. *Biologia (Bratislava),* **38:** 721–725.

Krahe, M., Antranikian, G. and Ma¨rkl, H. 1996. Fermentation of extremophilic microorganisms. *FEMS Microbiology Review,* **18:** 271 – 85

Krishnamurthy, S. 1989. Organometallic chemistry of diphosphazane ligands PhD thesis, Indian Institute of Science, Bangalore, India.

Kubackova, M., Karacsonyi, S., Bilisics. and Toman, R. 1978. Some properties of an endo-1,4-beta-D-xylanase from the ligniperdous fungus Trametes hirsute. *Folia Microbiologica,* **23:** 202-209.

Kuhad, R.C. and Singh, A. 1993. Lignocellulose biotechnology: Current and future prospects. *Critical Reviews in Biotechnology,* **13:** 151–72.

Kulkarni, N., Shendye, A. and Rao, M. 1999. Molecular and biotechnological aspects of xylanases. *FEMS Microbiology*, **23:** 411–456

Kumar, H.D. and Swati, S. 2001. Modern Concepts of Microbiology, second revised ed. Vikas Publishing House Pvt. Ltd., New Delhi, 455.

Laemmli, U.K. 1970. Cleavage of structural proteins during the assembly of the head of bacteriophage T4. *Nature*, **227:** 680-685.

Lakowicz, J. R. 1983. Principles of Fluorescence Spectroscopy. *Plenum Press, New York,* 76-78.

Lakowicz, J. R. 1999. Principles of Fluorescence Spectroscopy. *2nd Ed. Plenum Press, New York, 698.*

Lo, M.C. Aulabaugh, A., Jin, G., Cowling, R., Bard, J., Malamas, M. and Ellestad, G. 2004. Evaluation of fluorescence-based thermal shift assays for hit identification in drug discovery. *Analytical Biochemistry*, **332:** 153–159.

Lopez, G., Banares-Hidalgo, A. and Estrada, P. 2011. Xylanase II from Trichoderma reesei QM 9414: conformational and catalytic stability to Chaotropes, Trifluoroethanol, and pH changes. *Journal of Industrial Microbiology and Biotechnology*, **38:** 113-125.

Lüthi, E., Reif, K., Jasmat, N. B. and Bergquist, P. L. 1992. In vitro mutagenesis of a xylanase from the extreme thermophile *Caldocellum saccharolyticum*. *Applied Microbiology and Biotechnology*, **36:** 503-506.

Maat J., Roza M., Verbakel J., Stam H., daSilra M.J.S., Egmond M.R., Hagemans M.L.D., van Garcom R.F.M., Hessing J.G.M., van Derhondel C.A. and van Rotterdam, C. 1992. Xylanases and their application in bakery. Xylans and xylanases. *Elsevier, Amsterdam* 349–360

McCoy, M. 2000. Novozymes emerges. *Chemical and Engineering News*, **19:** 23-25.

Mc Guire, R. and Feldman, I. 1973. The quenching of tyrosine and tryptophan fluorescence by H_2O and D_2O. *Photochemistry and Photobiology*, **18:** 119–124.

Maheshwari, R., Bharadwaj, G. And Bhat, M. 2000. Thermophilic Fungi: Their Physiology and Enzymes. *Microgiology and Molecular Reviews*, **64:** 461-488.

Mathrani, I.M. and Ahring, B.K. 1991. Isolation and characterization of a strictly xylan-degrading *Dictyoglomus* from a man-made, thermophilic anaerobic environment. *Archives of Microbiology*, **157:** 13-17.

Matulis, D., Kranz, J.K., Salemme, F.R. and Todd, M.J. 2005.Thermodynamic stability of carbonic anhydrase: measurements of binding affinity and stoichiometry using ThermoFluor. *Biochemistry*, **44:** 5258–5266.

McCarter, J. D. and Withers, S. G. 1994. Mechanisms of enzymatic glycoside hydrolysis *Current Opinion in Structural Biology*, **4:** 885-892.

McCarthy, A.J., Peace, E. and Broda, P. 1985. Studies on extracellular activities of some thermophilic Actinomycetes. *Applied Microbiology Biotechnology*, **21:** 238-244.

Nath, D.S. 2001 Studies on xylan degrading enzymes from an alkalophilic thermophilic *Bacillus* sp. Ph. D Thesis. University of Poona. India.

Nelson, D. and Cox, M. 2000. *Principles of Biochemistry*. Macmillan Press, London, UK.

Niesen, F., Berglund, H. and Vedadi, M. 2007. The use of differential scanning fluorometry to detect ligand interactions that promote protein stability. *Nature Protocols*. **2:** 2212-2221.

Nordberg-Karlsson, E., Dahlberg, L., Torto, N., Gorton, L. and Holst, O. 1998. Enzymatic specificity and hydrolysis pattern of the catalytic domain of the xylanase Xyn1 from *Rhodothermus marinus*. *Journal of Biotechnology*, **60:** 23-25.

Okazaki, F., Shiraki, K., Tamaru, Y., Araki, T. and Takagi, M. 2005. The First Thermodynamic Characterization of b-1,3-Xylanase from a Marine Bacterium. *The Protein Journal*, **24:** 7–8.

Paice, M.G., Gurnagul, N., Page, D.H. and Jurasek, L. 1992. Mechanism of hemicellulose directed prebleaching of Kraft pulp. *Enzyme Microbial Technology*, **14:** 272–276.

Paladarni, A., Gianses, G., Bossa, F. and Pascarela, F. 2002. Structural plasticity of thermophilic serine hydroxymethyltransferases. *Proteins*, **50:** 122-134.

Pantoliano, M.W., Petrella, E.C., Kwasnoski, J.D., Lobanov, V.S., Myslik, J., Graf, E., Carver, T., Asel, E., Springer, B.A., Lane, P. and Salemme FR. 2001. High-

density miniaturized thermal shift assays as a general strategy for drug discovery. *Journal of Bimolecular Screening,* **6:** 429–440.

Patt, R., Kordsachia, O. and Fehr, J. 2006. European hardwoods versus Eucalyptus globulus as a raw material for pulping. *Wood Science Technology,* **40:** 39-48.

Perez, J., Dorado, J.M., de la Rubia, T. and Martinez, J. 2002. Biodegradation and biological treatments of cellulose, hemicellulose and lignin: an overview. *International Microbiology,* **5:** 53-63.

Poklar, N., Lah, J., Salobir, M., Macek, P. and Vesnaver, G. 1997. pH and temperature induced molten globule-like denatured states of equinatoxin II: a study by UV-melting DSC, far- and near-UV CD spectroscopy, and ANS fluorescence. *Biochemistry,* **36:** 14345–14352

Privalov, P.L. 1979. Stability of proteins: small globular proteins. *Advances in Protein Chemistry,* **33:** 167–241

Puchart, V., Katapodis, P., Biely, P., Kremnicky, L., Christakopoulos, P., Vrsanska, M., Kekos, D., Marcis, B.J. and Bhat, M.K. 1999. Production of xylanases, mannanases, and pectinases by the thermophilic fungus *Thermomyces lanuginosus*. *Enzyme and Microbial Technology,* **24:** 355–361.

Raja, S.M., Rawat, S.S., Chattopadhyay, A. and Lala, A.K. 1999. Localization and environment of tryptophans in soluable and membrane bound states of a pore-forming toxin from *Staphylococcus aureus*. *Biophysical Journal*, **76:** 1469-1479.

Rajan, M. 2004. Global market for industrial enzymes to reach $2.4 million by 2009. Business Communications Company, RC-147U Enzymes for Industrial Applications.

Rashid, F., Sharma, S. and Bano, B. 2005. Comparison of Guanidine Hydrochloride (GdnHCL) and Urea denaturation on Inactivation and Unfolding of Human Placental Cystatin (HPC). *The Protein Journal*, **24:** 283-292.

Rawn, D. J. 1989. Proteins, energy and metabolism. *Biochemistry.* Neil Patterson Publishers, Burlington, N.C.

Rizzati, A.C.S. and Sandrim, V.C. 2004. Influence of temperature on the properties of the xylanolytic enzymes of the thermotolerant fungus *Aspergillus phoenicis*. *Journal of Industrial Microbiology and Biotechnology* **31**: 88-93.

Roncero, M. B., Torres, A. L., Colom, J. F. and Vidal, T. 2000. Effects of Xylanase treatment on fibre morphology in totally chlorine free bleaching (TCF) of *Eucalyptus* pulp. *Process Biochemistry,* **36:** 45-50.

Rouvinen, J., Bergfors, T., Terri, T., Knowles, J. K. C. and Jones, T. A. 1990. Three-dimensional structure of cellobiohydrolase II from Trichoderma reesei. *Science,* **249:** 380-386.

Ruiz, C., Blanco, A., Javier Pastor, F.I., and Diaz, P. 2002. Analysis of Bacillus megaterium lipolytic system and cloning of LipaseA, a novel subfamily I.4 bacterial Lipase. *FEMS Microbiology Letters,* **217:** 263-267.

Sasaki, H., Iwata, E., Oshima, A., Ishida, A. and Nagata, S. 2009. Isolation of Extreme Halotolerant Bacteria from Asian Desert Dust; Molecular Phylogeny and Growth Properties of their Cells. *Research Journal of Microbiology,* **4:** 260-268.

Satyanarayana, L. 2006. Structural studies on phycocyanins from three *Cyanobacterial* Spp. and Xylanase from an alkalophilic *Bacillus* Sp. Doctoral thesis. Pune. University of Pune.

Scheepers, C.G., Rypstra, T., de Koker, T.H. and Janse, B.J.H. 2002. Biotechnological pitch control in the Kraft pulping of *Eucalyptus* spp. BioY2K Combined Millennium Meeting. Grahamstown.

Schellman, J.A. 1997. Temperature, stability and the hydrophobic interaction. *Biophysical Journal,* **73:** 2960–2964.

Schoemaker, H.E., Mink, D. and Wubbolts, M.G. 2003. Dispelling the myths – Biocatalysts in industrial synthesis. *Science*, **299:** 1694-1697.

Shao, W., DeBlois, S. and Wiegel, J. 1995. Purification and characterization of two thermostable acetyl xylan esterases from *Thermoanaerobacterium* sp. strain JW/SL-YS485. *Applied Environmental Microbiology*, **61:** 937-940.

Sharma, H.S.S. 1987. Enzymatic degradation of residual non-cellulosic polysaccharides present on dew-retted flax fibers. *Applied Microbiology and Biotechnology*, **26:** 358–362.

Sharma, R., Chisti, Y. and Banerjee, U.C. 2001. Production, purification, characterization and application of Lipases. *Biotechnology Advances*, **19:** 627-662.

Sharmili, J. and Rao, M. 2009. Fluorescence study on Interactions of α–Crystallin with the Molten Globule State of 1, 4–β–D–Glucan Glucanohydrolase from *Thermomonospora* sp. induced by guanidine hydrochloride. *Journal of Fluorescence,* **19:** 967-973.

Shashidhara, K. S. and Gaikwad, S. M. 2007. Fluorescence quenching and time-resolved fluorescence studies of α-mannosidase from *Aspergillus fischeri* (NCIM 508). *Journal of Fluorescence,* **7:** 559–605.

Shashidhara, K.S., Sushama, M. and Gaikwad, M. 2010. Conformational and Functional Transitions in Class II α mannosidase from *Aspergillus fischeri*. Journal of Fluorescence, **20:** 827-836.

Shatalov, A.A. and Pereira, H. 2007. Xylanase pre-treatment of giant reed organosolve pulps: Direct bleaching effect and bleach boosting. *Industrial Crops and Products,* **25:** 248-256.

Shortle, D. and Ackerman, M. S. 2001. *Persistence of native-like topology in a denatured protein in 8 M urea. Science,* **293:** 487–489.

Simons, S.S. and Johnson, D.F. 1978. Reaction of o-phthalaldehyde and thiols with primary amines: formation of 1-alkyl(and aryl)thio-2-alkylisoindoles. *The Journal of Organic Chemistry,* **43:** 2886-2891.

Simpson, H.D., Haufler, U.R. and Daniel, R.M. 1991. An extremely thermostable xylanase from the thermophilic eubacterium *Thermotoga*. *Biochemical Journal,* **277:** 413-417.

Singh, S., Madlala, A. M. and Prior, B.A. 2003. *Thermomyces lanuginosus*: properties of strains and their hemicellulases. *FEMS Microbiology Reviews,* **27**: 3-16

Sinnott, M. L. 1990. Catalytic mechanisms of enzymic glycosyl transfer. *Chemical Reviews,* **90:** 1171-1202.

Stephens, D.E. 2006. Protein engineering of a fungal xylanase. D.Tech thesis. Durban University of Technology.

Stirpe, A., Guzzi, R., Wijma, H., Verbeet, M.P., Canters, G.W, and Sportelli, L. 2005. Calorimetric and spectroscopic investigations of the thermal denaturation of wild type nitrite reductase. *Biochimica et Biophysica Acta,* **1752:** 47–55.

Spampinato, C.P., Ferreyra, M.L. and Andreo, C.S. 2007. Conformational changes of maize and wheat NADP-malic enzyme studied by quenching of protein native fluorescence. *International Journal of Biological Macromolecules*, **41:** 64-71.

Sunna, A. and Antranikian, G. 1997. Xylanolytic enzymes from fungi and bacteria. *Critical Reviews in Biotechnology,* **17:** 39-67.

Sunna, A., Puls, J. and Antranikian, G. 1996. Purification and characterization of two endo-1,4-β-D xylanases from *Thermotoga thermarum*. *Biotechnology and Applied Biochemistry,* **24:** 177-185.

Suresh Kumar, R. 2006. Investigation into the structure and activity of conjugated bile slt hydrolase and related penicillin acylase. Doctoral thesis. Pune. University of Pune.

Suzuki, T., Yasugi, M., Arisaka, F., Yamagishi, A. and Oshima, T. 2001. Adaptation f a thermophilic enzyme 3-isoprpylmalate dehydrogenase, to low temperatures. *Protein engineering,* **14:** 85-91.

Tan, L.U.L., Wong, K.K.Y., Yu, E.K.C. and Saddler J.N. 1985. Purification and characterization of two D-xylanases from *Trichoderma harzianum*. *Enzyme and Microbial Technology,* **7:** 425–430.

Tarvainen, K., Kanerva, L., Tupasela, O., Grenquist-Norden, B., Jolanki R., Estlander, T. and Keskinen, H. 1991. Allergy from cellulose and xylanase enzymes. *Clinical and Experimental Allergy,* **21:** 609–615.

Techapun, C., Poosarun, N., Wanatanabe, M. and Sasaki, K. 2003. Thermostable and alkali tolerant cellulose free xylanases produced from agricultural wastes and the properties required for use in pulp bleach processes: a review. *Process Biochemistry*. **38:** 1327-1340.

Thompson, G., Swain, J., Kay, M. and Forster, C.F. 2001. The treatment of pulp and paper mill effluent: a review. *Bioresource Techno*logy, **77:** 275–286.

Toniolo, C. 1970. Optical properties of methylisothiocyanate-amino acid adducts. *Tetrahedron,* **26:** 5479-5488.

Torronen, A. and Rouvinen, J. 1997. Structural and function properties of low molecular weight endo-1,4-β-xylanases. *Journal of biotechnology,* **57:** 137-149.

Torres, F.L, Melo, R. and Colodette, J. L. 2005. Bleached Kraft Pulp Production from *Pinus tecunumanii. Sociedade de Investigações Florestais,* **29:** 489-494.

Vazquez, M. C., Oberhauser, A. F., Fowler, S. B., Marszaler, P. E., Broedel, S. E., Clarke, J. and Fernandez, J. M. 1999. Mechanical and chemical unfolding of a single protein: a comparison. *Proccedings of the National Acadamy of Sciences of the United States of America,* **96:** 3694-369

Vedadi, M., Niesen, F.H., Allai-Hassani, A., Fedorov, O.Y., Finerty, P.J., Wasney, G.A., Yeung, R., Arrowsmith, C., Ball, L.J., Berglund, H., Hui, R., Marsden, B.D., Nordlund, P., Sundstrom, M., Weigelt, J. and Edwards, A.M. 2006. Chemical screening methods to identify ligands that promote protein stability, protein crystallization, and structure determination. *Proccedings of the National Academy of Sciences of the United States of America,* **103:** 15835–15840.

Vetri, V. and Militello, V. 2005. Thermal induced conformational changes involved in the aggregation pathways of beta-lactoglobulin. *Biophys Chemistry.* **113:** 83–91.

Vieille, C. and Zeikus, G.J. 2001. Hyperthermophilic Enzymes: Sources, uses and molecular mechanisms for thermostability. *Microbiology and Molecular Biology Reviews* **65**: 1-43.

Vivian, J.T. and Callis, P.T. 2001. Mechanisms of Tryptophan Fluorescence Shifts in Proteins. *Biophysical Journal,* **80:** 2093-2109.

Warren, R.A.J. 1996. Microbial hydrolysis of polysaccharides. *Annual Review of Microbiology,* **50:** 183-212.

Wang, Y., Srivastava, K.C., Shen, G.J. and Wang, H.Y. 1995. Thermostable alkaline Lipase from a newly isolated thermophilic *Bacillus* strain. *Journal of Fermentation and Bioengineering,* **79:** 433–438.

Wassenberg D., Schurig, H., Liebl, W. and Jaenicke R. 1997. Xylanase XynA from the hyperthermophilic bacterium *Thermotoga maritima*: structure and stability of the recombinant enzyme and its isolated cellulose-binding domain. *Protein Science,* **6:** 1718–1726

Wei, Z., and Song, J. 2005. Molecular mechanism underlying the thermal stability and pH-induced unfolding of *CHABII*. *Journal of Molecular Biology,* **348:** 205–218

Winterhalter, C. and Liebl, W. 1995. Two extremely thermostable xylanases of the hyperthermophilic bacterium *Thermotoga maritima* strain MSB. *Applied Environmental Microbiology,* **61:** 1810-1815.

Wintrode, P.L., Miyazaki, K. and Arnold, F.H. 2001. Patterns of adaptation in a laboratory evolved thermophilic enzyme. *Biochimica et Biophysica Acta,* **1549:** 1-8.

Withers, S.G. 2001. Mechanisms of glycosyl transferases and hydrolases. *Carbohydrate Polymers,* **44:** 325–337.

Wong, K. K. Y., Tan, L. U. L., and Saddler, J. N. 1988. Multiplicity of beta-1,4-xylanase in microorganisms: functions and applications. *Microbiological Review,* **52:** 305-317.

Wong, K.K.Y. and Saddler, J.N. 1992. Trichoderma xylanases, their properties and purification. *Critical Reviews in Biotechnology,* **12:** 413–435.

Wong, K.K.Y., Tan, L.U.L. and Saddler, J.N. 1988. Multiplicity of β-1,4-xylanase in microorganisms: Functions and applications. *Microbiological Review*, **52:** 305–17.

Wuthrich, K. 1994. NMR assignment as a basis for structural characterization of denatured states of globular proteins. *Current Opinion in Structural Biology*, **4:** 93-99.

Yin, E., Le, Y., Pei, J., Shao, W. and Yang, Q. 2008. High-level expression of the xylanase from Thermomyces lanuginosus in Escherichia coli. *World Journal of Microbiology and Biotechnology*, **24:** 275-280.

Yoshioka, H., Nagato, N., Chavanich, S. Nilubol, N. and Hayashida S. 1981. Production and characterization of themostable xylanase from *Talaromyces byssochlamydoides* YH-50. *Agricultural and Biological Chemistry,* **45:** 2425-2432.

Zavodszky, P., Kardos, J., Svingor, A. and Petsko G.A. 1998. Adjustment of conformational flexibility is a key event in the thermal adaptation of proteins. *Proceedings of the National Academy of Sciences,* **95:** 7406-7411.

www.ap-lab.com/circular_dichroism.htm

*** (2007) Fluorescence spectroscopy: A tool for Protein folding/unfolding study PC. 3267.